Maejo International Journal of Science and Technology

Volume 1, Issue 2 August - December 2007 ISSN : 1905-7873

- Green chemistry and sustainable development
- Multidisciplinary research and development : The biomedical engineering approach
- Antioxidant capacity and phenolic content of some Thai culinary plants

Coverage by Abstracting Service : This journal is covered by Chemical Abstracts, SciFinder Scholar, AGRIS and Google Scholar.

Available online at **www.mijst.mju.ac.th**

**Journal Information**

*Maejo International Journal of Science and Technology* (ISSN 1905-7873 © 2007), the international journal for the rapid publication of all preliminary communications in Science and Technology, is the first peer-refereed scientific journal of Maejo University (www.mju.ac.th). Intended as a medium for communication, discussion, and rapid dissemination of important issues in Science and Technology, articles are initially published online in an open access format which thereby gives authors the chance to communicate with a wide range of readers in an international community.

**Publication Information**

MIJST is published twice each year. Articles are available online and can be accessed free of charge at http://www.mijst.mju.ac.th. Printed and bound copies of each volume are produced and distributed to authors and selected groups or individuals. 

**Abstracting/Indexing Information**

MIJST is covered and cited by Chemical Abstract Service (CAS) and AGRIS. CAS is the global leader in chemical information that provides the most comprehensive databases in chemistry and related sciences. CAS makes this information available to researchers through SciFinder and STN, the best search retrieval tools for scientists and information professionals. AGRIS is another big database that provides worldwide biographic coverage of agricultural science and technology,

**Contact Information**

Editorial office: Maejo International Journal of Science and Technology (MIJST), 1st floor, Orchid Building, Maejo University, San Sai, Chiang Mai 50290, Thailand

Tels: +66-53-87-3880, +66-53-87-3651 Fax: +66-53-87-3897, +66-53-86-9410

Emails: duang@mju.ac.th , mijst@mju.ac.th or weerachai@mju.ac.th .

# MAEJO INTERNATIONAL JOURNAL OF SCIENCE AND TECHNOLOGY

# MAEJO INTERNATIONAL JOURNAL OF SCIENCE AND TECHNOLOGY

*The International Journal for the Rapid Publication of Preliminary Communications in Science and Technology*

http://www.mijst.mju.ac.th
ISSN 1905-7873 

# MAEJO INTERNATIONAL JOURNAL OF SCIENCE AND TECHNOLOGY

*Volume 1, Issue 2(August-December 2007)*


## CONTENTS

**Articles**
**Page**

http://www.mijst.mju.ac.th
ISSN 1905-7873 

MAEJO INTERNATIONAL JOURNAL
OF SCIENCE AND TECHNOLOGY

*Volume 1 (April – July 2007)*

## Author Index



http://www.mijst.mju.ac.th
ISSN 1905-7873 

# Instructions for Authors

## Manuscript Preparation

Manuscripts should be prepared in English using a word processor. MS Word for Macintosh or Windows, and .doc or .rtf files are preferred. Manuscripts may be prepared with other software, provided that the full document (with figures, schemes and tables inserted into the text) is exported to a MS Word format for submission. Times or Times New Roman font is preferred. The font size should be 12 pt. and the line spacing at least 17 pt. The printing area is 17.5cm x 24.7cm (6.9" x 9.73"). For A4 paper, margins must be 1.5 cm on top, 3.5cm at the bottom and 1.75 cm on both left and right sides of the paper. For US letter-sized paper, margins must be 1.5 cm (0.59") on top, 1.74 cm (0.68") at the bottom and 2.05 cm (0.8") on both left and right sides. Although our final output is in .pdf format, authors are asked NOT to send a manuscript in this format as editing them is much more complicated.

Authors' full mailing addresses, homepage addresses, phone and fax numbers, e-mail addresses and homepages can be included in the title page and these will be published in the manuscripts. The corresponding author should be clearly identified. It is the corresponding author's responsibility to ensure that all co-authors are aware of and approve of the content of a submitted manuscript.

A brief (200 word maximum) Abstract should be provided. The use in the Abstract of numbers to identify compounds should be avoided, unless these compounds are also identified by name.

A list of three to five keywords must be given, and placed after the Abstract. Keywords may be single words or very short phrases.

Although variations in accord with a manuscript's content are permissible, in general all papers should have the following sections: Introduction, Materials and Methods, Results and Discussion, Conclusion, Acknowledgments (if applicable), and References.

Authors are encouraged to prepare figures and schemes in color. Full color graphics will be published free of charge.

Tables should be inserted into the main text, and numbers and titles supplied for all tables. All table columns should have an explanatory heading. To facilitate the layout of large tables, smaller fonts may be used, but in no case should these be less than 10 pt. in size. Authors should use the Table option of MS Word to create tables, rather than tabs, as tab delimited columns are often difficult to format in .pdf for final output.

Figures and schemes should also be placed in numerical order in the appropriate place within the main text. Numbers, titles and legends should be provided for all schemes and figures. These should be prepared as a separate paragraph of the main text and placed in the main text before the figure or scheme. Chemical structures and reaction schemes should be drawn using an appropriate software package designed for this purpose. As a guideline, these should be drawn to a scale such that all the details and text are clearly legible when placed in the manuscript (i.e. text should be no smaller that 8-9 pt.).

For bibliographic citations the reference numbers should be placed in square brackets, i.e. [ ], and placed before the punctuation, for example [4] or [1-3], and all the references should be listed separately and as the last section at the end of the manuscript.

## Format for References

*Journal:*

1. Buddhasukh, D., J. R. Cannon, B. W. Metcalf, and A. J. Power, ″Synthesis of 5-n-Alkylresorcinol Dimethyl Ethers and Related Compounds *via* Substituted Thiophens", *Aust. J. Chem.*, **1971**, *24*, 2655-64.

*Text:*

2. Vogel, A. I. "A Textbook of Practical Organic Chemistry", 3rd Edn., Longmans, London, **1956**.

*Chapter in an edited Text :*

3. Gore, P. H., in "Friedel-Crafts and Related Reactions." (Ed. G. A. Olah.), Vol. 3, Interscience, London, **1964**, Ch. 31.

*Thesis / Dissertation :*

4. Chowwanapoonpohn, S. *PhD. Thesis*, **2003**, Chiang Mai University, Thailand.

*Patent:*

5. Miwa, K., S. Maeda, and Y. Murata, “Purification of Stevioside by Electrolysis", *Jpn. Kokai Tokkyo Koho 79 89,066* (**1979**).

### Referees

Authors should suggest at least 3 referees with the appropriate technical expertise, although the editors will not necessarily approach them. Their addresses, homepage addresses, phone and fax numbers and e-mail addresses should be provided as fully as possible.

### English corrections

This journal is published in English, so it is essential that for proper refereeing and quick publication all manuscripts be submitted in grammatically correct English. For this purpose we ask that non-native English speakers ensure their manuscripts are checked before submitting them for consideration. We suggest that for this purpose your manuscript be revised by an English speaking colleague before submission.

## Submission

Manuscripts should be submitted by e-mail to duang@mju.ac.th, mijst@mju.ac.th or weerachai@mju.ac.th .

*Mj. Int. J. Sci. Tech.* **2007**, *01(02)*, 95-97

***Maejo International***

***Journal of Science and Technology***

**ISSN 1905-7873**

Available online at www.mijst.mju.ac.th

*Invited Article*

# Green chemistry and sustainable development

**Margaret E. Kerr***

*Dr. Kerr received her B.S. degree in chemistry from the University of Maine and her Ph.D. from Wesleyan University in Middletown, CT (USA) in inorganic chemistry. She did post-doctoral research at the University of Florida and was offered a position as a Senior Staff Scientist at Fina Oil and Chemical in Houston, TX. She worked for two years developing metallocene catalysts for polypropylene synthesis before taking a position as a faculty member at Worcester State College in Worcester, MA. She is currently an Associate Professor with a focus on green chemistry in education. She was awarded a Fulbright Senior Scholar Grant in 2007 to go to Thailand to promote green chemistry curriculum development at Chulalongkorn University in Bangkok.*

* E-mail : Margaret.Kerr@worcester.edu

I am writing this article at the end of a 5-month Fulbright Senior Scholar grant that has provided me the opportunity to live in Bangkok, Thailand. I have worked closely with Thai scholars at my host institution, Chulalongkorn University, and at other institutions including Maejo University, Ubon Ratchatani University and Silpakorn University. During my stay in Thailand, I have been fortunate to interact with scientists and citizens who care deeply about the future of Thailand and of the world. As I have learned more about Thailand, I have been struck by how important the ideals of self-sufficiency and sustainability are in relation to the predominant culture. In the first edition of Maejo International Journal of Science and Technology, Dr. Thep Pongparnich, president of Maejo University, wrote an invited article that discussed some of the links between science and Thai culture and suggested that "Thai scientists should focus more on research that leads to self-dependency with a certain degree of freedom and on how to live a moderate life that is friendly with nature." If we take that a step further, the question becomes not whether we should promote sustainability and self-sufficiency but rather how do we attain that goal? As someone with a specialty in the field of green chemistry in education, I have become very interested in how the ideal of sustainable science can fit into a message that is acceptable by society as a whole.

My perspective as an American might be somewhat different than that of a Thai, but the fundamental role of science in the future will be the same everywhere. As chemists, we are concerned about the future of our field and are worried about what will happen when petroleum based starting materials

*Mj. Int. J. Sci. Tech.* **2007**, 01(02), 95-97

become scarce and more expensive. Scientists have both the burden and the privilege of being on the forefront in the development of solutions that will aid society in its progression into the future. As we work to train students and develop research programs, it is imperative that we teach students in concepts in sustainability. The practice of green chemistry, or sustainable chemistry, is a powerful tool that provides students with the opportunity to learn about how they can promote practices that are favorable to the environment and to humans when they get into the working world.

Green chemistry, by definition, promotes the reduction or elimination of hazardous substances in chemical processes [1]. Chemistry as it has been traditionally practiced is not on a sustainable trajectory and will be a major contributor to environmental degradation unless changes are made. According to Professor Walter Leitner [2], scientific editor of the journal *Green Chemistry*, "As the principles of green chemistry and the concepts of sustainability in chemical manufacturing are becoming part of the explicit corporate policy and aims in the chemical industry, there is a rapidly growing need for the education of chemists in the field." Increasingly, corporations are looking for employees who have training in areas such as hazard and risk management, toxicity, and life cycle assessment that are not taught in traditional chemistry programs.

Green chemistry has been defined as "the utilization of a set of principles that reduces or eliminates the use or generation of hazardous substances in the design, manufacture and application of chemical products." It has been referred to in numerous sources as "molecular-level pollution prevention". Green chemistry is not related to a specific discipline in chemistry, but instead provides any chemist with a framework in which to design molecular processes. The major difference between a green chemistry approach to environmental issues and more traditional approaches is that green chemistry utilizes the creativity of the scientists and engineers to develop novel and benign approaches to processes from the start rather than relying on regulatory restrictions after the process has been discovered to be toxic or polluting [3]. There are twelve principles associated with green chemistry and if all principles are utilized, a process can be considered benign [1].

Why is it important for students to study these concepts? If we focus on Thailand and Asia, we find that the Asian market is so vast that the future of the planet depends considerably on what happens there in the next generation [4]. There has been substantial economic growth in most countries in Asia over the previous 15 years. In Thailand for example, the economic growth averaged 6.2% from 2002-2004 and is expected to show continued growth of around 5% per year in the future [5]. A measure of economic growth worldwide is indicated by the Global Chemical Index. The 2003 Global Chemical Index showed East Asia, which includes China, with an annual growth of 11.0%. This can be compared with Central and Eastern Europe at 6.7% and the United States at 0.2%. While China shows the largest growth in eastern Asia, countries such as Thailand, Malaysia and Vietnam are also expected to see high growth [6]

While this growth has resulted in an overall reduction in poverty in Asia, it has also placed significant strains on the environment. In a study by the Asian Development Bank, Asian cities have substantially higher air pollution than other industrial countries. Higher levels of water and ground pollution also contribute to the overall environmental degradation of the area. In the Thailand Human Development Report 2007, written by the United Nations Development Program, it was found that Thailand imported

*Mj. Int. J. Sci. Tech.* **2007**, 01(02), 95-97

nearly two times the amount of pesticides in 2004 than it did in 2003. Additionally, samples taken from over 100,000 farmers showed dangerous levels of toxins from exposure to pesticides. While many overall quality of life indicators are improved there are growing problems with environmental issues. Factors such as water quality and industrial waste management indicate that unless changes are made, Thailand will show marked environmental deterioration in the future [7].

As we read statistics such as those above, the question becomes one of how to balance economic growth and environmental degradation. Sustainable development has been defined by the World Commission on Environment and Development as "a process in which the exploitation of resources, the direction of investment, the orientation of technological development, and institutional change are made consistent with future and present needs." According to *Sustainable Development in Asia* [5], "Sustainable development is an act of balancing economic, social, and environmental benefits through implementation of development policies, programs, and projects that will not enhance one type of benefit at the cost of others. Sustainable development also requires a major overhaul in the mindset, attitude, and behavior of the local people as well as of the international community." If the 11% growth of the Global Chemical Index of Asia in 2003 is compared with the percentages of hazardous wastes that are dumped in landfills or oceans, it becomes apparent that changes in the way chemistry and chemical manufacturing are done will have a major impact in the goal of sustainable development.

Research and education efforts in academic institutions and industrial laboratories throughout the world recognize the importance of designing more benign chemical processes and of utilizing sustainable development practices in order to bring about necessary changes. It is encouraging to read articles in leading journals describing the development of greener processes and to visit universities with ongoing programs in sustainable development. In Thailand, institutions such as Maejo University and Chulalongkorn University are on the forefront of the work being done in these areas. Green chemistry, coupled with the Thai ideal of self-sufficiency and living in harmony with nature, can provide a way to navigate the path toward a future where we can have the comforts we all as humans desire while at the same time not compromising the future of upcoming generations.

**References**

1. P.T. Anastas and J.C. Warner, "Green chemistry: theory and practice" Oxford University Press, 1998.
2. W. Leitner, "Focus on education in green chemistry", *Green Chem.*, **2004,** *6*, 351.
3. http://www.chemistry.org/portal/a/c/s/1/acsdisplay.html?DOC=greenchemistryinstitute\index.html (Accessed November, 2007)
4. Asian Development Bank, "Asian environment outlook 2005: making profits, protecting our planet," http://www.adb.org/Environment/aeo/events.asp#aeor . (Accessed November, 2007)
5. Asian Development Bank, "Asian development outlook 2006: Thailand," http://www.adb.org/Thailand/default.asp . (Accessed November, 2007)
6. a) I.Young, "Riding Asia's industry upcycle," *Chemical Week*, **2005**, *167(13)*, 28. b) K. Tyagarajan, "The global chemical industry—looking up as Asia leads," February, 2004, http://www.frost.com/prod/servlet/market-insight-print.pag? docid=10658071 . (Accessed November, 2007)
7. United Nations Development Program, "Thailand human development report 2007", http://www.undp.or.th/NHDR2007/index.html. (Accessed November, 2007)

*Mj. Int. J. Sci. Tech.* **2007**, *01(02)*, 98-99

***Maejo International***

***Journal of Science and Technology***

**ISSN 1905-7873**

Available online at www.mijst.mju.ac.th

# Multidisciplinary research and development: The biomedical engineering approach

**Assoc. Prof. Chatchai Tayapiwatna, PhD**


***A highly acclaimed and multi-awarded scientist in Thailand whose researches on clinical immunology and biomedical engineering are recognized internationally***

Division of Clinical Immunology, Faculty of Associated Medical Sciences and BioMedical Engineering Center, Chiang Mai University, Chiang Mai, 50200, Thailand
Email: asimi002@hotmail.com

---

The way we do science has tremendously changed. In particular, life sciences and engineering are becoming increasingly complex. Thus, an integrated approach to research and development is adopted to meet the burdens of each challenging problem. Advances in basic science and clinical medicine afford unprecedented opportunities for the conjoining of the life sciences with the physical sciences, mathematics, computer science, and engineering. The multidisciplinary research teams combine scientific talents, and they draw from the resulting blend of knowledge, skills, and experience to generate innovative solutions. Research and development activities range from fundamental science to production engineering of complex systems. The improvement of tools and techniques offers great potential for medical advances, and there is an increasing trend in the biomedical sciences to use an integrative rather than a disparate approach.

The biomedical research community at large does not understand the nature of bioengineering and technology and instrumentation development research. Although the rise of molecular and cell biology has made biology accessible to engineering science, most biomedical scientists are not aware of the contributions engineers can make. In fact, biomedical engineering development has a powerful impact on health researches. Radical changes in biomedical sciences are likely to occur from incorporating the engineering perspectives into the formulation of basic questions addressed in "hypothesis-driven research." On the one hand, the field of bioengineering has evolved by amalgamating with molecular and cellular biology and biochemistry (e.g., tissue engineering, drug and gene delivery, and biomimetic biomaterials), while on the other, it also continues to build upon its early roots in the physical sciences (e.g., magnetic resonance, computerized tomography, ultrasound imaging, and biomechanics). It advances fundamental concepts, creates knowledge from the molecular to the organ systems level, and develops innovative biologics, materials, processes, implants, devices and informatic approaches for the prevention, diagnosis, and treatment of disease, for patient rehabilitation, and for improving health. It is important for biomedical scientists to fully appreciate the ways in which engineers can contribute to the advancement of biomedical science and clinical medicine. Engineers need to learn to devise problems, not just solve them. They necessitate managing complexity and dealing with vagueness. Engineering education thus needs to become more integrative and ground-breaking.

Biomedical engineering, however, has received little recognition in Thailand. Some major funding mechanisms have not kept up with the increasingly multidisciplinary nature of its research and the need to innovate and take risks. An identified organizational structure would help foster biomedical engineering research, preferably an inter-institutional center for biomedical engineering with its own appropriation and platform for growth. Chiang Mai University has created an internal organization, BME Center, to provide a central focus for bioengineering issues. BME Center is composed of representatives from several Faculties. BME Center has a specific aim to improve the current mechanisms for reviewing biomedical engineering grant applications. Meanwhile, private support of biomedical researches is becoming increasingly important. Research collaborations, partnerships, and personnel exchanges should be encouraged to enhance biomedical engineering and other research disciplines.

*Mj. Int. J. Sci. Tech.*, **2007**, *01(02)*, 100-106

***Maejo International***

***Journal of Science and Technology***

**ISSN 1905-7873**

Available online at www.mijst.mju.ac.th

*Full Paper*

# Antioxidant capacity and phenolic content of some Thai culinary plants

**Wiwat Wangcharoen* and Wallaya Morasuk**

Department of Food Technology, Faculty of Engineering and Agricultural Industry, Maejo University, Chiangmai 50290, Thailand.

*Corresponding author, E-mail: wwwangcharoen@yahoo.com

*Received: 7 June 2007 / Accepted: 1st August 2007 / Published: 16 August 2007*

**Abstract:** The antioxidant capacity of red and green bird chili (*Capsicum frutescens* Linn.), red and green chili spur pepper (*Capsicum annuum* Linn. var. acuminatum Fingerh.), red and white holy basil (*Ocimum sanctum* Linn.), garlic (*Allium sativum* Linn.), and pumpkin (*Cucurbita moschata* Decne.), which have been normally used in Thailand as food ingredients, was estimated by three different methods: ferric reducing antioxidant power (FRAP) assay, improved ABTS radical cation decolorization assay, and DPPH free radical scavenging assay. Additionally, their total phenolic contents were analyzed by Folin-Ciocalteau micro method. The result showed that red holy basil and red bird chili seemed to be better sources of antioxidant compounds, followed by green bird chili and red chili spur pepper, white holy basil, green chili spur pepper, garlic and pumpkin, respectively. For results of total phenolic content analysis, they were significantly related to those of FRAP (r = 0.825), ABTS (r = 0.973) and DPPH (r = 0.683).

**Keywords**: antioxidant capacity, total phenolic content, chili, holy basil, garlic, pumpkin.

## Introduction

Most of culinary plants in Thailand, such as chilies, garlic, holy basil, pumpkin, etc., are also used as medicinal plants. Chilies have been recognized by many cultures around the world for their medicinal qualities. When chilies are eaten, capsaicin stimulates the release of endorphins, which give a pleasurable feeling. Moreover, chilies are believed to increase circulation, relieve rheumatic pain,

*Mj. Int. J. Sci. Tech.*, **2007**, *01(02)*, 100-106

treat mouth sores and infected wounds, reduce blood clots and aid digestion by stimulating saliva and gastric juice flow [1]. Garlic has a high concentration of sulfur-containing compounds. The thiosulfinates, including allicin, appear to be the active substances in garlic. Allicin is formed when alliin, a sulfur-containing amino acid, comes into contact with the enzyme alliinase when raw garlic is chopped, crushed, or chewed. The antimicrobial, hypolipidemic, antioxidant, and antithrombotic effects that have been attributed to garlic are thought to be related to allicin and other breakdown products [2].

Holy basil has a strong anise-like, slightly musky and lemony taste with a camphoraceous aroma. The dominant aroma component in holy basil is eugenol. This herb also has been used by Asian people in traditional medicine. It is used for most stomach disorders, cramps, diarrhea, headaches, whooping cough and head colds [1]. Pumpkin is a good source of beta – carotene, an important antioxidant, and it is also a good source of vitamin C, another good antioxidant [3].

The objective of this study was to compare the antioxidant capacity of bird chili (green and red), chili spur pepper (green and red), garlic, holy basil (red and white), and pumpkin available from fresh markets in Chiangmai, Thailand, by three different methods, viz. ferric reducing antioxidant power (FRAP) assay, improved ABTS radical cation decolorization assay, and DPPH free radical scavenging assay. The total phenolic contents of the above culinary plants were also estimated and related to their antioxidant capacity results.

## Materials and Methods

### *Chemicals*

Trolox (6-hydroxy-2,5,7,8-tetramethychroman-2-carboxylic acid) [Aldrich], TPTZ (2,4,6-tripyridyl-s-triazine), DPPH (2,2-diphenyl-1-picrylhydrazyl) [Sigma], ABTS (2,2'-azinobis (3-ethylbenzothiazoline-6-sulfonic acid)), Folin-Ciocalteau phenol reagent, ferric chloride, ferrous sulphate, gallic acid, glacial acetic acid, hydrochloric acid, sodium acetate, potassium persulphate, sodium carbonate, and vitamin C [Fluka], were all of analytical grade.

### *Sample extraction*

Fresh samples of the studied plants were purchased from fresh markets in Chiangmai. Their moisture contents were analyzed by the method of AOAC [4]. The sample extraction method of Leong and Shui [5] was modified for sample preparation. Edible portion of the fresh sample was homogenized using a blender. A mixture of deionized water and 95% ethanol was used as extraction solvent and 95% ethanol was selected for preliminary studies. Two grams of homogenized sample were added with 10 ml of the selected solvent. The extraction was done by using a vortex mixer for 60 seconds. The mixture was filtered and the filtrate was collected and used for FRAP, ABTS, DPPH, and total phenolic content assays. Milton Roy Spectronic 20D+ spectrophotometer was used for all assays.

*Mj. Int. J. Sci. Tech.*, **2007**, *01(02)*, 100-106

*Ferric reducing antioxidant power (FRAP) assay*

The FRAP was assessed according to Benzie and Strain [6]. Briefly, 6 ml of working FRAP reagent prepared daily was mixed with 20 - 100 µl of the extract. The absorbance at 593 nm was recorded after 30-min incubation at 37 °C. Absorbance increases were calculated as FRAP values by comparing with standard curves created by vitamin C (0 - 15 µg), and reported as mg vitamin C equivalent per gram of fresh weight.

*ABTS radical cation decolorization assay*

The ABTS method of Re *et al*. [7] was modified. ABTS radical cation ($ABTS^+$) was produced by reacting 7 mM ABTS stock solution with 2.45 mM postassium persulphate (final concentration) and allowing the mixture to stand in the dark at room temperature for 12 - 16 hours before use. The $ABTS^+$ solution was diluted with deionized water and 95 % ethanol (1:1) to an absorbance of 0.70 ($\pm$ 0.02) at 734 nm. The extract (20-100µl) was mixed with 6 ml of diluted $ABTS^+$ solution. The decrease of absorbance was recorded at 1 min after mixing. Absorbance decreases were calculated as ABTS values by comparing with standard curves created by vitamin C (0 - 20 µg), and the results were reported as mg vitamin C equivalent per gram of fresh weight.

*DPPH free radical scavenging activity*

The method of Brand-Williams *et al.* [8] was used with some modifications. DPPH radical solution (0.8 mM) in 95% ethanol was prepared. The extract (100-1000µl) was diluted to 5.4 ml by deionized water and 95 % ethanol (1:1) before 0.6 ml of the DPPH solution was added and mixed. The decrease of absorbance was recorded at 1 min after mixing. Absorbance decreases were calculated as DPPH values by comparing with standard curves created by vitamin C (0 - 40 µg), and the results were reported as mg vitamin C equivalent per gram of fresh weight.

*Total phenolic content*

The Folin-Ciocalteau micro method of Waterhouse [9] was used to estimate total phenolic content (TPC). The extract (60-300 µl) was diluted with deionized water to 4.8 ml, and 300 µl of Folin-Ciocalteau reagent was added and shaken. After 8 min, 900 µl of 20% sodium carbonate solution was added with mixing. The solution was left at 40°C for 30 min before reading the absorbance at 765 nm. Gallic acid (0 - 50 µg) was used as standard, and the results were reported as mg gallic acid equivalent per gram of fresh weight.

*Calculation and Statistical Analysis*

*Mj. Int. J. Sci. Tech.*, **2007**, *01(02)*, 100-106

The values of FRAP, ABTS, DPPH, and TPC (mg standard equivalent per gram of fresh weight) were calculated using the equation below:

$$\text{Values of FRAP, ABTS, DPPH, and TPC (mg standard equivalent per gram of fresh weight)} = \frac{[(SA - BA) / (Slope)]\,[10 / U]}{[2]\,[1{,}000]}$$

where: SA = Sample absorbance for FRAP value and TPC or absorbance decrease of sample for ABTS and DPPH values

BA = Blank (no extract) absorbance for FRAP value and TPC or absorbance decrease of blank for ABTS and DPPH values (extract was substituted by deionized water for blank)

Slope = Slope of standard curve

[10 / U] = Total volume of extract (10 ml) / Used volume of extract (ml)

[2] = Weight of used sample (g)

[1,000] = Factor for changing µg to mg.

Each experiment was performed in triplicate on different purchased samples. A randomized complete block design (RCBD) was used. Plants and market purchases served as treatment and block variables, respectively. Mean comparisons were performed by Duncan's new multiple range test (DMRT). The bivariate correlations between all antioxidant capacity assays and total phenolic contents were analyzed.

## Results and Discussion

The moisture content of each plant is shown in Table 1. From preliminary studies, 60% (v/v) of 95% ethanol was selected as extraction solvent for chilies and holy basil, while deionized water and 95% ethanol were chosen for garlic and pumpkin, respectively.

**Table 1** Moisture content of some Thai culinary plants.

| Thai culinary plant | Moisture content (%) |
|---|---|
| Bird chili, green | 78.46 $\pm$ 2.32 |
| Bird chili, red | 67.09 $\pm$ 1.58 |
| Chili spur pepper, green | 90.92 $\pm$ 1.15 |
| Chili spur pepper, red | 84.28 $\pm$ 2.32 |
| Garlic | 68.66 $\pm$ 2.22 |
| Holy basil, red | 86.44 $\pm$ 0.46 |
| Holy basil, white | 85.90 $\pm$ 0.61 |
| Pumpkin | 86.21 $\pm$ 2.15 |

*Mj. Int. J. Sci. Tech.*, **2007**, *01(02)*, 100-106

The results of the antioxidant capacity assessment of the studied plants as determined by FRAP, ABTS, and DPPH assays are shown in Table 2. These differences could be explained by different mechanisms of analytical methods. FRAP assay measures the ability to reduce a ferric tripyridyltriazine ($Fe^{3+}$-TPTZ) to a ferrous form ($Fe^{2+}$-TPTZ) of samples [5]. ABTS and DPPH assays are based on the reduction of ABTS [7] and DPPH free radicals [8] of samples, but values from DPPH assay might be lower than those from ABTS assay. Wang *et al*. [10] showed that some compounds which have ABTS scavenging activity may not show DPPH scavenging activity, and Arts *et al.* [11] found that some products of ABTS scavenging reaction may have a higher antioxidant capacity and can further react with remained ABTS radicals.

Table 2 shows that red holy basil had the highest antioxidant capacity analyzed by FRAP assay, followed by red bird chili and white holy basil, green bird chili and red chili spur pepper, green chili spur pepper, pumpkin and garlic, in that order. In ABTS assay, the plants with the highest antioxidant capacity were bird chili (red and green) and red holy basil, followed by red chili spur pepper and white holy basil, green chili spur pepper, garlic, and pumpkin, respectively. However, results of DPPH assay showed that red chili spur pepper had the highest antioxidant capacity, followed by bird chili (red and green) and holy basil (red and white), green chili spur pepper, garlic and pumpkin, respectively. For overall results, it might be concluded that red holy basil and red bird chili were better sources of antioxidant compounds in this study, followed by green bird chili and red chili spur pepper, white holy basil, green chili spur pepper, garlic and pumpkin, respectively. In case of total phenolic content analysis, it was found that red bird chili contained the highest amount of phenolic compounds, followed by green bird chili and red holy basil, red chili spur pepper and white holy basil, green chili spur pepper, garlic and pumpkin, respectively.

**Table 2.** Results of antioxidant capacity and total phenolic content estimation

| Thai culinary plant | FRAP* | ABTS* | DPPH* | TPC** |
|---|---|---|---|---|
| Bird chili, green | $1.68 \pm 0.04^{c}$ | $6.48 \pm 0.88^{a}$ | $0.66 \pm 0.09^{b}$ | $2.83 \pm 0.31^{b}$ |
| Bird chili, red | $2.34 \pm 0.16^{b}$ | $6.68 \pm 0.84^{a}$ | $0.79 \pm 0.07^{b}$ | $3.48 \pm 0.58^{a}$ |
| Chili spur pepper, green | $0.61 \pm 0.19^{d}$ | $1.32 \pm 0.05^{c}$ | $0.36 \pm 0.04^{c}$ | $0.85 \pm 0.20^{d}$ |
| Chili spur pepper, red | $1.56 \pm 0.20^{c}$ | $3.82 \pm 0.37^{b}$ | $1.23 \pm 0.31^{a}$ | $1.85 \pm 0.26^{c}$ |
| Garlic | $0.14 \pm 0.04^{e}$ | $1.06 \pm 0.11^{d}$ | $0.16 \pm 0.03^{d}$ | $0.41 \pm 0.10^{e}$ |
| Holy basil, red | $3.35 \pm 0.43^{a}$ | $5.91 \pm 0.49^{a}$ | $0.72 \pm 0.02^{b}$ | $2.65 \pm 0.27^{b}$ |
| Holy basil, white | $1.99 \pm 0.05^{b}$ | $4.23 \pm 0.19^{b}$ | $0.62 \pm 0.01^{b}$ | $1.78 \pm 0.16^{c}$ |
| Pumpkin | $0.19 \pm 0.03^{e}$ | $0.63 \pm 0.24^{e}$ | $0.11 \pm 0.01^{d}$ | $0.24 \pm 0.05^{e}$ |

* mg Vitamin C equivalent / g fresh weight.
** mg Gallic acid equivalent / g fresh weight.
Means ($\pm$ S.D.) with different superscripts in each column are significantly different ($p \leq 0.05$). Superscript a indicates the group with the highest value, while e belongs to the lowest value group.

The correlations between results of antioxidant capacity and TPC analysis are highly significant ($p<0.01$) as shown in Table 3. These correlations indicate that the phenolic compounds could be the main cause of antioxidant power of all plant samples, in accordance with the previous findings that many phenolic compounds in plants are good sources of natural antioxidants [12, 13]. However, some

*Mj. Int. J. Sci. Tech.*, **2007**, *01(02)*, 100-106

coefficients were not high, which may be due to the fact that some natural antioxidants, eg. vitamin C and carotenoids, are not phenolic compounds, and that each antioxidant compound may show different activities with different assays. In this study, the contribution of the phenolic content to ABTS values was greater than to FRAP and DPPH values. Thus, ABTS assay may preferably be a better method to study the antioxidant power which is mainly caused by phenolic compounds, than FRAP and DPPH methods, in that order.

**Table 3.** Bivariate correlation results of three antioxidant capacity assays and total phenolic content from all extracts.

| Results | Correlation coefficient | Sign (2-tailed) |
|---|---|---|
| TPC | 1.000 | - |
| FRAP | 0.825 | < 0.01 |
| ABTS | 0.973 | < 0.01 |
| DPPH | 0.683 | < 0.01 |

## Conclusion

This work has shown that chilies (bird chilies and chili spur peppers) and holy basils (white and red) could be good sources of natural antioxidants in Thai foods. However, they should be used with care because of their hot and pungent flavours. Garlic and pumpkin may be lower in antioxidant power but it is possible to consume them in higher quantity, especially for pumpkin.

## Acknowledgements

This work was a part of a research project supported by a grant from Office of Agricultural Research and Extension, Maejo University, Thailand.

## References and Notes

1. S. R. Uhl, “Spices, seasonings, & flavorings”, Technomic Publishing Co., Lancaster, **2000.**
2. H. P. Koch and L. D. Lawson, “Garlic: the science and therapeutic application of Allium sativum L. and related species.” 2nd Edn., Williams & Wilkins, Baltimore, **1996.**
3. N. R. Farnsworth and N. Bunyapraphatsara, “Thai medicinal plants recommended for primary health care system”, Medicinal Plant Information Center, Bangkok, **1992**.
4. AOAC (Official method of analysis of AOAC international), 16th Edn, The Association of Analytical Chemists, Arlington, **1997**.
5. L. P. Leong and G. Shui, “An investigation of antioxidant capacity of fruits in Singapore markets”, *Food Chem***., 2002**, *76*, 69-75.
6. I. F. F. Benzie, and J. J. Strain, “Ferric reducing / antioxidative power assay: direct measure of total antioxidant activity of biological fluids and modified version of simultaneous measurement of antioxidant power and ascorbic acid concentration”, *Methods Enzymol.*, **1999**, *299*, 15-27.

*Mj. Int. J. Sci. Tech.*, **2007**, *01(02)*, 100-106

7. R. Re, N. Pellegrini, A. Rroteggente, A. Pannala, M. Yang, and C. Rice-Evans, "Antioxidant activity applying an improved ABTS radical cation decolorization assay", *Free Radical Bio. Med.*, **1999**, *26*, 1231-37.
8. W. Brand-William, M. Cuelier, and M. E. Berset, "Use of free radical method to evaluate antioxidant activity", *Lebensm. Wiss. U. Technol.*, **1995**, *28*, 25-30.
9. A. Waterhouse, "Folin-Ciocalteau micro method for total phenol in wine.", (no date), retrieved May 4, 2005, from http://waterhouse.ucdavis.edu/phenol/folinmicro.htm.
10. M. F. Wang, Y. Shao, J. G. Li, N. Q. Zhu, M. Rangarajan, E. J. LaVoie, and C. T. Ho, "Antioxidative phenolic compounds from Sage (*Salvia officinalis*)", *J. Agric. Food Chem.*, **1998**, *46*, 4869-73.
11. M. J. T. J. Arts, G. R. M. M. Haenen, H. P. Voss, and A. Bast, "Antioxidant capacity of reaction products limits the applicability of the Trolox equivalent antioxidant capacity (TEAC) assay", *Food Chem. Toxicol.*, **2004**, *42*, 45-49.
12. C. T. Ho, in "Phenolic compounds in food and their effects on health I: analysis, occurrence, & chemistry" (Eds. C. T. Ho, C. Y. Lee, and M. T. Huang), American Chemical Society, New York, **1992,** Ch. 1.
13. M. J. Amiot, A. Fleuriet, V. Cheynier, and J. Nicolas, in "Phytochemistry of fruits and vegetables" (Eds. F. A. Tomas-Barberan and R. J. Robins), Clarendon Press, Oxford, **1997**, Ch. 4.

*Mj. Int. J. Sci. Tech.*, **2007**, *01(02)*, 107-119

***Maejo International***

***Journal of Science and Technology***

**ISSN 1905-7873**

Available online at www.mijst.mju.ac.th

*Full Paper*

# Identification of *Aeromonas hydrophila* infection with specific monoclonal antibodies

**Siwaporn Longyant[1], Kriengkrai Prahkarnkaeo[2], Vithaya Meevoothisom[3], Sirirat Rengpipat[4], Sombat Rukpratanporn[5], Weerawan Sithigorngul[l], Parin Chaivisuthangkura[1], Paisarn Sithigorngul[1*]**

[1]Department of Biology, Faculty of Science, Srinakharinwirot University, Bangkok 10110, Thailand.
[2]Department of Veterinary Clinic Science, Faculty of Veterinary Science, Mahidol University, Nakhon Pathom 73170, Thailand.
[3]Department of Microbiology, Faculty of Science, Mahidol University, Bangkok 10400, Thailand.
[4]Department of Microbiology, Faculty of Science, Chulalongkorn University, Bangkok 10330, Thailand.
[5]Center of Excellence for Marine Biotechnology at Chulalongkorn University, National Center for Genetic Engineering and Biotechnology (BIOTEC), Bangkok 10330, Thailand.
E-mail: paisarn@swu.ac.th, paisarn_sithi@hotmail.com

* Author to whom correspondence should be addressed. (Apply M_address)

*Received: 21 July 2007 / Accepted: 14 August 2007 / Published: Published: 16 August 2007*

---

**Abstract:** Whole cell of Aeromonas hydrophila 1234 was used for immunization to produce monoclonal antibodies (MAbs). Three different groups of MAbs specific to Aeromonas were obtained. The first group of MAbs demonstrated high specificity and bound to the A. hydrophila 1234 only but did not bind to the other two A. hydrophila isolates. This group of MAbs bound to a series of lipo-polysaccharides (LPS) with molecular masses range from 10 to190 kDa. The second group of antibodies recognized *A. hydrophila* 1234 and 2798 isolates, and bound to a series of LPS with molecular masses range from 5-200 kDa. The third group of MAbs recognized all three isolates of *A. hydrophila* and two isolates of *A. sobria*, and lightly bound to *A. caviae*. This group of MAbs also bound to an unknown protein with molecular mass of 20 kDa. The MAbs in group 1 and group 2 can be used to detect the bacteria in tissues by immunohistochemistry. Both groups of MAbs bound to LPS at different sites in which the MAbs in group 2 bound to the side chain of O antigen while

*Mj. Int. J. Sci. Tech.,* **2007**, *01(02),* 107-119

the MAbs in group 1 bound to the polymerization site at the core of oligosaccharide. All of the MAbs can be used to identify *Aeromonas* by dot blotting with the sensitivity range from $10^3$-$10^4$ CFU/μl. This study demonstrated a convenient immunological tool that can be used for simple and accurate identification of *A. hydrophila*, as well as for diagnosis of the *A. hydrophila* infection in animals. This immunological tool can replace costly and laborious biochemical tests.

**Keywords:** *Aeromonas hydrophila*, dot blotting, immunohistochemistry, monoclonal antibody, lipopolysaccharide (LPS), Western blotting.

---

## Introduction

*Aeromonas hydrophila* , a Gram negative motile rod, a member of the family Vibrionaceae, has been widely studied and regarded as the most important bacteria for causing "aeromonosis, or hemorrhagic septicemia or motile aeromonas septicemia" in fish ]1,2,3] and other aquatic animals such as frog [4,5], prawn [6], crab [7] and mussel [8] (Maki et al., 1998). The pathological conditions include tail/fin rot and hemorrhagic septicemias in freshwater fish species and occasionally in marine fish [1,9]. The motile aeromonads has classically been divided into three biochemically different groups, namely *A. hydrophila*, *A. caviae* and *A. sobria*. These also contain at least 13 mesophilic genomospecies, and also a psychrophillic group of nonmotile *A. salmonicida* which causes disease among salmonids called "furunculosis" [10]. During the past decade the interest in *Aeromonas* spp. has gone beyond the boundaries of fish pathology due to the increasing reports of acute diarrhea in humans caused by *Aeromonas* spp. [11,12]. Up to date *A. hydrophila* has been well established as a food borne pathogen and has been isolated from both animal and plant food products [13].

Epidemiological investigation has been hampered by either the lack of rapid identification method, or taxonomic complexicities of various isolates. The conventional methods necessary to identify this pathogen are laborious, time consuming and uninventive. Recently immunoassays and molecular methods using DNA probes or PCR have been proven useful for direct detection of microorganisms present in clinical samples [2, 14]. However, most of the molecular methods for diagnosing the bacterial agents can only be effectively used by well-trained personnel and in a well-equipped setting. This limits their use in laboratories. Development of efficient (specific and sensitive), simple-to-use and rapid diagnostic methods, such as immunoassays based on monoclonal antibody (MAb) , are in general essential for detecting etiologic agents and various stages of the disease. Also, specific polyclonal antibody (PAb) against *A. hydrophila* can be used either for diagnosis [15-18, or for studying the role of flagella on bacterial invasion [19]. However, PAb could give a false positive result and an unspecific background of antigen-antibody reaction, especially in the characterization of epitopes of the target antigens. By contrast, MAb specific to *A. hydrophila* has been characterized against LPS of *A. hydrophila* type I isolates [20], and also another MAb against a 110 kDa protein of *A. hydrophila* with low cross reactivity to other *Aeromonas* spp. and various bacterial species [21]. In

*Mj. Int. J. Sci. Tech.,* **2007**, *01(02)*, 107-119

this study, we demonstrated a series of MAbs specific to *A. hydrophila* isolates and *Aeromonas* spp. in order to use them as a tool for immunodiagnosis of *Aeromonas* infection.

## Materials and Methods

### *Bacterial culture and antigen preparation*

*Aeromonas hydrophila* 1234 (AH1) isolated from carp's kidney was kindly provided by Veterinary Medical Aquatic Research Center (VMARC), Chulalongkorn University, Thailand. *A. hydrophila* 04082 (AH2) was obtained from Aquatic Animal Health Research Institute, Department of Fisheries Thailand. *A. hydrophila* 2798 (AH3) was obtained from Department of Medical Sciences, Ministry of Public Health, Thailand. Other sources of other bacteria used for cross-reactivity testing were indicated in Table 1. The bacteria were grown with agitation at 37$^{o}$C in a 250 ml flask containing tryptic soy broth (TSB; Merck) to log phase. The TSB supplemented with 2% (w/v) NaCl was used for *Vibrio parahaemolyticus*. The culture was harvested by centrifugation at 3,500 X *g* for 20 min at 4 $^{o}$C. Bacterial pellets were washed twice with sterile 0.15 M phosphate buffered saline (PBS) pH7.2, suspended in PBS, heat-killed at 60 $^{o}$C for 30 min, and finally adjusted to the O.D. of 1 at 600 nm (approximately $10^{9}$ CFU/ml). The bacterial suspension was divided into aliquots and stored at -70$^{o}$C until used.

Three preparations (heat-killed, denatured and formalin-fixed) of *A. hydrophila* 1234 (AH1) were used for immunization. The denatured antigen was prepared by mixing the bacteria with a treatment buffer containing an equal volume of 4% sodium dodecyl sulfate (SDS) and 10% mercaptoethanol, boiling for 1 min, and then dialyzing against an excess volume of PBS three times at 12 h interval. Formalin fixed antigen was prepared by mixing the bacteria with 20% formalin at a ratio of 1:1 (v/v) for 2 h and dialyzing as before.

### *Immunization*

The mixture of 3 preparations of *A. hydrophila* 1234 was prepared at a ratio 1:1:1. Four 6-week old female Swiss mice purchased from National Laboratory Animal Center, Mahidol University, were injected intraperitoneally with 50 μl of a prepared mixture ($10^{8}$ CFU/ml) of *A. hydrophila* 1234 mixed with an equal volume of complete Freund's adjuvant. They were subsequently injected 3 more times with the same inoculum mixed with incomplete Freund's adjuvant at two-week intervals. One week after the fourth injection, mouse antisera were collected by eyebleeding and preabsorbed with an excess number of *V. parahaemolyticus* cells for partial elimination of the antibodies that can recognize common epitopes of both *Vibrio* and *Aeromonas*. The antisera from four mice were tested against *A. hydrophila* 1234 by Western blotting. After the best performing mouse was identified, it was boosted with the same *A. hydrophila* preparation for 3 days before hybridoma production.

*Mj. Int. J. Sci. Tech.,* **2007**, *01(02)*, 107-119

**Table 1**. List of bacterial isolates and sources used in this study.

| **Bacteria** | **Sources** | **Remarks** |
|---|---|---|
| *Aeromonas hydrophila* 1234 | VMARC | Isolated form carp kidney |
| *A. hydrophila* 04082 | AAHRI | |
| *A. hydrophila* 2798 | DMST | Isolated from stool |
| *A. sobria* 12056 | NCIMB | |
| *A. sobria* 12446 | DMST | Isolated from stool |
| *A. caviae* 13016 | NCIMB | |
| *Plesiomonas shigelloides* | DMST | Isolated from rectal swab |
| *Vibrio alginolyticus* 22082 | DMST | Isolated from stool |
| *V. cholerae* Non O1 non O139 | SWU | Isolated from *Penaeus vannamei* |
| *V. fluvialis* 22085 | DMST | Isolated from stool |
| *V. harveyi* 639 | CENTEX | Isolated from *P. monodon* |
| *V. mimicus* 22088 | DMST | Isolated from food |
| *V. parahaemolyticus* 22091 | DMST | Isolated from stool |
| *V. vulnificus* | DABU | Isolated from sea bass |
| *Enterobacter cloacae* | DMSM | |
| *Escherichia coli* ATCC 25922 | CPF | |
| *Klebsiella pneumoniae* | DMSM | |
| *Morganella morganii* | DMSM | |
| *Proteus vulgaris* | DMSM | |
| *Pseudomonas auroginosa* | DMSM | |
| *Salmonella* Enteritidis 7108 | DMST | |
| *Salmonella* Typhi | DMSM | |
| *Salmonella* Typhimurium ATCC 1408 | CPF | |
| *Shigella flexneri* | DMSM | |

Notes:
AAHRI = Aquatic Animal Health Research Institute, Dept. of Fisheries, Ministry of Agriculture
CENTEX = Centex Shrimp, Faculty of Science, Mahidol University
CPF = Charoen Pokphand Foods Public Co. Ltd.
DABU = Dept.of Aquatic Science, Burapa University
DMSM = Dept. of Microbiology, Faculty of Science, Mahidol University
DMST = Dept. of Medical Science, Ministry of Public Health Thailand
NCIMB = National Collection of Industrial Marine and Food Bacteria, UK
SWU = Dept. of Biology, Srinakharinwirot University
VMARC = Veterinary Medical Aquatic Research Center, Chulalongkorn University

*Hybridoma production*

A cell fusion protocol used in this study was modified according to the methods developed by Köhler and Milestein [22] and Mosmann et al. [23]. A P3X myeloma cell line was used as the fusion partner. Fusion products from 1 mouse were plated on 30 microculture plates (96 wells/plate). After identification of the positive cultures by screening methods including dot blotting, Western blotting

*Mj. Int. J. Sci. Tech.,* **2007**, *01(02)*, 107-119

and immunohistochemistry as described below, the cells were cloned by the limiting dilution method, and stored in liquid nitrogen.

*Dot-blotting*

Heat-killed *A. hydrophila* and other bacterial preparations containing approximately $10^8$ CFU/ml of various bacteria were used for screening. Bacterial samples (1 µl/spot) were spotted onto nitrocellulose membrane, baked at 60$^o$C for 10 min, and incubated in each conditioned medium from hybridoma culture at 1:200 dilution in 5% Blotto (5% nonfat drymilk, 0.1% Triton X-100 in PBS) for 5 h. After extensive washing in 0.5% Blotto, the membrane was incubated in horseradish peroxidase labeled with goat anti-mouse gamma immunoglobulin heavy and light-chain specific antibody (GAM-HRP, Bio-Rad) at 1:1500 dilution for 3 h. The membrane was then washed as before in Blotto and incubated for 5 min in substrate mixture containing 0.03% diaminobenzidine (DAB), 0.006% hydrogen peroxide, and 0.05% cobalt chloride in PBS [24]. Hybridoma cultures that displayed immunoreactivity against *A. hydrophila* were confirmed for bacterial specificity by Western blotting and immunohistochemistry before cloning and cryopreservation for further investigation.

*SDS-PAGE and Western blotting analysis*

Heat-killed *A. hydrophila* and other bacterial preparations were separated by 15% sodium dodecyl sulfate – polyacrylamide gel electrophoresis (SDS-PAGE) according to the method described by Laemmli [25]. Samples were electrophoresed for 6 h at 30 V and gels were stained with Coomassie Brilliant Blue R-250. For Western blotting, samples resolved by SDS-PAGE were electro-blotted onto nitrocellulose membrane using Transblot apparatus (Bio-Rad). The nitrocellulose membrane was incubated in 5% Blotto for 10 min, treated with 1:200 hybridoma conditioned medium for 5 h, and then performed as described above in the dot blotting section. Low molecular weight markers (Bio-Rad) were used as a standard.

*Immunohistochemistry*

Ten Nile tilapia, *Oreochromis niloticus,* 1-2 g weight (purchased from Jatujak fish market, Bangkok) was artificially infected with *A. hydrophila* 1234 (50 µl of $10^7$ CFU/ml) by intraperitoneal injection. When the fish exhibited pathogenic symptoms such as external ulcer, lethargy and swollen abdomen, they were killed in the cold water and fixed in Davidson fixative for 24 h and processed for paraffin sectioning.

Serial sections (8 µm thickness) were prepared and processed for indirect immunoperoxidase staining using various MAbs and GAM-HRP diluted 1:1000 with 10% calf serum in PBS. Peroxidase activity was revealed by incubation with 0.03% DAB and 0.006% hydrogen peroxide in PBS. Preparations were counter-stained with haematoxylin and eosin Y (H&E), dehydrated in graded

ethanol series, cleared in xylene and mounted in permount [24]. Positive immunoreactivity was visualized as brown coloration against the pink and purple colors of H&E.

*Class and subclass determination.*

Class and subclass of mouse immunoglobulins produced by the hybridomas were determined by sandwich ELISA using Zymed's Mouse MonoAb ID Kit (HRP).

*Sensitivity of MAb for detection of A. hydrophila determined by dot-blotting.*

Ten-fold serial dilution of *A. hydrophila* (begining with $10^8$CFU/ml) in PBS was performed and 1 µl of each dilution was spotted onto a nitrocellulose membrane before fixing in 10% formalin for 10 min and processing for dot blotting using various MAbs as described above. The lowest bacterial dilution that showed distinct and clear immunoreactivity was determined.

.

**Results and Discussion**

After the fourth immunization, the antisera from four mice at dilution of 1:20,000 were preabsorbed with the lysate of *Vibrio parahaemolyticus* before determination of the specificity by Western blotting. All antisera demonstrated a series of numerous bands without cross-reactivity to *V. parahaemolyticus* and *Escherichia coli*. The serum from mouse number 2 demonstrated the strongest immunoreactivity, therefore, it was used as spleen donor for hybridoma production.

From one fusion, the cell mixture were laid in 30 microculture plates and about half (1500 wells) contained hybridoma colonies from which approximately 200 wells gave positive reaction in the first screening by dot blotting against *A. hydrophila* 1234. After the second screening by Western blotting, antibody-producing clones with strong positive immunoreactivity and high specificity and some limited cross-reactivity to related bacteria were selected and recloned. Only 10 hybridoma clones were selected, cloned and established as high stability cell lines which can be divided into 3 groups according to their specificities (Table 2, Fig.1, 2, 3).

MAbs in group 1 consisted of 4 MAbs (AH32, 63, 66, 76) and all of them were IgG1. These MAbs bound to only one isolate of the *A. hydrophila* (1234) and did not show any cross-reactivity to the other two isolates of *A. hydrophila* (04082 and 2798) and other bacterial species (Fig.1A). The MAbs bound to a series of lipopolysaccharides (LPS) ranging from 10 to 200 kDa with increasing step of 5 kDa (Fig.2B). These MAbs can be used to detect *A. hydrophila* infection in the infected Nile tilapia by immunohistochemistry (Fig 3).

*Mj. Int. J. Sci. Tech.,* **2007**, *01(02),* 107-119

**Table 2.** Specificity of monoclonal antibodies

| Group | MAb (isotype) | Sensitivity Dot Blotting (CFU/ml) | Antigen Western blotting (kDa) | IHC | Bacterial immunoreactivity (Dot blotting) |
|---|---|---|---|---|---|
| 1 | AH 32,63, 66, 76 (G1) | $10^6$ | 10-200 | +++ | AH1(+++) |
| 2 | AH 29 (G2a), 59 (G2b) | $10^6$ | 5-200 | +++ | AH1, AH3 (+++) |
| 3 | AH 17, 53 (G1), 56, 65 (G2b) | $10^7$ | 20 | - | AH1, AH2, AH3, AS1, AS2 (+++) AC (+) |

Notes: The binding of antibodies to various bacteria was determined by dot blotting using bacteria at approximately $10^8$ CFU/ml: AH1 = *A. hydrophila* 1234, AH2 = *A. hydrophila* 04082, *A. hydrophila* 2798, AS1 = *A. sobria* 12056, AS2 = *A. sobria* 12446, AC = *A. caviae*13016. The intensity of staining was arbitrarily scored as +++ = very intense staining, + = light staining, ± very light staining - = not staining. IHC = immunohistochemistry

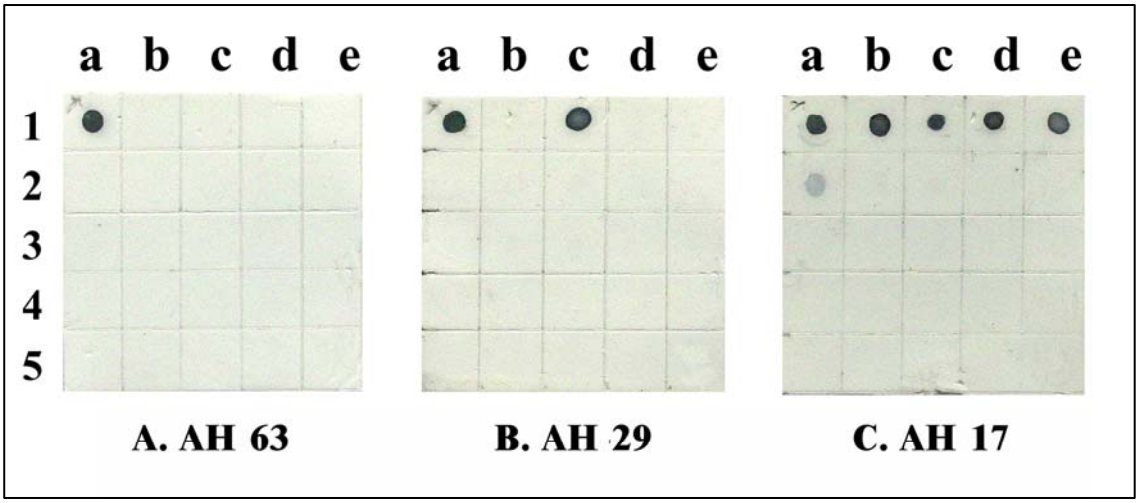


**Figure 1.** Cross-reactivity of MAbs assayed by dot blotting.
Heat killed bacteria ($10^9$ CFU/ml) were spotted on nitrocellulose membrane (1µl/spot) and treated with various MAbs: (A) AH63, (B) AH29, (C) AH17 (only one of representative for each group was demonstrated).
Row 1. a. *A. hydrophila* 1234, b. *A. hydrophila* 04082, c. *A. hydrophila* 2798, d. *A. sobria* 12446, e. *A. sobria* 12056.
Row 2. a. *A. caviae* 13016, b. *Vibrio penaeicida*, c. *V. vulnificus*, d. *V. parahaemolyticus*, e. *V. mimicus*.
Row 3. a. *V. harveyi*, b. *V. fluvialis*, c. *V. cholerae*, d. *V. alginolyticus*, e. *Pseudomonas auroginosa.*
Row 4. a. *Klebsiella pneumoniae*, b. *Proteus vulgaris*, c. *Plesiomonas shigelloides*, d. *Escherichia coli*, e. *Salmonella* Typhi.
Row 5. a. *Shigella flexneri*, b. *Morganella morganii*, c. *Enterobacter cloacae*, d. *Salmonella* Enteriditis, e. *Salmonella* Typhimurium.

*Mj. Int. J. Sci. Tech.,* **2007**, *01(02)*, 107-119

MAbs in group 2 consisted of two MAbs (AH29 and AH59) having two different subclasses (IgG2a and IgG2b). They bound to *A. hydrophila* (1234 and 2798 isolates) but did not bind to *A. hydrophila* 04082 and other bacterial species (Fig.1B). The antibodies recognized a series of LPS ranging from 5 to 200 kDa with increasing step of 5 kDa (Fig.2C). This evidence suggested that the MAbs in the second group bound to epitope at the side chain of O antigen of LPS while the antibodies in the first group bound to the epitope at the core oligosaccharide on polymerization site of LPS. The antibodies in the second group also recognized the bacteria in the infected tissues similar to that of the MAbs in the first group (Fig.3-3).

MAbs in group 3 consisted of four MAbs: AH17, 53 (IgG1), 56, 65 (IgG2b). The MAbs recognized all three isolates of *A. hydrophila* and demonstrated cross-reactivity to two isolates of *A. sobria*, and one isolate of *A. caviae* (Fig. 1C). However, the immunoreactivity against *A. caviae* was weaker than the immunoreactivity to *A. hydrophila* and *A. sobria*. (Fig. 1C). These antibodies did not recognize the bacteria in the tissues by immunohistochemistry. Nevertheless, these MAbs demonstrated broad specificity against all *Aeromonas* spp. tested, the range of specificity being narrower than that of previously reported MAbs. The MAbCX9/15 was generated against *E. coli* and recognized all members of bacteria in the family *Enterobacteriaceae* with exception of *Erwinia chrysanthemi* [26]. Therefore, the third group of antibodies can be generally used for identification *Aeromonas* spp. In order to improve the sensitivity to all three *Aeromonas* spp. the additional MAb specific to *A. caviae* is required.

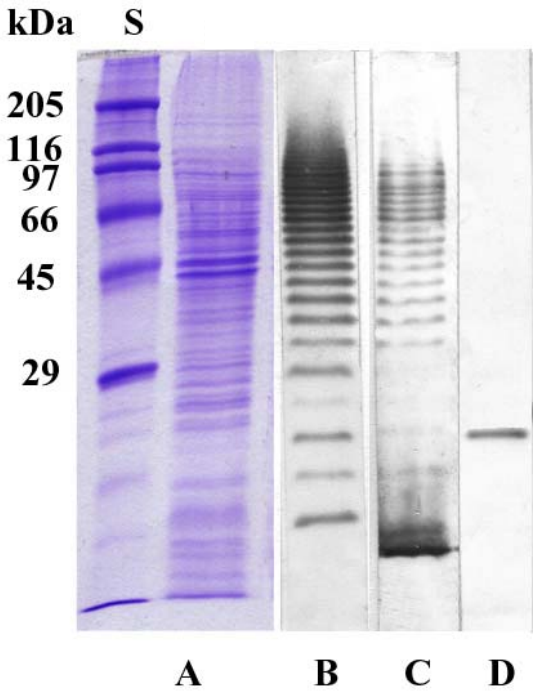


**Figure 2.** SDS-PAGE and Western blotting analysis.
Heat-killed *A. hydrophila* homogenate was separated by SDS-PAGE and (A) stained with Coomassie Blue. Proteins in another part of the gel was transferred to nitrocellulose membrane and treated with MAbs from each group, (B) AH63, (C) AH29, (D) AH17. S = standard marker proteins.

*Mj. Int. J. Sci. Tech.*, **2007**, *01(02)*, 107-119

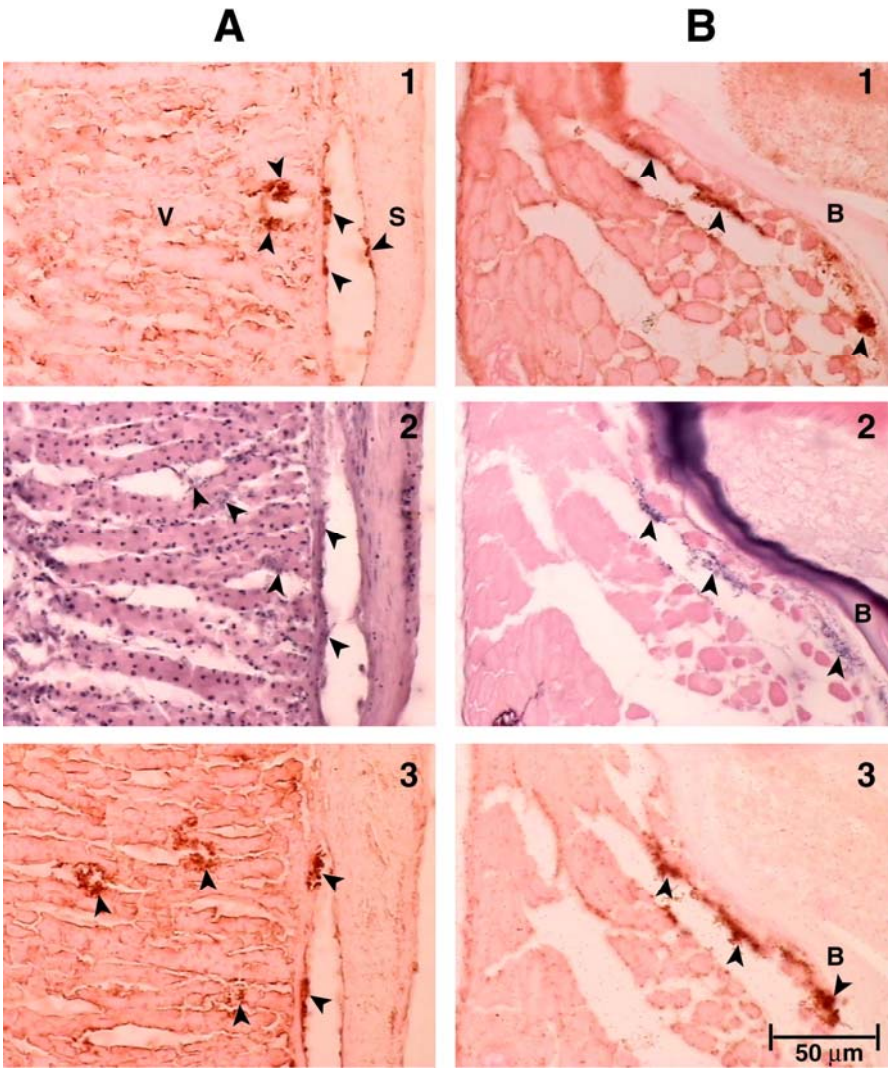


**Figure 3**. Immunohistochemistry.

Indirect immunoperoxidase staining of (A) intestine, and (B) skeleton muscle from experimentally infected Nile tilapia *Oreochromis niloticus* using Mabs; (1) AH63, and (3) AH29 then counterstained with eosin Y, or (2) staining with H & E without first antibody treatment. Arrow heads indicate the areas with heavy infection which were hardly observed with regular staining. B = rib bone, S = smooth muscle, V = villi.

The sensitivity testing for detection of *A. hydrophila* with dot blot assay were ranged from $10^6$ to $10^7$ CFU/ml depending on the group of MAbs (Table 2). Since the volume of dot blot assay was small (1 µl), the development of other types of enzyme immuno-assay such as sandwich ELISA would improve the sensitivity as the sample volume was increased by over a hundred fold. Pre-enrichment of the sample in TSB for 6 h before performing dot blotting would increase the detection sensitivity up to 1-10 CFU/ml. The *A. hydrophila* specific antibodies (group 1 and 2) can be used for detection of *A.*

*Mj. Int. J. Sci. Tech.,* **2007**, *01(02),* 107-119

*hydrophila* in the tissues of infected fish by means of immunohistochemistry. The immunoreactivity appeared at the surface of bacteria and soluble components in the intercellular space of various tissues (Fig.3). The detection of bacterial infection can be observed even in the area with light infection containing only a few bacterial cells or fragments which could not be observed with regular haematoxylin and eosin staining (Fig. 3B). The reason for the third group of antibodies that could not recognize the bacteria in the tissues may be due to the fact that the antibodies were specific to intracellular components. Therefore, after tissue fixation the high density of cell wall may prevent the accessibility of antibody into the cell.

The MAbs in the first group were highly specific to *A. hydrophila* 1234 without any cross-reactivity to the other two isolates of *A. hydrophila*. This evidence indicated the uniqueness among the heterogeneity of *A. hydrophila* in which different serotypes usually contain a unique epitope for each serotype.

The MAb specific to the common epitopes among the three *A. hydrophila* isolates was not obtained in this study. This evidence suggested that all three isolates of *A. hydrophila* used in this experiment were immunologically different. Previous report showed that MAb 5F3 recognized a protein of 110 kDa and could react with all 12 isolates of *A. hydrophila* from different sources including human stool, human wound and cold blood animals with very light reaction against *A. sobria*. [21]. The production of MAbs specific to various isolates of *A. hydrophila* is required in order to obtain MAbs that can react to most of the *A. hydrophila* isolates.

The antigen recognized by MAbs group 1 and 2 is expected to be a lipopolysaccharide (LPS) as described previously [20]. However, the difference in the lowest band of antigen recognized by group 1 and group 2 antibodies indicated that the epitope recognized by MAbs in group 2 may be on the O antigen with highly repetitive carbohydrate side chains of LPS monomer, while the epitope recognized by MAbs in group 1 may be on the polymerization site at the core of oligosaccharide. Therefore, the antibodies in group 1 could not recognize the smallest monomer of 5 kDa band. A MAb specific to LPS of *A. hydrophila* (F26P5C8) from previous report recognized many virulent and avirulent isolates of *A. hydrophila* isolated from diseased and healthy fish from Malaysia and Philippines. However, this antibody recognized only some isolates from diseased fish from Japan [20]. This evidence indicated that there are heterogeneity among *A. hydrophila* LPS recognized by the MAb. An experiment on production of rabbit antisera against various serotypes of motile *Aeromonas* revealed that various species of *Aeromonas* are different not only in LPS components but also in extracellular products among various serotypes and in the member of the same serotype as well [27]. Similar report on production of MAb against LPS of *A. salmonicida* demonstrated that three MAbs against core-oligosaccharide recognized all 10 typical isolates, 5 atypical isolates of *A. salmonicida,* and cross-reacted to two isolates of *A. hydrophila,* while three other MAbs recognized only *A. salmonicida* [28]. This evidence indicated that specific and common epitopes on LPS are present among various *Aeromonas* spp. and possibly can be recognized by the antibody. In our case, MAbs specific to *A. hydrophila* 1234 were generated; therefore, more production of monoclonal antibodies against different isolates of *A. hydrophila* is needed in order to provide immunological tools for identification of various isolates of *A. hydrophila*.

*Mj. Int. J. Sci. Tech.,* **2007**, *01(02)*, 107-119

## Conclusion

This study demonstrated that MAbs can be used for simple and accurate identification of *Aeromonas* spp. and some pathogenic isolates of *A. hydrophila* by dot blotting and immunohistochemistry. This immunological tool can replace costly and laborious biochemical tests and molecular identification. However, production of more MAbs specific to other isolates of *A. hydrophila* is required.

## Acknowledgements

This work was supported by the National Center for Genetic Engineering and Biotechnology (BIOTEC) Thailand. The authors are also indebted to all institutes in Table 1 for providing bacterial species for cross-reaction testing of the antibodies.

## References

1. S. L. Angka, T. J. Lam, and Y. M. Sin, "Some virulence characteristics of *Aeromonas hydrophila* in walking catfish (*Clarias gariepinus*)", *Aquaculture,* **1995**, *130*, 103-112.
2. Y. L. Zhang, C. T. Ong, and K. Y. Leung, "Molecular analysis of genetic differences between virulent and avirulent strains of *Aeromonas hydrophila* isolated from diseased fish", *Microbiol.*, **2000**, *146*, 999-1009.
3. M. H. Rhaman, S. Suzuki, and K. Kawai, "The effect of temperature on *Aeromonas hydrophila* infection in goldfish, *Carassius auratus*", *J. Appl. Ichthyol.*, **2001,** *17*, 282-285.
4. D. W. Hird, S. L. Diesch, R. G. McKinnell, E. Gorham, F. B. Martin, C. A. Meadows, and M. Gasiorowsky, "*Enterobacteriaceae* and *Aeromonas hydrophila* in Minnesota frogs and tadpoles (*Rana pipiens*)", *Appl. Environmental Microbiol*., **1983,** *46*, 1423-1425.
5. G. Huys, M. Pearson, P. Kampfer, R. Denys, M. Cnockaert, V. Inglis, and J. Swings, "*Aeromonas hydrophila* subsp. *ranae* subsp. Nov., isolated from septicaemic farmed frogs in Thailand", *International J. Systematic and Evolutionary Microbiol.*, **2003**, *53*, 855-891.
6. G. Vivekanandhan, K. Savithamani, A. A. M. Hatha, and P. Lakshmanaperumalsamy, "Antibiotic resistance of *Aeromonas hydrophila* isolated from market fish and prawn of South India", *International J. Food Microbiol*., **2002**, *76*, 165-168.
7. M. E. Nielsen, L. Hϕi, A. S. Schmidt, D. Qian, T. Shimada, J. Y. Shen, and J. L. Larsen, "Is *Aeromonas hydrophila* the dominant motile Aeromanas species that causes disease outbreaks in aquaculture production in the Zhejiang province of China?", *Dis. Aquat. Org*., **2001**, *46*, 23-29.
8. J. S. Maki, G. Patel, and R. Mitchell, "Experimental pathogenicity of *Aeromonas* spp. for the zebra mussel, *Dreissena polymorpha*", *Current Microbiol.*, **1998**, *36*, 19-23.

9. T. Kuge, K. Takahashi, I. Barcs, and F. Hayashi, "*Aeromonas hydrophila*, a causative agent of mass mortality in cultured Japanese catfish larvae (*Silurus asotus*)", *Gyobyo Kenkyu*. **1992**, *27*, 57-62.
10. S. L. Abbott, W. K. W. Cheung, and J. M. Janda, "The genus *Aeromonas*: Biochemical characteristics, atypical reactions, and phenotypic identification schemes", *J. Clin. Microbiol*, **2003**, *41*, 2348-2357.
11. A. K. Chopra and C. W. Houston, "Enterotoxins in Aeromonas-associated gastroenteritis. *Microbes and Infection*" **1999,** *1*, 1129-1137.
12. C. J. Gonzalez-Serrano, J. A. Santos, M. L. Garcia-Lopez, and A. Otero, "Virulence markers in *Aeromonas hydrophila* and *Aeromonas veronii* biovar sobria isolates from freshwater fish and from a diarrhoea case", *J. Appl. Microbiol.*, **2002**, *93*, 414-419.
13. H. Daskalov, "The importance of *Aeromonas hydrophila* in food safety", *Food Control*, **2006**, *17*, 474-483.
14. H. J. Oakey, L. F. Gibson, and A. M. George, "DNA probes specific for *Aeromonas hydrophila* (HG1)" *J. Appl. Microbiol*., **1999,** *86*, 187-193.
15. R. M. Sendra, C. Esteve, and E. Alcaide, "Enzyme-linked immunosorbent assay for detection of *Aeromonas hydrophila* serogroup O:19", *FEMS Microbiol. Lett.,* **1997,** *157*, 123-129.
16. S. Korbsrisate, S. Dumnin., R. Chawengkirttikul, V. Gherunpong, B. Eampokalap, C. Gongviseisoog, K. Janyapoon, K. Lertpocasombat, and T. Shimada, "Distribution of *Aeromonas hydrophila* serogroups in different clinical samples and the development of polyclonal antibodies for rapid identification of the genus *Aeromonas* by direct agglutination", *Microbial Immunol*., **2002,** *46*, 875-879.
17. S. V. Allavandi, and S. Ananthan, "Biochemical characteristics, serogroups, and virulence factors of *Aeromonas* species isolated from cases of diarrhea and domestic water samples in Chennai", *Indian J. Med. Microbiol*., **2003**, *21*, 233-238.
18. P. Swain, S. K. Nayak, A. Sahu, P. K. Meher, and B. K. Mishra, "High antigenic cross-reaction among the bacterial species responsible for diseases of cultured freshwater fishes and strategies to overcome it for specific serodiagnosis", *Comp. Immunol. Microbiol*., **2003**, *26*, 199-211.
19. S. Merino, X. Rubires, A. Aguilar, and J. M. Tomas, "The role of flagella and motility in the adherence and invasion to fish cell lines by *Aeromonas hydrophila* serogroup O:34 strains", *FEMS Microbiol. Lett.,* **1997**, *151*, 213-217.
20. G. A. Cartwright, D. Chen, P. J. Hanna, N. Gudkovs, and K. Tajima, "Immunodiagnosis of virulent strains of *Aeromonas hydrophila* associated with epizootic ulcerative syndrome (EUS) using monoclonal antibody", *J. Fish Disease,* **1994**,*17*, 123-133.
21. A. P. L. Delamare, S. Echeverrigaray, K. R. Duarte, L. H. Gomes, and S. O. P. Costa, "Production of a monoclonal antibody against *Aeromonas hydrophila* and its application to bacterial identification", *J. Appl. Microbiol.*, **2002**, *92*, 936-940.
22. G. Köhler and C. Milestein, "Derivation of specific antibody producing tissue culture and tumor lines cell fusion", *Eur. J. Immunol.,* **1976,** *6*, 511-519.

23. T. R. Mosmann, R. Baumal, and A. R. Williamson, "Mutations affecting immunoglobulin light chain secretion by myeloma cells I: Functional analysis by cell fusion", *Eur. J. Immunol.*, **1979**, *9*, 511-516.
24. W. Sithigorngul, S. Rengpipat, A. Tansirisittikul, S. Rukpratarnporn, S. Longyant, P. Chaivisuthangkura, and P. Sithigorngul, "Development of monoclonal antibodies for simple identification of *Vibrio alginolyticus*", *Lett. Appl. Microbiol.*, **2006,** *43*, 436-442.
25. U. K. Laemmli, "Cleavage of structural proteins during the assembly of the head of bacteriophage T4", *Nature,* **1970**, *227*, 680-685.
26. S. Lavasseur, M. O. Hussoan, R. Leitz, F. Merine, F. Laurent, F. Peladan, J. L. Drocourt, H. Leclerc, and M. Van Hoegaergen, "Rapid detection of members of the family Enterobaceae by a monoclonal antibody", *Appl. Environ. Microbiol.*, **1992**, *58*, 1524-1529.
27. Y. Santos, I. Bandin, and A. E. Toranzo, "Immunological analysis of extracellular products and cell surface components of motile *Aeromonas* isolated from fish", *J. Appl. Bacteriol.*, **1996,** *81*, 585-593.
28. D. Hädge, I. Lachmann, U. Wagner, and K. Drössler, "Characterization of core-oligosaccharide-specific monoclonal antibodies against *Aeromonas salmonicida* LPS binding to typical and atypical *Aeromonas salmonicida* isolates", *Aquaculture,* **1997**, *157*, 157-171.

*Mj. Int. J. Sci. Tech.*, **2007**, *01(02)*, 120-136

***Maejo International Journal of Science and Technology***

**ISSN 1905-7873**

Available online at www.mijst.mju.ac.th

*Review Article*

# An overview of aerosol particle sensors for size distribution measurement

**Panich Intra [1,*] and Nakorn Tippayawong [2]**

[1*] Energy Research Center, Maejo University, Chiang Mai 50290, Thailand,
E-mail: panich_intra@yahoo.com

[2] Department of Mechanical Engineering, Faculty of Engineering, Chiang Mai University, Chiang Mai 50200, Thailand

* Author to whom correspondence should be addressed.

*Received: 15 June 2007 / Accepted: 4 August 2007 / Published: 18 August 2007*

**Abstract:** Fine aerosols are generally referred to airborne particles of diameter in submicron or nanometer size range. Measurement capabilities are required to gain understanding of these particle dynamics. One of the most important physical and chemical parameters is the particle size distribution. The aim of this article is to give an overview of recent development of already existing sensors for particle size distribution measurement based on electrical mobility determination. Available instruments for particle size measurement include a scanning mobility particle sizer (SMPS), an electrical aerosol spectrometer (EAS), an engine exhaust particle sizer (EEPS), a bipolar charge aerosol classifier (BCAC), a fast aerosol spectrometer (FAS) a differential mobility spectrometer (DMS), and a CMU electrical mobility spectrometer (EMS). The operating principles, as well as detailed physical characteristics of these instruments and their main components consisting of a particle charger, a mobility classifier, and a signal detector, are described. Typical measurements of aerosol from various sources by these instruments compared with an electrical low pressure impactor (ELPI) are also presented.

**Keywords:** aerosol, electrical mobility, nanoparticles, size distribution, spectrometer

*Mj. Int. J. Sci. Tech.,* **2007**, *01(02)*, 120-136

**Introduction**

A recent particulate air pollution episode has affected Chiang Mai adversely. Aerosol is one of the most important environmental topics and particulate air pollution has become a major national concern. Emissions to air arise from human activities and natural processes. Anthropogenic emissions occur during extraction, distribution and combustion of fossil fuels from various industrial processes, from waste treatment and disposal, from agriculture, and from a range of consumer products. High fine particle concentrations in Chiang Mai were identified to be associated with a number of open fires observed during the months from February to April. Additionally, automotive vehicles have long been recognized as a major source of particulate air pollution. Emissions from road transport are growing steadily in line with increasing traffic. Any solid or liquid material suspended in air with diameter in the range of 1 nm to 100 μm can be considered as particulate matter [1]. It is a complex mixture of liquid and solid particles that exist in dynamic equilibrium with gaseous components in surrounding air and can be classified into two categories, viz. primary (directly emitted to the atmosphere) and secondary (formed at a later stage with atmospheric reactions) particles. The aerosol undergoes a number of complex reactions, affecting both the physical and chemical characteristics of ambient particulate matter. These particles have significant effects on the human health, Earth's climate, air quality and processes in various industries such as food, pharmaceutical and medical, electronic and semiconductor industries. Important physical properties of airborne particles are size, number, surface area, density and shape. Knowledge of these properties of aerosols is of great practical importance in aerosol science, air pollution, process control industry and epidemiological studies among others. In air pollution studies, photochemical reactions in the atmosphere often begin with nanometer-sized particles. In nucleation and condensation processes which are the basic of many technological applications, nanometer particles serve as the incipient nuclei for many processes. In the electronic and semiconductor industry, the contamination control of nanometer-sized particles is needed to prevent the formation and deposition of these particles on semiconductor devices during fabrication, because the size of the next generation 1-gigabit DRAM devices will have a minimum feature size smaller than 180 nm [2]. Using the common 1/3 or 1/5 rule for micro-contamination control, particles as small as 35 nm need to be measured and controlled. In industrial hygiene and epidemiological studies, the health consequences of these particulates depend on their ability to penetrate and deposit in the respiratory system. Particles with size larger than 10 μm are screened out quite easily at the upper inhalation system. For particles in the size range between 1 to 10 μm, they can penetrate the alveoli and bypass the upper respiratory tract. These particles are small enough to allow deposition at places where they can do the most damage. Particles with a diameter of less than 1 μm can penetrate deep into the respiratory system in the human lungs and are difficult to remove by lung clearance mechanisms, and for this reason they are considered to be the most dangerous. There is therefore a need to develop efficient respirators for protecting workers exposed to environments containing nanometer sized particles. Measurement and characterization of these particles is also needed in order to better understand and control them. A particle size instrument is one of the valuable tools for these applications.

There are several common instruments using various methods of measuring particle sizes. The techniques include diffusion method, inertial impaction method, light scattering method, electron microscopy method and aerodynamic method. However, they can only be used to measure super-

micrometer sized particles or are painstakingly difficult and slow to obtain results for sub-micrometer or nanometer-sized particles. The most efficient and widely used technique for measuring these submicron particles is essentially an electrical mobility determination method. Electrical mobility method was initially developed to measure ions in gases [3, 4] and in the atmosphere [5, 6]. Rohmann [7] later investigated and employed the method to measure atmospheric airborne particles. There have been numerous studies and developments on the electrical aerosol measurement in the past several decades. Among the first studies were carried out by Whitby and Clake [8], Tammet et al. [9], Knutson and Whitby [10] and Liu and Pui [11] over a few decades ago. An electrical aerosol analyzer and a differential mobility analyzer (DMA), capable of guaging the diameter to 10 nm - 1 μm were developed and later improved and refined by a number of researchers such as Kousaka et al. [12], Lehtimaki [13, 14], Stolzenburg [15] and Winklmayr et al. [16]. Chen et al. [17] employed the numerical method to improve DMA design. The results were in good agreement with experimental data [18 - 20]. Seto et al. [21] studied the performance of DMA under low pressure conditions to measure nanometer-sized particles in the size range between 4 - 10 nm. New developments were constantly tested and compared to assess their performance and to expand the measurement range [22-26]. Kulon et al. [27 - 29] described similar development concerning a bipolar charge aerosol classifier (BCAC). It uses electrostatic technique and is capable of simultaneously measuring particle charge as well as size. With respect to recent development on a similar instrument, Tammet et al. [30 - 31] designed and developed an electrical aerosol spectrometer (EAS) which can classify particles in a similar fashion to, but faster than a typical DMA due to its multi-channel measurement capability. In his PhD work, Graskow [32] developed a fast aerosol spectrometer (FAS) to measure nanometer-sized particles. His FAS prototype has better time response than the EAS. Reavell et al. [33 -35] and Biskos [36 - 41] reported a further development of a differential mobility spectrometer (DMS), derived from Graskow's concept. Based on similar principle to previously mentioned instruments, Intra and Tippayawong [42 - 46] designed, built and tested a multi-channel electrical mobility sensor for aerosol size distribution measurement. Although these instruments are all designed to measure airborne particle size distribution using the same principles, they are also different in terms of specific applications, construction, cost, measurement range, as well as time response and resolution.

In this paper, an overview of the state-of-the-art electrical mobility sizers for nanoparticle size measurement is described. Some of these instruments are commercially available and others are still laboratory prototypes. A detailed description of the operating principle of these instruments as well as main components, including the particle charger, the mobility classifier, and the signal detector are presented. Typical measurements of aerosol from various sources are also shown.

## Electrical Mobility Operating Principle

This section describes the operating principles of the particle sizer based on the electrical mobility technique. The basic principle of the electrical mobility technique is shown in Figure 1. This instrument consists of the corona charger, the mobility classifier, and the particle detector. Particle charging is accomplished by exposing aerosol sample to the cloud of unipolar corona ions inside the particle charger, and then charged via ion-particle collisions. The charged aerosol passes into the electrical mobility classifier, configured as coaxially cylindrical electrodes. A DC high voltage ranging

*Mj. Int. J. Sci. Tech.*, **2007**, *01(02)*, 120-136

from 1 to 5 kV is applied to the inner electrode. There are two separate streams: aerosol and sheath air flow. The charged aerosols enter the analyzer column. An electric field formed between the electrodes makes the particles deflect radially outward, and particles having specific mobility are collected on electrically-isolated electrometer rings, positioned at the inner surface of the outer electrode. Electrometers connected to these electrode rings measure currents corresponding to the number concentration of particles of a given mobility which is related to the particle size. Signal currents are

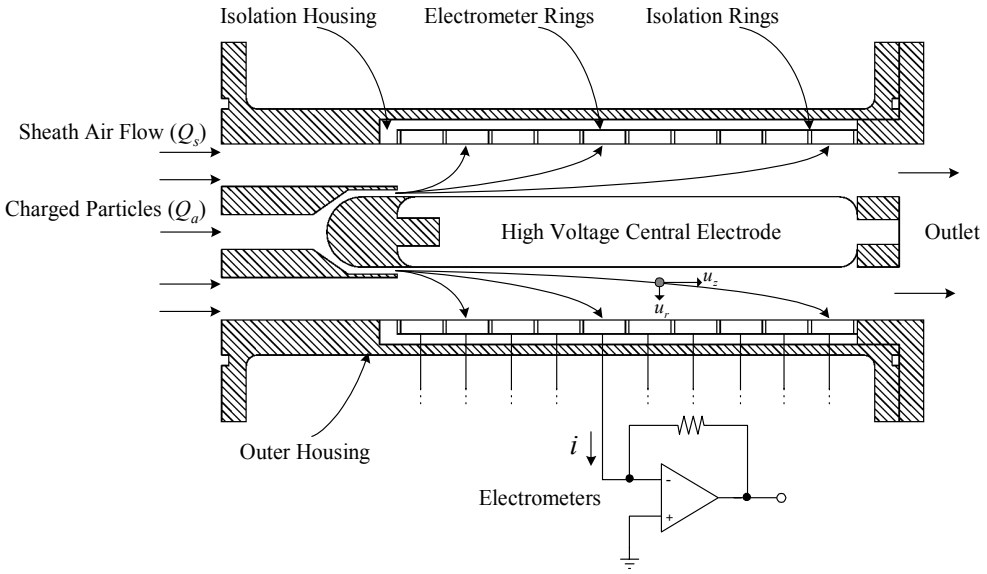


Figure 1. Basic principle of the electrical mobility technique [43].

then recorded and processed by a data acquisition system. The particle mobility diameter deposited on each electrometer ring can be calculated by the following expression [45]:

$$d_{p,i} = \frac{2VL_i n_p e C_c}{3\mu Q_t \ln\left(r_2/r_1\right)} \tag{1}$$

where $V$ is the central rod voltage, $L_i$ is the axial position between the aerosol entry location and the midpoint of the electrometer ring, $n_p$ is the net number of charges per particle, $e$ is the elementary charge on an electron, $C_c$ is the Cunningham slip correction factor, $\mu$ is the air viscosity, $Q_t$ is the total flow rate through the classifier column (sum of aerosol flow, $Q_a$ and sheath air flow, $Q_s$), $r_1$ is the central rod electrode radius, and $r_2$ is the outer electrode radius. The electric signal current from deposited charged particles on each electrometer ring along the inner surface of the outer electrode of the classifier column corresponds to the total number concentration of particles. The aerosol number concentration, $N_{p,i}$, of particles in relation to the signal current, $I_i$, at each electrometer ring is given by

$$N_{p,i} = \frac{I_i}{n_p(d_p)eQ_a} \tag{2}$$

where $n_p(d_p)$ is the average number of elementary charges carried by particles with diameter $d_p$ and is given by following equation [44]:

*Mj. Int. J. Sci. Tech.*, **2007**, *01(02)*, 120-136

$$n_p(d_p) = \frac{d_p kT}{2K_E e^2} \ln\left(1 + \frac{\pi K_E d_p \bar{c}_i e^2 N_i t}{2kT}\right) \tag{3}$$

where $\bar{c}_i$ is the mean thermal speed of the ions (240 m/s), $k$ is the Boltzmann's constant ($1.380658 \times 10^{-23}$ J/K, for air), $T$ is the temperature, $K_E$ is the constant of proportionality, $N_i$ is the ion concentration, and $t$ is the residence time of the charger. For the corona-wire charger [44], an approximate expression for the $N_i t$ product can be derived:

$$N_i t(r) = \frac{(r_{2c}^2 - r_{1c}^2) I_c}{2rZ_i e E_c(r) Q_c} \tag{4}$$

where $r_{1c}$ and $r_{2c}$ are the radial position of the outer and inner charger cylinder, respectively, $I_c$ is the charging current, $Z_i$ is the mobility of ion (equal to 0.00014 $m^2$/V.s for the positive ion), $E_c(r)$ is the charging electric field as a function of radial position, and $Q_c$ is the total flow rate through the charger. To obtain size distribution, the geometric midpoint diameter $d_{p,i}^{\text{mid}}$ is calculated as [44]:

$$d_{p,i}^{\text{mid}} = \sqrt{d_{p,i}^{\text{min}} \times d_{p,i}^{\text{max}}} \tag{5}$$

where $d_{p,i}^{\text{min}}$ is the particle diameter with minimum mobility in channel $i$, and $d_{p,i}^{\text{max}}$ is the particle diameter with maximum mobility in channel $i$. The geometric midpoint particle number concentration in channel $i$ can be approximated as [44]:

$$N_{p,i} = \frac{I_{e,i}}{n_p(d_{p,i}^{\text{mid}}) e Q_a} \tag{6}$$

The measured size channel $i$ distribution results correspond to the channel concentration $N_{p,i}$ divided by the channel geometric width [44]:

$$\frac{N_{p,i}(d_{p,i}^{\text{mid}})}{d\log(d_{p,i})} = \frac{N_{p,i}}{\log\left(d_{p,i}^{\text{max}} / d_{p,i}^{\text{min}}\right)} \tag{7}$$

## Available Aerosol Particle Sizers

*Scanning Mobility Particle Sizer*

The Scanning Mobility Particle Sizer (SMPS) is commercially available from Thermo-System, Incorporated (TSI) [47] and used to measure number-weighted particle size distributions in the range of 3 – 1000 nm. A schematic diagram of the SMPS is shown in Figure 2. The SMPS consists of three main parts: the particle charger, the differential mobility analyzer (DMA) and the detection system. As shown on the diagram, the SMPS uses a bipolar charger (neutralizer) before the DMA in order to bring particle charge levels to a Boltzmann equilibrium charge distribution. The polydisperse aerosols are then passed through the DMA near the inner surface of the outer electrode, which consists of a high voltage inner electrode concentrically surrounded by a grounded outer electrode. A laminar flow of particle-free sheath air (usually at a 10:1 ratio with respect to the aerosol flow rate) is passed through

*Mj. Int. J. Sci. Tech.*, **2007**, *01(02)*, 120-136

the DMA, near the inner electrode. Depending on their charge (positive and negative), particles are attracted or repelled by the inner electrode at different rates, depending on the electrical mobility of each particle. Particles of high electrical mobility precipitate close to the aerosol inlet while particles of lower mobilities precipitate further down the column. Particles within a narrow range of electrical mobility diameter exit the DMA through the monodisperse sample flow (a circumferential slit on the inner electrode located downstream of the aerosol inlet). These particles are referred to as the monodisperse aerosol. The monodisperse aerosol is then transferred to the condensation particle counter (CPC) where the number concentration of the particles is measured. All the remaining particles exit the DMA via the excess flow. The time response of the SMPS is typically 60 – 120 seconds. The particle number concentration that the SMPS can measure is approximately $10^4$ – $10^9$ particles/cm$^3$.

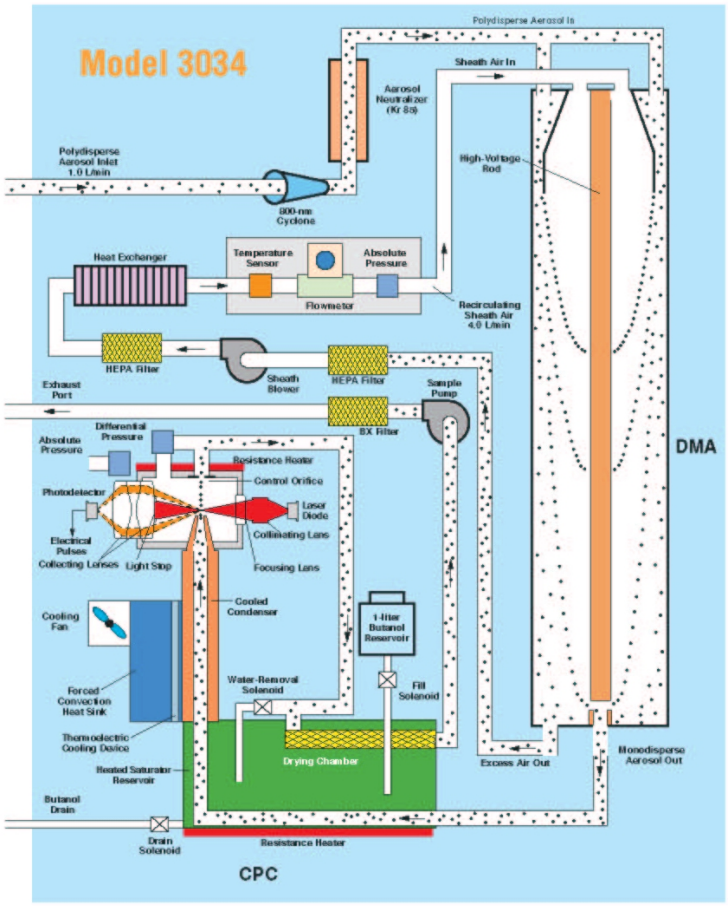


Figure 2 Schematic diagram of the Scanning Mobility Particle Sizer [47].

*Electrical Aerosol Spectrometer*

The Electrical Aerosol Spectrometer (EAS) developed at Tartu University, Estonia, is an instrument for measuring number-weighted particle size distributions in the range of 10 nm to 10 μm using electrical mobility methods [30 - 31]. The design of the EAS is shown in Figure 3. The EAS is designed on the full parallel measuring principle. It contains two mobility analyzers, one provided with a weak electric field or diffusion charger (D-analyzer), and the other with a strong electric field

charger (E-analyzer). High sensitivity has been achieved by unipolar charging of particles. Positive polarity of charge is used. Unipolar diffusion charging is the dominant mechanism for particles less than 0.5 μm in diameter, whereas unipolar field charging is the dominant mechanism for particles larger than 0.3 μm in diameter. For the particles in the size range of 0.3-0.5 μm in diameter, the combined field and diffusion charging is used in this size range. The mobility analyzers are cylindrical capacitors consisting of particle repulsive inner electrode and particle collecting outer electrode. The collecting electrodes of the mobility analyzers are divided into isolated sections each of which is provided with an electrometric amplifier (electrometer). Each section together with its electrometer corresponds to a measuring channel of the spectrometer. The EAS has 32 measuring channels. The aerosol is sucked into the analyzers through preconditioning facilities (laminarizers, dischargers) and through charging zones of the chargers close to the inner (repulsive) electrodes. Charging conditions in the chargers are stabilized by feedback circuits. Charged particles moving in radial electric field of the mobility analyzers precipitate on the different sections of the mobility analyzers according to their electrical mobility. The electric currents carried over these sections by particles are measured by electrometers and form output signals vector of the apparatus (apparatus record). The time uncertainty of measurement is reduced by measuring the same aerosol sample, synchronously with its movement in the analyzer. A special controller has been designed to control the measurement and record data. Maximum resolution of the electrometric signal is 0.25 mV making about $2.5 \times 10^{-16}$ A on the scale of the aerosol electric current. The main spectrometer parameters such as charging currents and air flow rates are also controlled. The time response of the EAS is approximately 1 second for fastest sampling rate. However, for statistically significant size distribution measurement a typical time of 5 seconds is required. Particle number concentration that the EAS can measure ranges between $10^2$ - $10^5$ particles/cm$^3$ for particles as small as 10 nm, and between $2 \times 10^{-2}$ - $5 \times 10^1$ particles/cm$^3$ for particle size up to 10 μm.

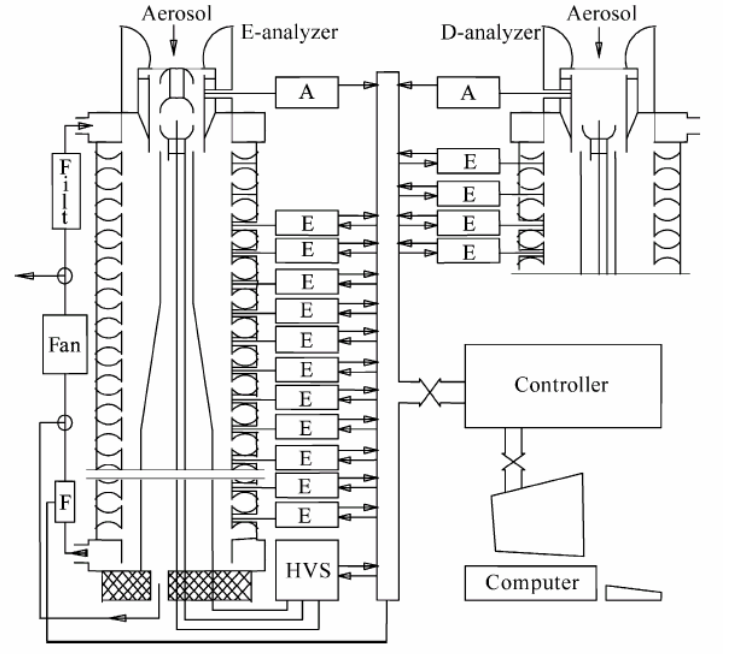


Figure 3 Schematic diagram of the Electrical Aerosol Spectrometer of Tartu University [30 - 31].

*Engine Exhaust Particle Sizer*

*Mj. Int. J. Sci. Tech.*, **2007**, *01(02)*, 120-136

The Engine Exhaust Particle Sizer (EEPS) is a very recent instrument for fast response aerosol measurement in the diameter range of 5.6 to 560 nm [48]. The EEPS commercially available from TSI is similar to the EAS described previously. Schematic diagram of the EEPS is shown in Figure 4. It employs a unipolar diffusion charger to charge the incoming aerosol sample, and an "inside-out" electrostatic classifier to separate particles according to their electrical mobility. It detects and measures particle concentration by a series of 22 electrometer rings along the column classifier. The particle size distribution is then estimated using the current measurements from individual channel and a data inversion algorithm. The time response of the EEPS is approximately 100 milliseconds.

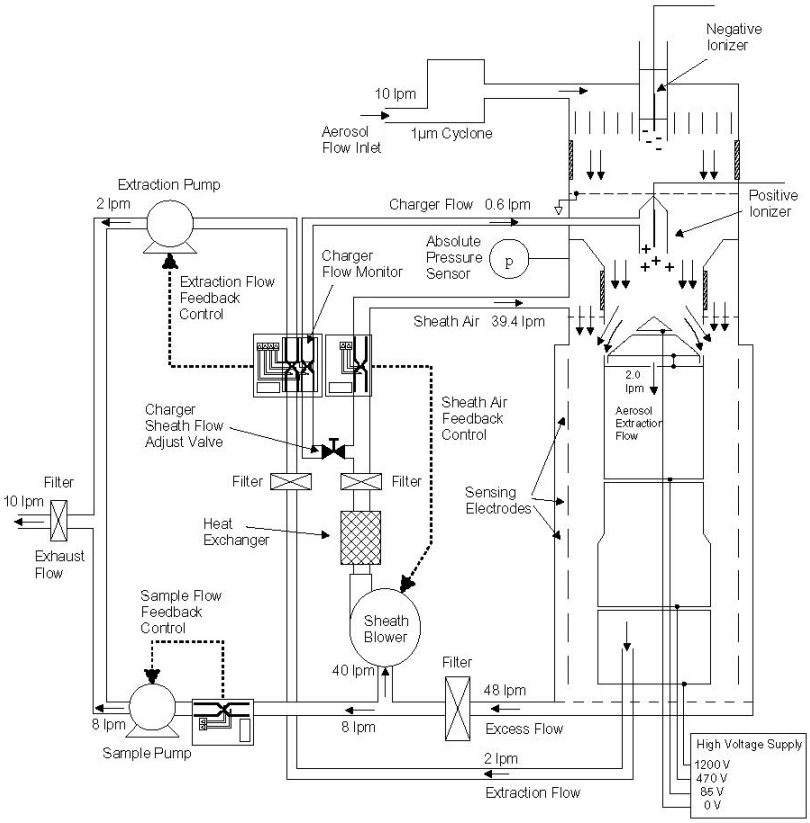


Figure 4 Schematic diagram of the Engine Exhaust Particle Sizer [48].

*Bipolar Charge Aerosol Classifier*

The Bipolar Charge Aerosol Classifier (BCAC) developed at Brunel University, UK, is an instrument for measuring aerosol bipolar charge distribution by electrical mobility technique [27 - 29]. A schematic diagram of the BCAC is shown in Figure 5. The BCAC system incorporates a front-end cylindrical arrangement consisting of 10 well-insulated sections. Each of these sections is composed of a cylindrical capacitor with a coaxial wire electrode maintained at a DC high potential. Aerosol is drawn through a separator using a suction pump, and subjected to an appropriate electric field. Depending on the electric field distribution and air flow rate, charged particles of the same polarity as that of the potential applied to the wire electrodes are deflected toward an outer collecting wall and give up their charge. Accumulated charge on each of the electrodes are measured with a Keithley 6517A electrometer incorporating low current, 10-channel 6522 scanner card. All devices are

interfaced to a personal computer via an IEEE-488 interface and port input/output (PIO) card and controlled by TestPoint software. The time response of the BCAC is approximately 10 seconds.

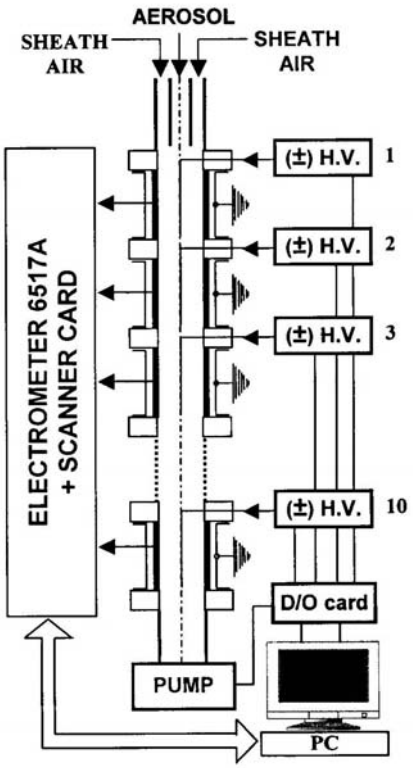


Figure 5 Schematic diagram of the Bipolar Charge Aerosol Classifier [27 - 29].

*Fast Aerosol Spectrometer*

The Fast Aerosol Spectrometer (FAS) developed at University of Cambridge, UK, is an instrument for fast measurement of number-weighted aerosol size distribution for particles in the size range of approximately 1 – 100 nm by electrical mobility method [32]. A schematic diagram of the FAS is shown in Figure 6. The overall design and operating principle of the FAS is similar to the EAS. However, there is a difference between the two instruments in that particle charging of the FAS is accomplished by photoelectric charger, resulting in bipolarly charged aerosol particles. The FAS is composed of an aerosol charger, a size classification column and a signal current detector. Particle charging is carried out by exposing the aerosol sample to intense monochromatic UV light which results in photoelectric ejection of electrons from particle surfaces. The UV lamp used is a KrCl excimer which produces photons at a wavelength of 222 nm (hv = 5.6 eV) [32]. It is powered by an AC source of a ±4 kV triangle wave pulse at a frequency of 40 kHz with charging residence time of approximately 100 ms. Downstream of the charger, the charged particles then enter the size classification section similar to the DMA. The FAS classifier consists of two coaxial electrodes with the central rod being maintained at a positive high voltage range varying between 1 and 10 kV and the outer chassis of the classification section being grounded. The central rod is made of a stainless steel rod with 20 mm diameter and the outer chassis is made of a stainless steel tube with 50 mm diameter and 150 mm in length. There are two streams which are the aerosol and the sheath air flow. The

*Mj. Int. J. Sci. Tech.*, **2007**, *01(02)*, 120-136

charged particles are introduced into the classification section near the central rod by a continuous flow of air, and surrounded by a sheath air flow. Since the central rod is kept at a positive voltage, the charged particles are deflected outward radially according to their electrical mobility and they are collected on a series of eleven isolated electrode rings at the inner surface of the outer chassis of the FAS classifier. Each electrode ring is 10 mm wide with a 0.6 mm gap between the electrometer rings for isolation. The electric currents due to the charged particles are measured by an electrometer and are then translated to particle number concentrations corresponding to the size range collected on each electrode ring. It was reported that the time response of the FAS is approximately 38 ms.

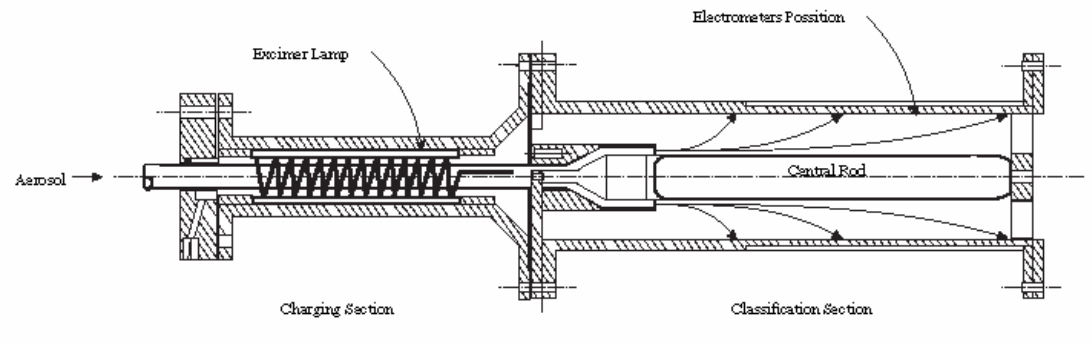


Figure 6 Schematic diagram of the Fast Aerosol Spectrometer [32].

*Differential Mobility Spectrometer*

The Differential Mobility Spectrometer (DMS) manufactured by Cambustion, UK, is similar to the FAS [33 - 41]. However, there are two main differences between the two instruments. Firstly, particle charging is accomplished by a corona-wire diffusion charger resulting in unipolarly charged aerosol particles. Secondly, the DMS operates at pressure below ambient (0.25 atm). Figure 7 shows a schematic diagram of the DMS. It is capable of fast response aerosol measurements in the range of 5 to 1000 nm in diameter, with a time response of 200 ms. The DMS consists of three main parts: the particle charger, the classification column, and the detection system. Aerosol particles are passed through a corona-wire diffusion charger, a Hewitt-type single-wire corona charger, to charge the sample aerosol prior to entrance to the column. The charger is maintained at 0.25 bar in order to increase mobility resolution for particles with diameter greater than 100 nm [33]. Following the charger, the charged particles enter the classification column, which is 700 mm long with an internal diameter of 53 mm. The DMS column (operating at the same pressure as the charger) consists of two concentric electrodes with an axially increasing electric field established in between. This varying electric field is created by a linearly increasing (from the aerosol inlet to the end of the column) potential along the central rod. This varying electric field results in a better resolution of particle size distribution. The actual number concentration of the charged particles is determined by a series of 26 metallic rings connected to sensitive electrometers placed in the inner surface of the outer electrode of the column. The first eight rings from inlet are 14.5 mm wide, while the rest have a width of 29.5 mm. The start of the first electrometer ring is located 18.5 mm downstream of the aerosol inlet, and a 0.5 mm gap is allowed between the electrometer rings for isolation. The actual size distribution of the

input aerosol can be determined by deconvoluting the electrometer current readings. The DMS can measure particle size with the number concentration in the range of approximately $1 \times 10^3 - 4 \times 10^7$ particles/cm$^3$.

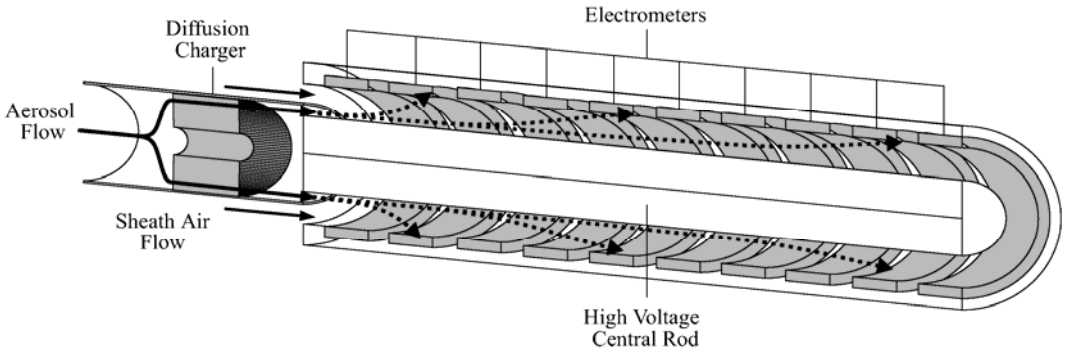


Figure 7 Schematic diagram of the Differential Mobility Spectrometer [36 - 41].

*Electrical Mobility Spectrometer*

The Electrical Mobility Spectrometer (EMS) has been developed at Chiang Mai University, Thailand, under the support from the National Electronic and Computer Technology Center (NECTEC), National Science and Technology Development Agency [42 - 46]. The EMS is a multi-channel size analyzer capable of measuring the aerosol size distribution near real time in the size range of approximately 10 – 1000 nm. Nonetheless, there are collective differences between the EMS and each of the existing instruments, which are as follows: (i) the concept of the present instrument is based on a compact, inexpensive and portable unit. Short column classifier and a small number of detection channels are used to reduce diffusion effect of the particle inside the classifier. Overall dimensions and weight are such that it is easy to handle and move around; (ii) the instrument adopts a tangential aerosol inlet upstream of the first electrode ring to ensure uniform particle distribution across the annular aerosol entrance to the classifier column; (iii) rather than diffusion charging, the instrument employs unipolar corona (diffusion and field) charging method; and (iv) the applied voltage is set to maintain at low level, well below the corona onset voltage, to avoid unintentional charging of the particles inside the classifier. The schematic diagram of the EMS is shown in Figure 8. The spectrometer has one short column which consists of coaxially cylindrical electrodes. The advantage of cylindrical geometry is that distortion of electric field between electrodes is minimal due to the absence of corners and edges. Operation and performance of the instrument depend upon aerosol transport under the influence of flow and electric fields. It is important to ensure that both flow and electric fields are laminar and uniformly distributed inside the classifying column. There are two streams which are the aerosol and sheath air flow. The two flows are regulated and controlled via mass flow controllers. The inside of the annular is constructed in such a way that smooth wall and turbulence free merging of the two gas flows are ensured. The flow field inside the apparatus is checked by solving numerically the continuity and Navier-Stokes equations using a commercial computational fluid dynamic software package. The charged particles enter the analyzer column near

*Mj. Int. J. Sci. Tech.*, **2007**, *01(02)*, 120-136

the central rod by a continuous flow of air. Since the central rod is kept at a positive high voltage, the charged particles are deflected radially outward. They are collected on electrically isolated electrometer rings positioned at the inner surface of the outer electrode of the column. A Keithley 6517A electrometer incorporating a Keithley 6522 low current scanner card connected to these electrodes measures currents corresponding to the number concentration of particles of a given mobility which is related to the particle size. The signal current from the electrometer is interfaced to an external personal computer via RS-232 serial port interface. Electrical current detection method is considered to be easier and faster than direct particle detection measurements. In addition, the applied high voltage is maintained at a lower value than the corona onset voltage to avoid unintentional charging of the particles within the classifier.

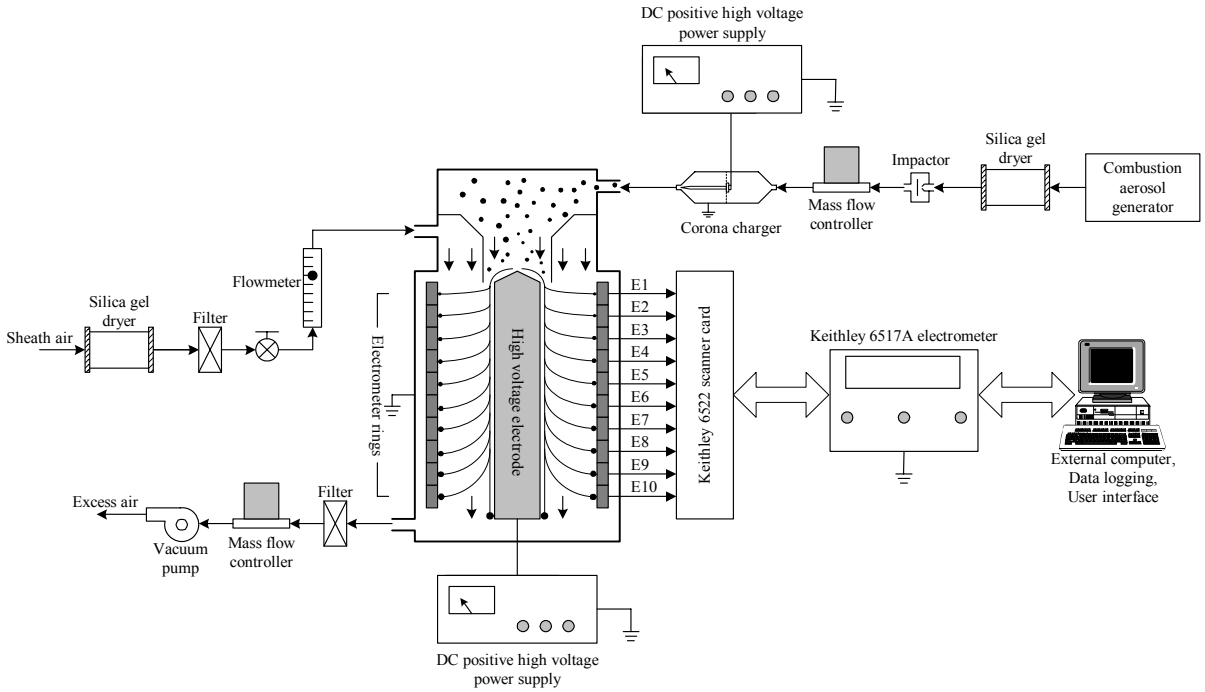


Figure 8 Schematic diagram of the Electrical Mobility Spectrometer developed at Chiang Mai University [42 - 46].

## Comparison of Available Instruments' Characteristics

Comparison of these instruments is made and shown in Table 1. Recent instrumentation developments allow the size distribution measurement of nanometer particles in the size range from 1 to 10,000 nm using the electrical mobility technique. Applications of these instruments are found in such diverse fields as materials synthesis, biotechnology, semiconductor manufacturing, pharmaceutical products, nano-composites and ceramics, electronics and computing, and exhaust gas

Table 1 Comparison of available aerosol particle sensors.

| | SMPS (TSI [47]) | EAS (Tammet et al. [30 - 31]) | EEPS (TSI [48]) | DMS (Biskos et al. [33 - 41]) | FAS (Graskow [32]) | BCAC (Kulon et al. [27 - 29]) | EMS (Intra and Tippayawong [42 - 46]) |
|---|---|---|---|---|---|---|---|
| Measurement technique | Electrical mobility | Electrical mobility | Electrical mobility | Electrical mobility | Electrical mobility | Electrical mobility | Electrical mobility |
| Size range | 3 - 1,000 nm | 10 - 10,000 nm | 5.6 - 560 nm | 5 - 1,000 nm | 1 - 100 nm | < 3,000 nm | 10 - 1,000 nm |
| Concentration range | $10^4$ – $10^{11}$ particles/$m^3$ | $10^4$ - $10^{11}$ particles/$m^3$ | $10^9$ - $10^{13}$ particles/$m^3$ | $10^9$ - $10^{13}$ particles/$m^3$ | n/a | n/a | $10^{11}$ - $10^{13}$ particles/$m^3$ |
| Time response | 60 – 120 s | < 1 s | 100 ms | 200 ms | 100 ms | 10 s | 30 s |
| Charger type | Neutralizer | Corona charger | Corona charger | Corona charger | KrCl excimer | Corona charger | Corona charger |
| Charging method | Bipolar charging | Unipolar diffusion and field charging | Unipolar diffusion charging | Unipolar diffusion charging | Photoelectric ejection | Bipolar diffusion charging | Unipolar diffusion and field charging |
| Particle detector | Condensation particle counter | Electrometers | Electrometers | Electrometers | Electrometers | Electrometers | Electrometers |
| Channels | 1 | 26 | 22 | 26 | 10 | 10 | 10 |
| Aerosol inlet technique | n/a | n/a | n/a | n/a | n/a | n/a | Tangential inlet |
| Aerosol flow rate | 1 l/min | 12 l/min | n/a | 5 l/min | 5 l/min | 2 l/min | 1 l/min |
| Sheath air flow rate | 10 l/min | 36 l/min | n/a | 35 l/min | 55 l/min | 58 l/min | 10 l/min |
| Operating pressure | n/a | n/a | n/a | 25.3 kPa | n/a | n/a | 34.5 kPa |
| Electrode applied voltage | 0 – 10 kV | 800 V | n/a | 5 kV to 10 kV | 1 to 10 kV | 5 kV | 500 V to 3 kV |
| Classifier length | n/a | n/a | n/a | 700 mm | 150 mm | 2000 mm | 131 mm |
| Inner electrode radius | n/a | n/a | n/a | 12.5 mm | 20 mm | 1.5 mm | 10 mm |
| Outer electrode radius | m/a | n/a | n/a | 26.5 mm | 25mm | 25 mm | 25 mm |

n/a: information not available

particles. Figure 9 shows typical ambient aerosol size distribution measurement results from the DMS, the SMPS and the Electrical Low Pressure Impactor (ELPI). The background size spectrum is more

*Mj. Int. J. Sci. Tech.*, **2007**, *01(02)*, 120-136

clearly shown at a single time point with a SMPS scan at approximately the same time. An example of size distribution of diesel engine vehicle exhaust particles measured by the CMU-EMS and ELPI is shown in Figure 10. The normal log nature of distribution is clearly illustrated. The CMU-EMS measured particle size distribution is in agreement with that obtained from the ELPI.

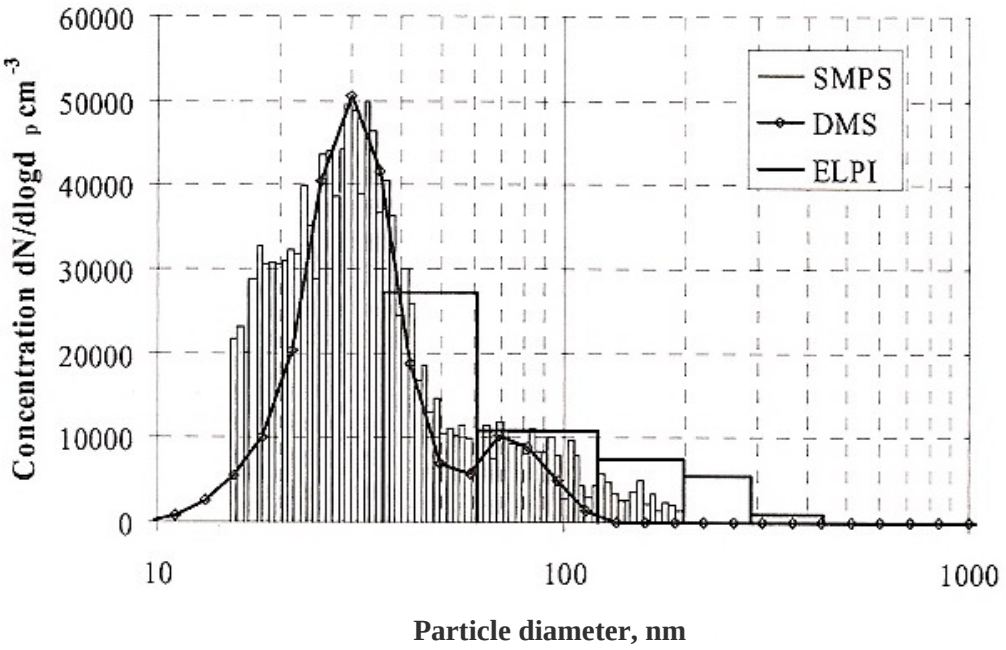


Figure 9 Typical ambient aerosol size distribution measurements results from SMPS, DMS and ELPI [34 - 35].

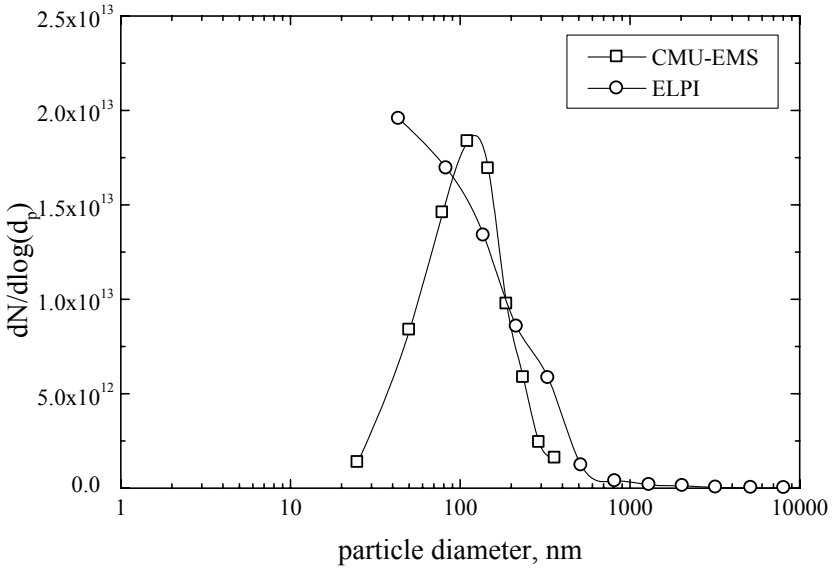


Figure 10 Size distribution of exhaust diesel engine vehicle particles measured by the CMU-EMS and ELPI [43].

**Summary**

An electrical mobility sizer is a valuable tool for measuring the airborne nanoparticle size distribution based on electrostatic classification technique. An overview of existing electrical mobility

sizers has been presented in this paper. These sensors include the SMPS, the EAS, the EEPS, the BCAC, the FAS, the DMS and the CMU-EMS. A description of the operating principle of each sizer and its components have also been given. This achievement will make a significant contribution to the investigation of the physics of nanoparticles as well as their applications.

**Acknowledgements**

The authors wish to express their deepest gratitude to the National Electronic and Computer Technology Center, National Science and Technology Development Agency, for its support during the course of the EMS development.

**References**

1. W. C. Hinds, "Aerosol Technology", John Wiley & Sons, New York, **1999**.
2. D. R. Chen, D. Y. H. Pui, D. Hummes, H. Fissan, F. R. Quant, and G. J. Sem, "Design and evaluation of a nanometer aerosol differential mobility analyzer (Nano-DMA)", *J. Aerosol Sci.*, **1998**, *29*, 497-509.
3. J. Zeleny, "The distribution of mobilities of ions in moist air", *Phys. Review*, **1929**, *34*, 310-334.
4. S. H. Zhang and R. C. Flagan, "Resolution of the radial differential mobility analyzer", *J. Aerosol Sci.*, **1996**, *27*, 1179-1200.
5. H. A. Erikson, "On the nature of the negative and positive ions in air, oxygen and nitrogen", *Phys. Review*, **1922**, *20*, 117-126.
6. H. A. Erikson, "On the effect of the medium on gas ion mobility", *Phys. Review*, **1927**, *30*, 339-347.
7. H. Rohmann, "Methode sur Messung der Grosse von Schwebeteilchen", *Zeitschrift fur Physik*, **1923**, *17*, 253 - 265.
8. K. T. Whitby and W. E. Clake, "Electric aerosol particle counting and size distribution measuring system for the 0.015 to 1 μm size range", *Tellus*, **1966**, *18*, 573-586.
9. H. F. Tammet, "The aspiration method for the determination of atmospheric ion spectra", Israel Program for Scientific Translations, Jerusalem, **1970**.
10. E. O. Knutson and K. T. Whitby, "Aerosol classification by electric mobility : apparatus, theory, and applications", *J. Aerosol Sci.*, **1975**, *6*, 443-451.
11. B. Y. H. Liu and D. Y. H. Pui, "On the performance of the electrical aerosol analyzer", *J. Aerosol Sci.*, **1975**, *6*, 249-264.
12. Y. Kousaka, K. Okuyama, M. Adachi, and T. Mimura, "Effect of Brownian diffusion on electrical classification of ultrafine aerosol particles in differential mobility analyzer", *J. Chem. Eng. Japan*, **1986**, *19*, 401-407.
13. M. Lehtimaki, "Studies of aerosol measuring techniques", *Ph.D. Thesis*, **1986**, Tampere University of Technology, Finland.
14. M. Lehtimaki, "New current measuring technique for electrical aerosol analyzers", *J. Aerosol Sci.*, **1987**, *18*, 401-407.

15. M. R. Stolzenburg, "An ultrafine aerosol size distribution measuring system", *Ph.D. thesis*, **1988**, University of Minnesota, USA.
16. W. Winklmayr, G. P. Reischl, A. O. Lindner, and A. Berner, "A new electromobility spectrometer for the measurement of aerosol size distribution in the size range from 1 to 1000 nm", *J. Aerosol Sci.*, **1991**, *22*, 289-296.
17. D. R. Chen and D. Y. H. Pui, "Numerical modeling of the performance of differential mobility analyzers for nanometer aerosol measurement", *J. Aerosol Sci.*, **1997**, *28*, 985-1004.
18. D. Hummes, S. Neumann, H. Fissan, D. R. Chen, D. Y. H. Pui, F. R. Quant, and G. J. Sem, "Nanometer differential mobility analyzer (Nano-DMA): Experimental evaluation and performance verification", *J. Aerosol Sci.*, **1996**, *27*, s135-s136.
19. D. Hummes, S. Neumann, F. Schmidt, M. Drodoom, K. Fissan, K. Deppert, T. Junno, J. O. Malm, and L. Samuelson, "Determination of the size distribution of nanometer-sized particles", *J. Aerosol Sci.*, **1996**, *27*, s163-s164.
20. D. Hummes, F. Stratmann, S. Neumann, and S. Fissan, "Experimental determination of the transfer function of a differential mobility analyzer (DMA) in the nanometer size range", *Particle and Particle System Characterization*, **1996**, *13*, 327-332.
21. T. Seto, T. Nakamoto, K. Okuyama, M. Adachi, Y. Kuga, and K. Takeuchi, "Size distribution measurement of nanometer-sized aerosol particles using DMA under low-pressure conditions", *J. Aerosol Sci.*, **1997**, *28*, 193-206.
22. H. Fissan, D. Hummes, F. Stratmann, P. Buscher, S. Neumann, D. Y. H. Pui, and D. Chen, "Experimental comparison of four differential mobility analyzers for nanometer aerosol measurements", *Aerosol Sci. Tech.*, **1996**, *24*, 1-13.
23. W. Brimili, F. Stramann, A. Wiedensohler, D. Covert, L. M. Russel, and O. Berg, "Determination of differential mobility analyzer transfer function using identical instruments in series", *J. Aerosol Sci.*, **1996**, *27*, 215-223.
24. B. G. Martinsson, M. N. A. Karlsson, and G. Frank, "Methodology to estimate the transfer function of individual differential mobility analyzers", *Aerosol Sci. Tech.*, **2001**, *35*, 815-823.
25. K. S. Seol, J. Yabumoto, and K. Takeeuchi, "A differential mobility analyzer with adjustable column length for wide particle size range measurements", *J. Aerosol Sci.*, **2002**, *33*, 1481-1492.
26. M. N. A. Karlsson and B. G. Martinsson, "Methods to measure and predict the transfer function size dependence of individual DMAs", *J. Aerosol Sci.*, **2003**, *34*, 603-625.
27. J. Kulon and W. Balachandran, "The measurement of bipolar charge on aerosols", *J. Electrostatics*, **2001**, *51-52*, 552-557.
28. J. Kulon, S. Hrabar, W. Machowski, and W. Balachandran, "A bipolar charge measurement system for aerosol characterization", *IEEE Trans. Ind. Appl.*, **2001**, *37*, 472-479.
29. J. Kulon, B. Malyan, and B. Balachandran, "The bipolar charge aerosol classifier", *IEEE Trans. Ind. Appl.*, **2001**, *4*, 2241-2248.
30. H. Tammet, A. Mirme, and E. Tamm, "Electrical aerosol spectrometer of Tartu University", *J. Aerosol Sci.*, **1998**, *29*, s427-s428.
31. H. Tammet, A. Mirme, and E. Tamm, "Electrical aerosol spectrometer of Tartu university", *Atmospheric Res.*, **2002**, *62*, 315 – 324.

32. B. R. Graskow, "Design and development of a fast aerosol size spectrometer", *Ph.D. Thesis*, **2001**, University of Cambridge, UK.
33. K. Reavell, "Fast response classification of fine aerosols with a differential mobility spectrometer", *Proc. 13th Annual Conference of Aerosol Society*, **2002**, Lancaster.
34. K. Reavell, T. Hands, and N. Collings, "Determination of real time particulate size spectra and emission parameter with a differential mobility spectrometer", *6th International ETH Conference on Nanoparticle Measurement*, 19-20 August **2002**, Zurich, Switzerland.
35. K. Reavell, T. Hands, and N. Collings, "A fast response particulate spectrometer for combustion aerosols", *Society of Automotive Engines*, **2002**, paper no. 2002-01-2714, p.283-289.
36. G. Biskos, K. Reavell, T. Hands, and N. Collings, "Fast measurements of aerosol spectra", *European Aerosol Conference,* September, **2003**, Madrid, Spain.
37. G. Biskos, "Theoretical and experimental investigation of the differential mobility spectrometer", *Ph.D. Thesis*, **2004**, University of Cambridge, UK.
38. G. Biskos, E. Mastorakos, and N. Collings, "Monte-Carlo simulation of unipolar diffusion charging for spherical and non-spherical particles", *J. Aerosol Sci.,* **2004**, *35*, 707-730.
39. G. Biskos, K. Reavell, and N. Collings, "Electrostatic characterization of corona-wire aerosol charges", *J. Electrostatics*, **2005**, *63*, 69-82.
40. G. Biskos, K. Reavell, and N. Collings, "Unipolar diffusion charging of aerosol particles in the transition regime", *J. Aerosol Sci.*, **2005**, *36*, 247-265.
41. G. Biskos, K. Reavell, and N. Collings, "Description and theoretical analysis of a differential mobility spectrometer", *Aerosol Sci. Tech.*, **2005**, *39*, 527-541.
42. P. Intra and N. Tippayawong, "An electrical mobility spectrometer for aerosol size distribution measurement", *Technology and Innovation for Sustainable Development Conference (TISD2006)*, 25-27 January **2006**, Khon Kaen, Thailand.
43. P. Intra, "Aerosol size measurement using electrical mobility technique", *Ph.D. Thesis*, **2006**, Chiang Mai University, Thailand.
44. P. Intra and N. Tippayawong, "Aerosol size distribution measurement using multi-channel electrical mobility sensor.", *J. Aerosol Res. Japan*, **2006**, *21*, 329-340.
45. P. Intra and N. Tippayawong, "An electrical mobility spectrometer for aerosol size distribution measurement" *International Conference on Technology and Innovation for Sustainable Development*, 25-27 January **2006**, Khon Kaen, Thailand.
46. P. Intra and N. Tippayawong, "Numerical simulation of flow and electric fields in an electrical mobility spectrometer", *International Symposium on Nanotechnology in Environmental Protection and Pollution (ISNEPP 2005)*, 12-14 January **2005**, Bangkok, Thailand.
47. Thermo-Systems Inc., "Operation and Service Manual, Revision L, for Scanning Electrical Mobility Sizer™ (SMPS™) Spectrometer, Model 3936", Minnesota, **2006**.
48. Thermo-Systems Inc., "Operation and Service Manual, Revision B, for Engine Exhaust Particle Sizer™ Spectrometer, Model 3090", Minnesota, **2004**.

*Mj. Int. J. Sci. Tech.* **2007**, *01(2)*, 137-144

***Maejo International***

***Journal of Science and Technology***

**ISSN 1905-7873**

Available online at www.mijst.mju.ac.th

*Full Paper*

# Preference direction study of Job's-tears ice cream

**Waraluck Khongjeamsiri, Wiwat Wangcharoen*, Suthaya Pimpilai and Wichittra Daengprok**

Department of Food Technology, Faculty of Engineering and Agricultural Industry, Maejo University, Chiangmai 50290, Thailand.

*Corresponding author, E-mail: wwwangcharoen@yahoo.com

*Received: 9 July 2007 / Accepted: 27 July 2007 / Published: 6 September 2007*

**Abstract:** Job's-tears (*Coix lachryma-jobi* L.) is a kind of cereal commonly used in Asia as food and medicine, but it is still not widely consumed in Thailand. Four prototype products of Job's-tears ice cream were developed by varying 2 levels of glucose syrup (16 and 32% of Job's-tears used) and coconut milk (50 and 100 % of Job's-tears used). Their sensory attribute profiles were evaluated by 3 groups of 10 selected panelists using Ratio profile test (RPT), and their acceptances, hedonic scores, were evaluated by 100 consumers. Results showed that there were significant effects of coconut milk quantity on several attributes, such as appearance (whiteness), texture (hardness, smoothness), and flavour (coconut milk aroma, sweetness, saltiness), but the effect of glucose syrup quantity was significant on hardness only. Acceptance data were analyzed by cluster analysis to find out the difference of preference directions and 3 clusters ($n_1$ = 39, $n_2$ = 25, $n_3$ = 36) were found. The first cluster preferred Job's tears ice cream containing high glucose syrup and low coconut milk, whilst the second preferred high level of only one of these two ingredients, and the third preferred high level of both ingredients. External preference maps were created from RPT and acceptance data to express the preference direction of each cluster.

**Keywords**: Job's-tears, ice cream, preference direction, ratio profile test, external preference map

*Mj. Int. J. Sci. Tech.* **2007**, 01(2), 137-144

## Introduction

Job's-tears (*Coix lacryma-jobi*), coixseed, adlay, or adlai, is a tall grain-bearing tropical plant of the family Poaceae, or grass family [1]. It is listed as a serious weed in Polynesia, a principle weed in Italy and Korea, a common weed in Australia, Borneo, Burma, Cambodia, China, Congo, Colombia, Costa Rica, Dominican Republic, Fiji, Ghana, Guatemala, Hawaii, Honduras, Hong Kong, India, Iran, Iraq, Japan, Melanesia, Micronesia, Nepal, Pakistan, Peru, Philippines, Puerto Rico, Rhodesia, Senegal, South Africa, Sudan, Thailand, United States, and Venezuela [2]. Like other cereals, there are many cultivars of Job's-tears, including soft-shelled, easily-threshed types with a sweet kernel. In some, the hulled grain is adapted for parching or boiling like rice, while in others it can be milled, ground into flour and baked into bread. The grains are also utilized in soups, porridge, drinks and pastries. In India, the Nagas use the grain for brewing a beer called “Zhu” or “Dzu”. A Japanese variety called "Ma-Yuen" is brewed into a tea and an alcoholic beverage, and roasted seeds are made into a coffee-like drink [3]. In Korea, a thick drink called “Yulmu Cha” is made from powdered Job's tears. A similar drink, called “Yì Mí Shǔi”, also appears in Chinese cuisine, and is made by simmering whole polished Job's tears in water and sweetening the resulting thin, cloudy liquid with sugar. The grains are usually strained from the liquid but may also be consumed separately or together [1].

One hundred grams of Job’s-tears grain contain 380 calories, 11.2 g water, 15.4 g protein, 6.2 g fat, 65.3 g total carbohydrate, 0.8 g fiber, 1.9 g ash, 25 mg Ca, 435 mg P, 5.0 mg Fe, 0 µg beta-carotene equivalent, 0.28 mg thiamine, 0.19 mg riboflavin, 4.3 mg niacin, and 0 mg ascorbic acid [4]. According to Hager's Handbook [5], there are 50-60% starch, 18.7% protein (with glutamic acid, leucine, tyrosine, arginine, histidine, and lysine), and 5-10% fatty oil (with glycerides of myristic and palmitic acids).

For medicinal uses, the fruits are anodyne, anti-inflammatory, antipyretic, antiseptic, antispasmodic, hypoglycemic, hypotensive, sedative and vermifuge [4,6]. The seed, with the husk removed, is antirheumatic, diuretic, pectoral, refrigerant and tonic [4, 7, 8]. A tea from the boiled seeds is drunk as part of a treatment to cure warts [9]. It is also used in the treatment of lung abscess, lobar pneumonia, appendicitis, rheumatoid arthritis, beriberi, diarrhea, oedema and difficult urination [7].

In Thailand, Job’s-tears is used as an ingredient in a few recipes and usually consumed by some people. Two commercial drinking products, Pro-fit and P-life, are now available but they are still not popular enough. This work tried to develop a prototype product of Job’s tears-based ice cream and to study the preference direction of consumers for improving this product further.

## Experimental Section

### *Ice cream preparation*

The ice cream was prepared accordingly. Job’s-tears were washed and soaked in water for 2 hours. It was then boiled for 40 minutes and blended with water in a ratio 1:2 (boiled Job’s-tears: water). The total solid of blended Job’s-tears was adjusted to 12 % (w/v) with water. Blended Job’s-tears and the other ingredients for each treatment were mixed following the formulation given in Table 1. The resulting mixture was pasteurized at 79 °C for 25 seconds and then cooled rapidly. It was then stored

*Mj. Int. J. Sci. Tech.* **2007**, 01(2), 137-144

overnight in the refrigerator. The mixture was made into ice cream using an ice cream maker, then packed and kept in a freezer.

**Table 1.** Ingredients for preparing ice cream from 500 grams of blended Job's-tears**.**

| Treatment | Ingredient (grams) | | | | |
|---|---|---|---|---|---|
| | BlendedJob's-tears | Glucose syrup | Coconut milk | Sucrose | Salt |
| 1 | 500 | 80 | 250 | 60 | 4 |
| 2 | 500 | 160 | 250 | 60 | 4 |
| 3 | 500 | 80 | 500 | 60 | 4 |
| 4 | 500 | 160 | 500 | 60 | 4 |

*Sensory evaluation*

1) Creating sensory attribute profile of 4 prototype products

Three groups of 10 selected panelists were trained to evaluate the products by Ratio profile technique (RPT) [10] before they were requested to taste and evaluate 4 prototype products on 18 sensory attributes created by our research team. The 10 cm-line scale with suitable descriptors at the two ends was used for rating the intensity of each sensory attribute.

2) Preference study of 4 prototype products

One hundred panelists (50 males and 50 females) were requested to express their preference by rating 4 prototype products on 9-point hedonic scale (1 = dislike extremely, 5 = neither like nor dislike, 9 = like extremely).

*Statistical analysis*

1) Identifying the difference of preference direction

Hedonic scores of each panelist were standardized. Their standard scores were differentiated by cluster analysis.

2) Analysis of variance

Effects of glucose syrup and coconut milk quantities on the intensity of each sensory attribute (from RPT) and hedonic scores (from each cluster) of 4 prototype products were analyzed by 2x2 Factorial design. All data were tested for normality and homogeneity of variance before analysis of variance was applied.

3) Creating external preference maps

The data reduction by Principal component analysis (PCA) was applied to RPT data, and the position of each sensory attribute and prototype product on each PC was estimated. Bivariate correlations between product positions and hedonic scores (from each cluster) were analyzed. Each

pair of related PCs was used to create an external preference map for each cluster. Finally preference direction of each cluster was created by regressing product positions and their hedonic score means.

## Results and Discussion

*The difference of preference direction*

The result of cluster analysis showed that the difference of preference direction was found and 100 panelists could be separated into 3 different clusters (groups) depending on their preference direction. The number of member in cluster 1, cluster 2, and cluster 3 were 39, 25, and 36 persons, respectively.

*Effect of glucose syrup and coconut milk quantities on the intensity of each sensory attribute.*

Results (Table 2) showed that there were significant effects of coconut milk quantity on several attributes but the effect of glucose syrup quantity was significant only on hardness. If coconut milk quantity was increased, the product looked brighter, smoother, but lesser in quantity of blended Job's-tears. Also, the coconut milk odor would be stronger but Job's-tears taste, sweetness, and saltiness would be milder**.** Additionally, the product became harder and slower melting, but less in stickiness and teeth and tough sticking after swallowing. If glucose syrup quantity was added, the product became softer.

*Effect of glucose syrup and coconut milk quantities on hedonic scores of each cluster.*

The difference of three consumer clusters is shown in Table 3. Cluster 1 preferred Job's-tears ice cream containing high glucose syrup and low coconut milk (Treatment 2), whilst cluster 2 preferred high glucose syrup and low coconut milk (Treatment 2) or low glucose syrup and high coconut milk (Treatment 3), and clusters 3 preferred high levels of both glucose syrup and coconut milk (Treatment 4).

*Creating external preference maps.*

The principal component (PC) analysis reduced 18 sensory attributes into only 6 PCs with 66.4 % variance explained as shown in Table 4. Bivariate correlations showed that there was an optimum point of products on PC3 and PC6 for cluster 1 and it meant they wanted products with optimum texture (hardness, melting rate, and number of ice crystals) and coconut milk odour. The optimum point was also found on PC1, PC3, and PC5 for cluster 2. It meant products with optimum Job's-tears flavour and texture (hardness, melting rate, and number of ice crystal) would be preferred. For cluster 3, the direction of preference was found on PC2 (+) and PC4 (-). It meant that this cluster preferred smooth and rich, but not sticky and sweet products. External preference maps were created as shown in Figure 1, but the equation of preference direction could be created for cluster 3 only, because more

*Mj. Int. J. Sci. Tech.* **2007**, 01(2), 137-144

data points were needed for non-linear regression in case of cluster 1 and 2, who wanted optimum products. However, the optimum area might be considered from hedonic score means of products for cluster 1 and it should be located close to the origin point (0,0), but the optimum area for cluster 2 could not be identified because of the small difference between hedonic score means of products. The preference direction equation for cluster 3 was: Hedonic score = 6.61 - 2.26 PC2 - 2.76 PC4. This equation expressed that products located on quadrant 3 (-,-) would be preferred by this consumer cluster. This result did not agree with the bivariate correlation result for PC2 (smoothness and richness), and it meant that too smooth and rich products were not preferred by this cluster either.

**Table 2**. Intensity means of prototype products' sensory attributes at low and high levels of glucose syrup and coconut milk.

| | Glucose syrup | | Coconut milk | |
|---|---|---|---|---|
| | 80 grams | 160 grams | 250 grams | 500 grams |
| **Appearance** | | | | |
| 1. Whiteness (bright to dark) | 5.42 | 5.01 | 6.87[a] | 3.56[b] |
| 2. Quantity of blended Job's-tears (least to most) | 5.09 | 5.51 | 6.31[a] | 4.29[b] |
| 3. Smoothness by looking (least to most) | 5.92 | 5.70 | 5.40[b] | 6.22[a] |
| **Odour** | | | | |
| 4. Coconut milk odour (mild to strong) | 5.30 | 5.32 | 4.69[b] | 5.94[a] |
| 5. Job's-tear odour (mild to strong) | 4.31 | 4.38 | 4.61 | 4.08 |
| **Taste** | | | | |
| 6. Coconut milk taste (least to most) | 5.78 | 5.77 | 5.52 | 6.03 |
| 7. Job's-tear taste (least to most) | 5.45 | 5.54 | 6.05[a] | 4.94[b] |
| 8. Sweetness (least to most) | 4.87 | 4.96 | 5.29[a] | 4.53[b] |
| 9. Saltiness (least to most) | 5.00 | 5.09 | 5.46[a] | 4.63[b] |
| **Texture** | | | | |
| 10. Hardness (soft to hard) | 5.91[a] | 5.05[b] | 4.87[b] | 6.08[a] |
| 11. Smoothness by taste (least to most) | 5.39 | 5.03 | 5.29 | 5.13 |
| 12. Richness (least to most) | 5.76 | 5.53 | 5.67 | 5.63 |
| 13. Stickiness (least to most) | 4.81 | 5.14 | 5.58[a] | 4.38[b] |
| 14. Number of ice crystal (least to most) | 4.61 | 4.17 | 4.18 | 4.60 |
| 15. Melting rate (fast to slow) | 4.71 | 5.20 | 4.64[b] | 5.26[a] |
| **Others** | | | | |
| 16. Off-flavour (least to most) | 2.02 | 2.13 | 2.11 | 2.05 |
| 17. Teeth and tough sticking after swallow (least to most) | 5.56 | 5.50 | 5.97[a] | 5.09[b] |
| 18. Mouth coating after swallow (least to most) | 5.41 | 5.80 | 5.44 | 5.77 |

a, b ; Mean pairs with different letters were significantly different ($p<0.05$).

*Mj. Int. J. Sci. Tech.* **2007**, 01(2), 137-144

**Table 3.** Hedonic score means for 4 prototype products of each consumer cluster**.**

| Treatment | Cluster 1 ($n_1$ = 39) | Cluster 2 ($n_2$ = 25) | Cluster 3 ($n_3$ = 36) |
|---|---|---|---|
| 1 | $5.90 \pm 1.45^{c}$ | $6.44 \pm 0.87^{bc}$ | $6.61 \pm 1.10^{b}$ |
| 2 | $7.21 \pm 1.06^{a}$ | $6.80 \pm 1.00^{ab}$ | $5.97 \pm 1.28^{c}$ |
| 3 | $5.36 \pm 1.44^{d}$ | $6.92 \pm 1.00^{a}$ | $6.69 \pm 1.12^{b}$ |
| 4 | $6.72 \pm 1.07^{b}$ | $6.12 \pm 1.13^{c}$ | $7.22 \pm 1.10^{a}$ |

a, b,.. ; Means with different letters in each column were significantly different ($p<0.05$).

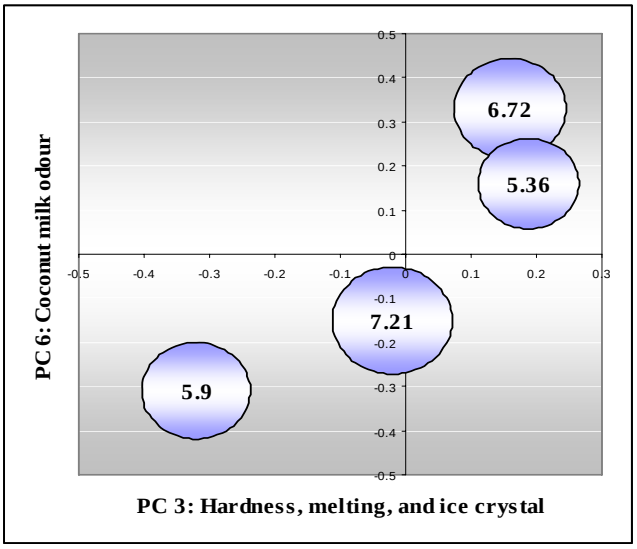


**Cluster 1**: Product located on the origin point (0,0) area would be preferred..

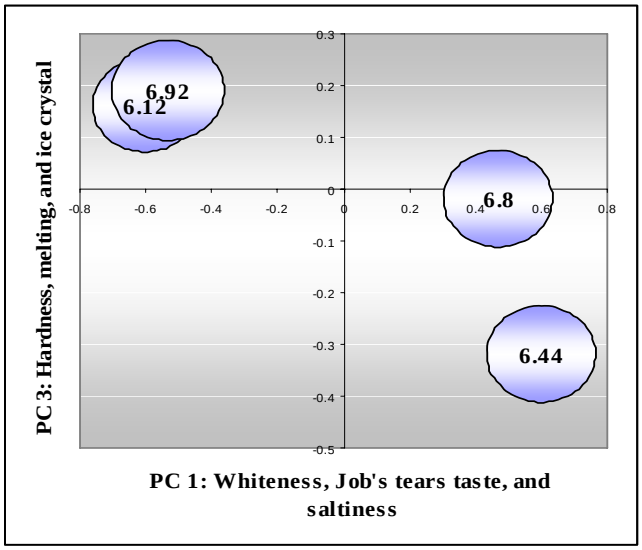


**Cluster 2:** Area of preferred products could not be identified for this cluster since there was a small difference between hedonic scores of all products (6.12 – 6.92).

*Mj. Int. J. Sci. Tech.* **2007**, 01(2), 137-144

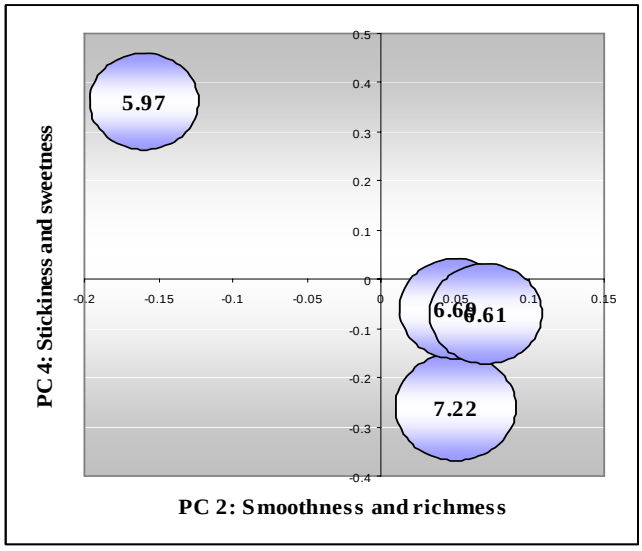


**Cluster 3:** Product located on the minus area of both PC2 and PC4 would be preferred.
(Hedonic score = 6.61 - 2.26 PC2 - 2.76 PC4**)**

**Figure 1.** External preference maps created from the results of the principal component analysis

**Table 4.** Results of the RPT data reduction by Principal component analysis**.**

| PC | % Variance explained | Highly related attributes |
|---|---|---|
| 1 | 15.4 | Whiteness (+), quantity of blended Job's-tears (+), Job's-tears taste (+), saltiness (+), and teeth and tough sticking after swallowing (+). |
| 2 | 14.2 | Smoothness by looking (+), smoothness by tasting (+), richness (+), and mouth coating after swallowing (+). |
| 3 | 10.1 | Hardness (+), melting rate (+), and number of ice crystals (+). |
| 4 | 9.7 | Stickiness (+), sweetness (+), and off-flavour (+). |
| 5 | 8.7 | Job's-tears odour (+), and coconut milk taste, (-). |
| 6 | 8.3 | Coconut milk odour (+). |
| Total | 66.4 | |

*Mj. Int. J. Sci. Tech.* **2007**, 01(2), 137-144

## Conclusion

The study on the difference of preference direction could provide more information about consumers' preference to the developed product. It guided the direction to improve products for each target consumer group. This work also showed the opportunity to develop Job's tears-based ice cream for cluster 1 and cluster 2, but for cluster 3 Job's-tears flavoured ice cream seemed to be more interesting to them.

## Acknowledgements

This work is a part of a research project supported by Faculty of Engineering and Agro Industry, Maejo University, Chiangmai, Thailand.

## References

1. A. Pink, "Gardening for the million", EText-No. 11892**, 2004**; Retrieved Feb 20, 2007, from: http://www.gutenberg.org/etext/11892.
2. L. G. Holm, J. V. Pancho, J. P. Herberger, and D. L. Plucknett, "A geographical atlas of world weeds", John Wiley & Sons, New York, **1979.**
3. A. Arber. The Gramineae--A Study of Cereal, Bamboo, and Grass. Wheldon & Wesley, New York, **1965.**
4. J. A. Duke and E. S. Ayensu, "Medicinal plants of China", Reference Publications, Michigan, **1985.**
5. P. H. List and L. Horhammer, "Hager's handbuch der pharmazeutischen praxis", Vol. 2-6, Springer-Verlag, Berlin, **1969-1979.**
6. D. Bown, "Encyclopaedia of herbs and their uses", Dorling Kindersley, London, **1995.**
7. H. Yeung, "Handbook of Chinese herbs and formulas", Institute of Chinese Medicine, Los Angeles, **1985.**
8. R. N. Chopra, S. L. Nayar, and I. C. Chopra, "Glossary of Indian medicinal plants" (including the supplement), Council of Scientific and Industrial Research, New Delhi, **1986.**
9. Brooklyn Botanic Garden, "Oriental herbs and vegetables", Vol. 39 (No. 2), New York, **1986.**
10. H. R. Cooper, M. D. Earle, and C. M. Triggs, in "Ratios of ideals–a new twist to an old idea", (Ed. L. S. Wu : Product testing with consumers for research guidance), American Society for Testing and Materials (ASTM), Philadelphia, **1989.**

*Mj. Int. J. Sci. Tech.* **2007**, *01(2)*, 145-156

***Maejo International***

***Journal of Science and Technology***

**ISSN 1905-7873**

Available online at www.mijst.mju.ac.th

*Full Paper*

# Selective fiber used for headspace solid-phase microextraction of abused drugs in human urine

**Sunanta Wangkarn [1*], and Wisitsak Wutiadirek [1]**

[1] Department of Chemistry, Faculty of Science, Chiang Mai University 50200, Thailand

* Corresponding author, e-mail : sunanta@chiangmai.ac.th

*Received: 2 August 2007 / Accepted: 24 August 2007 / Published: 11 September 2007*

**Abstract:** A sensitive and selective fiber for simultaneous analysis of three drugs of abuse (amphetamine, methamphetamine and ephedrine) in urine samples was explored using headspace solid phase microextraction and gas chromatography with flame ionization detection. Several parameters affecting extraction, viz. extraction temperature, extraction time, pH of solution, and salt addition were investigated. Among five commercially available fibers, divinylbenzene/carboxen/ polydimethylsiloxane was the most sensitive and selective fiber at the extraction temperature of 80 °C for 20 minutes and solution pH of 9.5-10.0, with added NaCl and desorption temperature of 220 °C for 2 minutes. Under these optimal conditions, the proposed solid phase microextraction method provided good linearity in the ranges of 0.1-10 µg/ml for amphetamine and methamphetamine and 0.5-20 µg/ml for ephedrine. The detection limits for amphetamine, methamphetamine and ephedrine were 9, 3 and 30 ng/ml, respectively. The recoveries of the three drugs in urine samples exceeded 85%.

**Keywords:** amphetamine, methamphetamine, ephedrine, solid phase microextraction.

## Introduction

Amphetamine (AMP), methamphetamine (MET) and ephedrine (EPH) are closely related in chemical structure (Figure 1). They are a class of central nervous system stimulants, usually without producing hallucination [1]. AMP and MET are generally manufactured in clandestine laboratories. They are significantly abused drugs in Thailand over the past 10 years. Called “ya ba” (crazy medicine) in Thai, AMP and MET are thought to come largely from small mobile production units across the border of the country. Synthesized MET is mainly produced from EPH. The varieties of

illicit samples have been found to contain MET or MET mixed with EPH [2]. Since 2001, the most commonly abused drugs in Thailand have been amphetamine-type stimulants. Although Thailand has laws prohibiting the sale and use of amphetamines, the use of amphetamines has increased [3].

The determination of abused drugs usually begins with the extraction of target compounds from the sample. Generally, liquid-liquid extraction (LLE) is widely used for extracting abused drugs. The method requires an excessive amount of organic solvent and it is time consuming. Solid phase extraction (SPE) is an alternative to LLE with the advantages of being cheaper and faster, however it requires a large variety of adsorbents and toxic solvents still have to be used as in LLE [4-7].

Solid phase microextraction (SPME) is a sample preparation technique which has been widely applied to extract AMP and MET from biological samples such as urine [8-12], hair [13-14], blood [15] and saliva [16]. The method does not require any organic solvent as the analytes are directly adsorbed onto a fiber usually made of fused silica. The fiber works as a cross-linked or stationary phase coated onto the fiber surface. The additional advantages are that SPME requires small sample volume and possesses extraction simplicity.

SPME-GC-MS analysis has been employed for synthetic drugs in hair samples [13] with detection limits of 1.29 and 0.37 ng/mg for AMP and MET, respectively. Solid-phase dynamic extraction (SPDE) using a stainless steel needle coated with a 50 μm film of polydimethylsiloxane (PDMS) and 10% of activated carbon was used for determining AMP and synthetic drugs in hair samples [14]. Limits of detection were found to be 0.04 ng/mg for AMP and 0.05 ng/mg for MET. Namera et al. used polydimethylsiloxane (PDMS) fiber for the extraction of AMP and MET in whole blood [15] with a detection limit of 10 ng/ml for AMP and MET.

Several groups have also reported the analysis of amphetamine-like drugs and their derivatives in urine samples using various fibers, for example, the PDMS fiber [8, 9, 11, 17], the carboxen polydimethylsiloxane (CAR/PDMS) and polydimethylsiloxane divinylbenzene (PDMS/DVB) fibers [17], the heptakis (2,6-di-*O*-methyl)-β-cyclodextrin blended with hydroxyl-terminated silicone oil (DM-β-CD/OH-TSO) fiber [18]. Yashiki et al. [9] reported that the minimum detectable levels of both AMP and MET were 100 ng/ml whereas the limit of detection values of those compounds was 30 ng/ml as reported by Raikos et al. [11]. The detection limits obtained using the PDMS fiber derivatized with heptafluorobutyric anhydride were 0.05 and 0.02 ng/ml for AMP and MET, respectively [17]. Employing the DM-β-CD/OH-TSO fiber, the limits of detection were 0.60 and 0.33 ng/ml for MET and EPH, respectively [18].

As stated earlier, many methods for the determination of AMP and MET in urine samples using the PDMS fiber either with or without derivatization have been developed. However, few methods on extraction of EPH using commercial SPME fiber were reported. Recently, EPH mixed with MET has been used extensively in the production of the so called “ya ba” stimulant drugs. In this study, the selectivity of SPME fiber for simultaneous analysis of MET, AMP and EPH was investigated using five commercially available SPME fibers. Variables affecting the SPME process, viz. extraction temperature, extraction time, pH of solution and salt addition were evaluated and optimized.

*Mj. Int. J. Sci. Tech.* **2007**, *01(2)*, 145-156

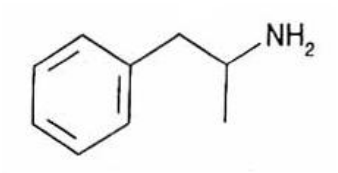


Amphetamine (AMP)

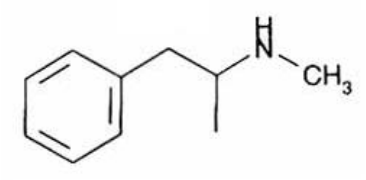


Methamphetamine (MET)

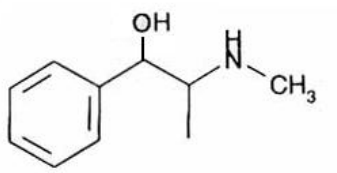


Ephedrine (EPH)

**Figure 1.** Chemical structures of abuse drugs used in this study.

## Materials and Methods

### *Materials*

Amphetamine sulfate, methamphetamine hydrochloride, ephedrine hydrochloride and phentermine hydrochloride (used as internal standard) were obtained from Medical Science Department (Bangkok, Thailand). All chemicals were of analytical grade with purity above 99 %.

Five different fibers: PDMS with coating thickness 100 μm, polyacrylate (PA) 85 μm, carboxen/polydimethylsiloxane (CAR/PDMS) 75 μm (Stable Flex), carbowax/divinylbenzene (CW/DVB) 65 μm (Stable Flex), and DVB/CAR/PDMS 50/30 μm (Stable Flex) were purchased from Supelco (Bellefonte, PA, USA). All fibers were conditioned according to the supplier's instructions.

### *Gas chromatography*

The gas chromatograph used was a Hewlett Packard HP-5890 Series II equipped with a flame ionization detector. The column was HP-5MS (30m x 0.25 mm I.D., 0.25 μm film thickness). The oven temperature was: initial 55 °C, held for 0.5 min, programmed to 230 °C at 20 °C/min, and then held for 2 minutes. The carrier gas was nitrogen maintained at a flow rate of 1.2 ml/min. The temperature of injector and detector were set at 220 °C and 260 °C, respectively. A split/splitless injector was used in the splitless mode.

### *SPME procedure*

The parameters that affect the SPME process such as fiber type, extraction temperature, extraction time, pH of solution and salt addition were evaluated and optimized. Spiked aqueous solutions used for extraction efficiency were adjusted to pH 9.5 with 1.0 M sodium hydroxide.

First of all, the selection of the fiber type was investigated. Each spiked aqueous solution (2 ml; 1 μg/ml of each analyte) and 0.6 g sodium chloride, adjusted to pH 9.5 with 1.0 M sodium hydroxide was placed in a 10-ml headspace vial. The vial was sealed with a septum and aluminum cap. Then it was immersed in a thermostatic water bath at 80 °C and stirred at speed of 300 rpm. The fiber was then exposed to the headspace over the solution for 20 minutes and thermally desorbed in the GC injection port for 2 minutes.

The effect of extraction temperature was investigated by varying in the range of 50-90 °C. The extraction time was evaluated from 5 to 30 minutes. Then the pH of the aqueous solutions was varied from 8.5 to 11.0. Finally, the influence of salt types on the extraction was evaluated employing

aqueous solutions containing sodium chloride or sodium sulfate. All experiments were carried out in the spiked aqueous solutions. For recovery test, urine samples were spiked with appropriate concentrations of the three abused drugs and 0.1 µg/ml of phentermine hydrochloride was also added as internal standard. To avoid carry-over, each fiber was kept in the GC injection port for another 10 min before the next run. It was also confirmed that no carry-over effect was observed after 10 minutes.

## Results and Discussion

*Selection of fiber*

In order to achieve maximum efficiency of extraction of the three target drugs from the spiked aqueous solution, five different fibers, viz. PDMS, PA, CAR/PDMS, CW/DVB and DVB/CAR/PDMS, were initially evaluated in this study. The result of the evaluation showed that all three drugs (Figure 1) could be sufficiently extracted by the fibers, except for the CAR/PDMS fiber (Figure 2). This may be rationalized by the fact that the CAR/PDMS is semi-polar fiber while the PDMS fiber is nonpolar, whereas the PA, CW/DVB and DVB/CAR/PDMS fibers are polar. As indicated in Figure 2, all fibers exhibited somewhat lower efficiency for extracting EPH. This is because the existence of the β-hydroxyl group of EPH makes it more soluble in water [19]. Also, small and broad peaks for EPH were observed. Among the five fibers studied, the DVB/CAR/PDMS provided high extraction efficiency, particularly for AMP and MET as observed in Figure 2. On the other hand, the CAR/PDMS is least sensitive to the three drugs studied. The DVB/CAR/PDMS was therefore selected for further method development and applications

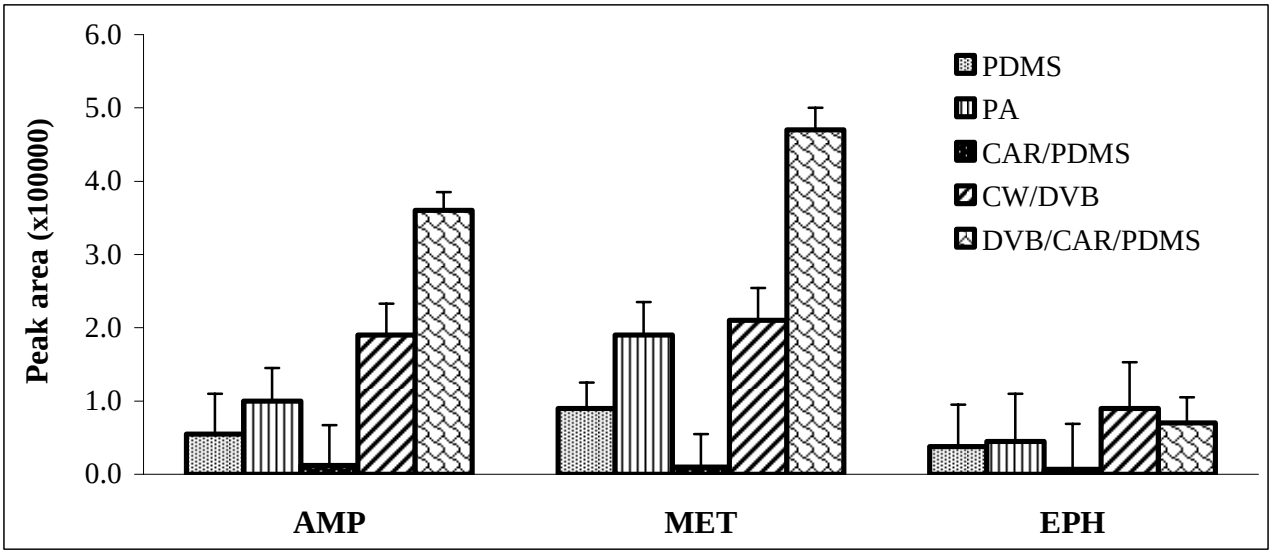


**Figure 2.** Effect of fiber coating type on extraction amount and percent relative standard deviation (%RSD) of three abused drugs (n = 3). Spiked water samples containing 1 µg/ml of each compound and 0.6 g sodium chloride, adjusted to pH 9.5 with 1.0 M sodium hydroxide were extracted at 80 °C for 20 min.

*Mj. Int. J. Sci. Tech.* **2007**, *01(2)*, 145-156

*Effect of extraction temperature and extraction time*

For the SPME method, temperature is an important factor in the extraction efficiency as it affects the kinetics of the reaction and diffusion of the analytes [20]. The effect of temperature on extraction yield, as represented by the peak area, was investigated by extracting a spiked aqueous solution in a thermostatic water bath for 15 minutes. The extraction temperature was increased in 5-10°C steps from 50 to 90°C. The extraction yield of AMP and MET increased with temperature until it reached a maximum at 80 °C, whereas the extraction yield of EPH continued to increase with temperature until 90 °C (Figure 3). This is because EPH is more soluble in water and can form more hydrogen bonding, which makes it more difficult to volatilize. The peak areas of AMP and MET obtained at 80 °C were increased by 2 and 3 times respectively, as compared to those obtained at 50°C. In order to avoid water boiling, the temperature selected for the extraction of the three drugs was 80°C.

Extraction time was also found to affect the extraction efficiency of the three drugs as shown in Figure 4. At extraction time from 5 to 20 minutes, peak areas were increased 61%, 74% and 67% for AMP, MET and EPH, respectively. Increasing extraction time beyond this period provided lower amounts of analytes extracted. Thus, the results at 80°C indicated that extraction time of 20 minutes was suitable for determining AMP, MET and EPH in aqueous solution.

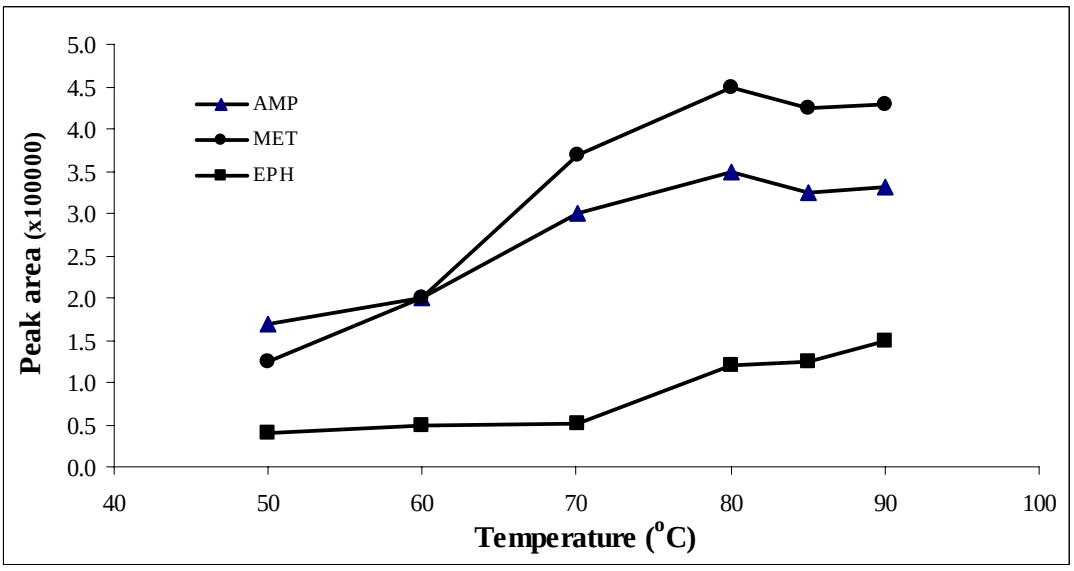


**Figure 3.** Temperature profiles for the extraction of three drugs using DVB/CAR/PDMS fiber.

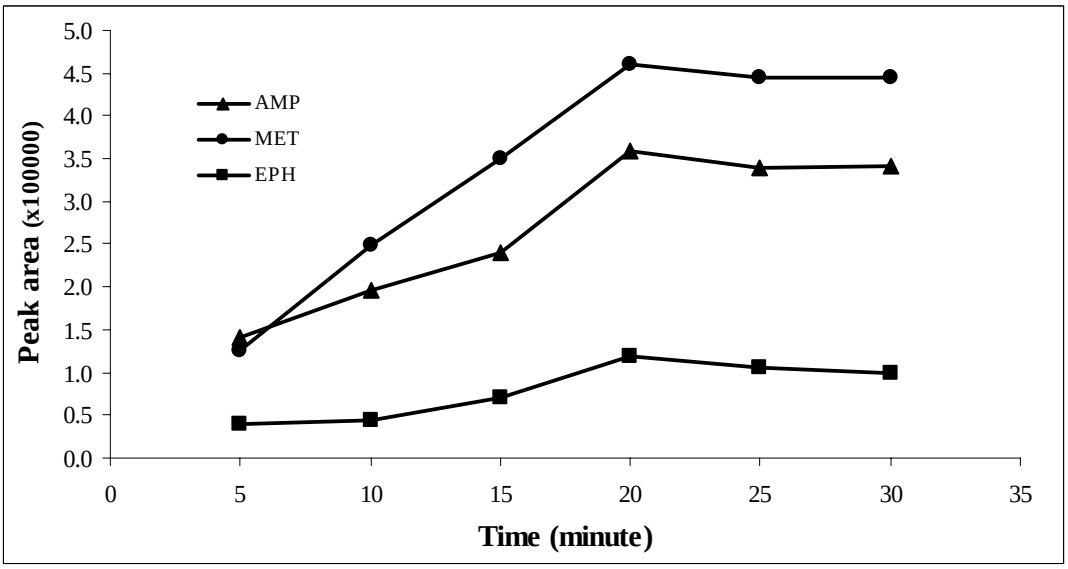


**Figure 4.** Extraction time profiles for the extraction of three drugs using DVB/CAR/PDMS fiber at 80 °C.

*Effect of solution pH*

It has been reported that the determination of AMP, MET and their derivatives is satisfactory in alkaline solution [8, 11, 12, 21]. In this work, the pH of solution was varied from 8.5 to 11.0 for SPME of AMP, MET and EPH. As shown in Figure 5, the extracted amount of the three drugs (the peak area) increased with increasing pH to a maximum at 9.5 (for AMP and MET) and 10 (for EPH). This may be explained by the fact that at a high pH, the acid-base equilibria of the three drugs, all being a weakly basic compound, significantly shift toward the neutral forms [22, 23], which have a higher affinity for the fiber, thereby increasing the amounts extracted. At still higher pH, however, the extraction efficiency began to decrease. This might be due to the formation of the new ionized forms of the three drugs starting to occur, thereby decreasing the neutral forms available for adsorption onto the fiber.

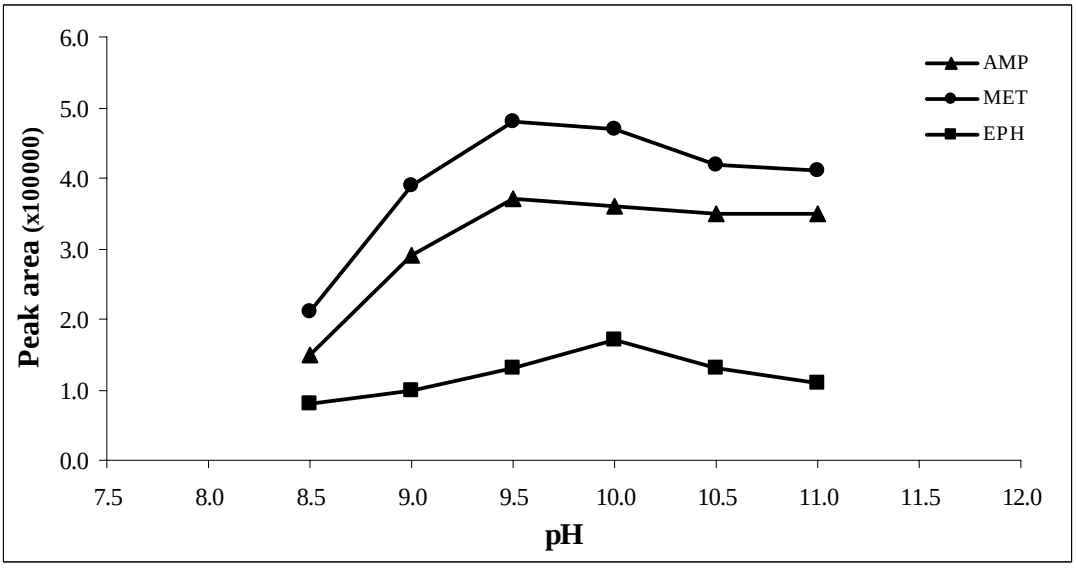


**Figure 5.** Effect of solution pH on the extraction of the three drugs using DVB/CAR/PDMS fiber at 80°C.

*Mj. Int. J. Sci. Tech.* **2007**, *01(2)*, 145-156

*Effect of salt addition*

In order to enhance the extraction efficiency, two types of salt (sodium chloride and sodium sulfate) added at the amount of 0.4 g in the aqueous solution (2 ml) containing 1 μg/ml of each drug were investigated. This effect was studied in solutions of pH 10.0 (adjusted with 1.0 M sodium hydroxide). As demonstrated in Figure 6, the extracted amounts of the three drugs increased significantly with the addition of each salt (5 times for AMP, MET and 7 times for EPH compared to the absence of salt). This may be explained by the fact that the addition of salt to the aqueous solution causes a decrease in solubility of the drugs in the aqueous phase, consequently increasing adsorption of the drug onto the fiber surface [22, 24]. The results obtained for AMP and MET are in good agreement with other reports [8, 22, 24]. In addition, the extraction efficiency obtained using sodium chloride and sodium sulfate was similar. Sodium chloride was therefore selected for further investigation.

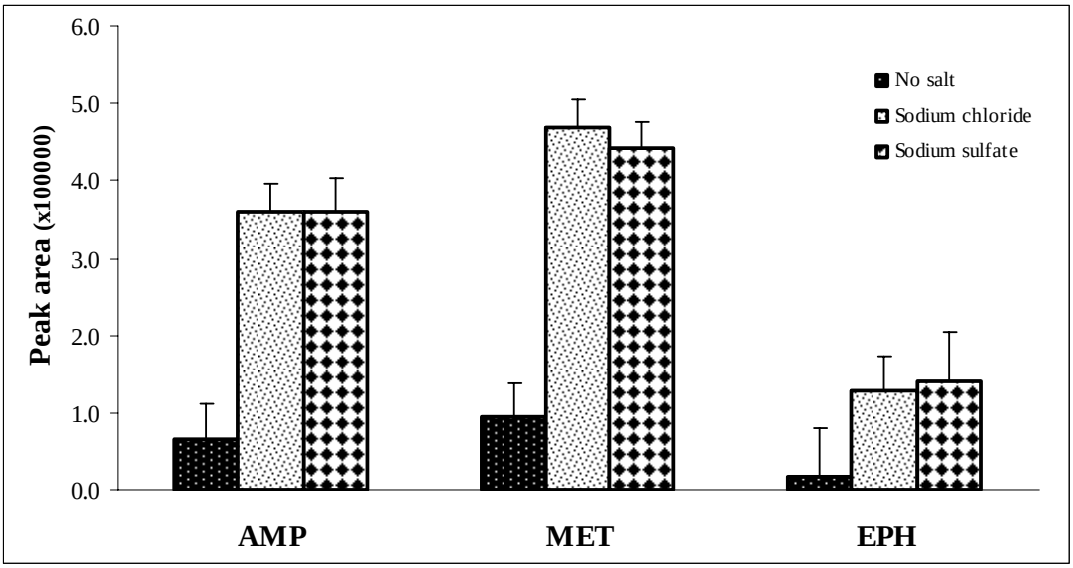


**Figure 6.** Effect of salt type on the extraction of the three drugs using DVB/CAR/PDMS fiber at 80 °C.

*Characteristics of the developed HS-SPME method*

An example of the chromatograms of the abused drug standards obtained by HS-SPME method under SPME optimum conditions is depicted in Figure 7. Calibration data obtained using phentermine hydrochloride as internal standard, limits of detection (LOD) and limits of quantitation (LOQ) are summarized in Table 1. Excellent linearity was obtained over the entire concentration ranges with correlation coefficient ($r^2$) greater than 0.999. The LOD calculated from low concentration value calibration curves were 9 ng/ml for AMP, 3 ng/ml for MET and 30 ng/ml for EPH with a signal-to-noise ratio of 3 (S/N = 3). The LOD of AMP and MET obtained in this work are lower than those presented by other groups employing a commercial PDMS fiber [9, 11]. Although the LOD values of MET and EPH are higher than those reported by Zhou and Zeng [18], a simple commercial fiber instead of a sophisticated fiber was used in this study. In addition, the LOD and LOQ obtained in this

study are lower than the concentration (e.g., 10 µg/ml for EPH) which is regarded as positive for illegal use of amphetamine drugs. The extraction time of SPME method was less than that reported by Zhou and Zeng [18].

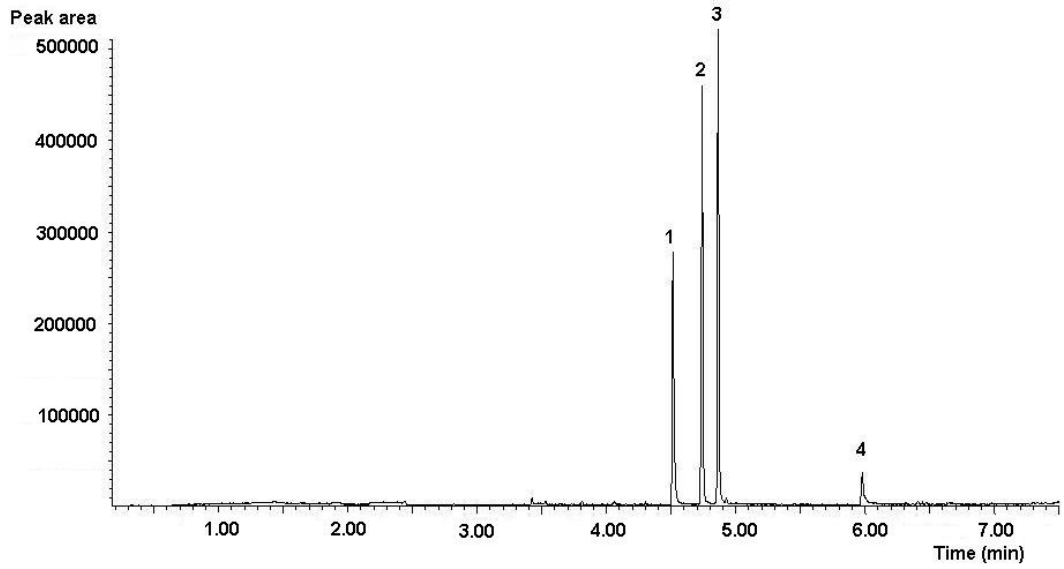


**Figure 7.** Chromatogram of standard mixture of the three abused drugs obtained using the DVB/CAR/PDMS fiber under SPME optimum conditions. Peak assignment: (1) amphetamine, (2) phentermine, (3) methamphetamine and (4) ephedrine.

**Table 1.** Linearity, detection limit and quantitation limit of the developed method

| Compound | Range of linearity (µg/ml) | Correlation coefficient ($r^2$) | Limit of detection (ng/ml) | Limit of quantitation (ng/ml) |
|---|---|---|---|---|
| AMP | 0.1-10 | 0.9993 | 9 | 30 |
| MET | 0.1-10 | 0.9999 | 3 | 10 |
| EPH | 0.5-20 | 0.9990 | 30 | 100 |

The accuracy and precision values of the three standards spiked at two concentration levels in blank urine from different sources were investigated to determine the effect of different matrices of urine samples. The results demonstrated that the developed HS-SPME-GC method provides good recovery in the range of 86-98%, with the standard deviation (SD) ranging from 1.1 to 3.1, as shown in Table 2. The intra-day and inter-day RSD values at two different concentrations ranged from 1.8-4.9% and 3.8-6.8%, respectively (Table 2).

*Mj. Int. J. Sci. Tech.* **2007**, *01(2)*, 145-156

**Table 2.** Recovery and relative standard deviation of intra-day and inter-day analysis of the three drugs.

| Concentration (μg/ml) | Compound | Recovery (%) (mean ± SD) | RSD (%) | |
|---|---|---|---|---|
| | | | Intra-day (n =5) | Inter-day (n = 5) |
| 0.5 | AMP | 89.2 ± 2.1 | 3.7 | 4.9 |
| | MET | 91.7 ± 1.5 | 2.2 | 4.2 |
| 1.0 | AMP | 94.6 ± 1.8 | 1.8 | 4.5 |
| | MET | 98.5 ± 1.1 | 1.3 | 3.8 |
| | EPH | 85.8 ± 3.1 | 4.9 | 6.8 |
| 2.0 | EPH | 91.3 ± 2.3 | 3.3 | 5.1 |

*Application to real samples*

The developed HS-SPME-GC method was applied to the analysis of AMP, MET and EPH in urine samples collected from three suspected persons. An example of the chromatograms of the abused drugs in urine samples is shown in Figure 8. All resulting chromatograms were obtained without endogenous interferences. The amounts of AMP and MET in all urine samples were found in the range of 23-128 ng/ml, whereas EPH was not present (Table 3).

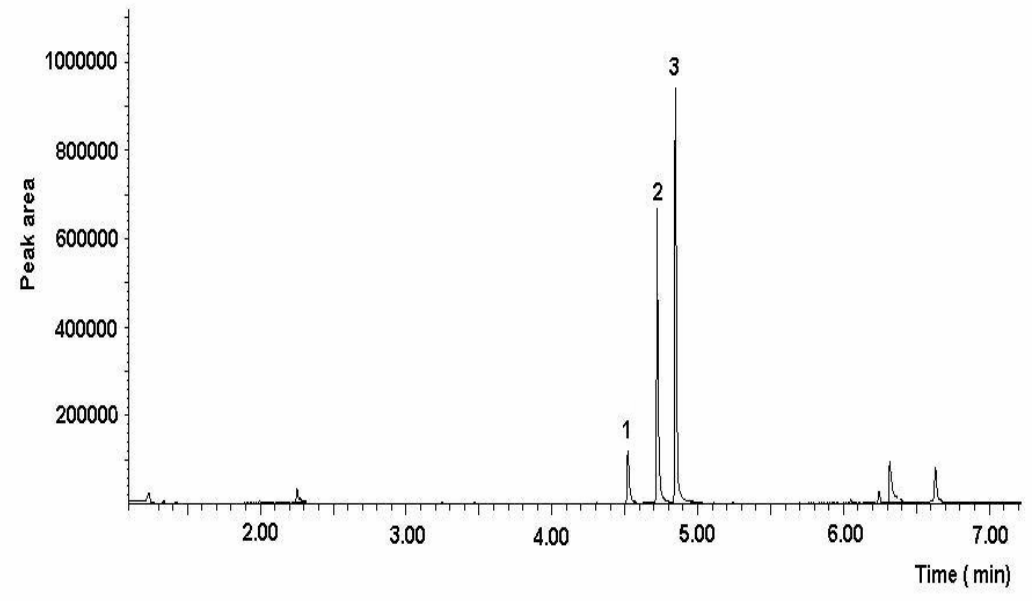


**Figure 8.** Chromatogram of abused drugs present in a urine sample using DVB/CAR/PDMS fiber under SPME optimum conditions. Peak assignment: 1 = amphetamine, 2 = phentermine, 3 = methamphetamine.

**Table 3**. Concentrations of the three drugs in urine samples

| Sample | Amount±SD (ng/ml) | | |
|---|---|---|---|
| No. | AMP | MET | EPH |
| 1 | 28.3±1.2 | 127.7±1.1 | ND |
| 2 | 22.9±2.3 | 91.3±1.9 | ND |
| 3 | 34.9±1.1 | 103.2±1.3 | ND |

ND: not detected.

## Conclusion

Headspace SPME coupled with GC-FID is a rapid and simple method for extraction and quantitative analysis of AMP, MET and EPH in human urine. In this study, the DVB/CAR/PDMS fiber was found to give higher extraction efficiency than other commercially available fibers, especially PDMS. Under the proposed method, the results were obtained with low limits of detection, good precision, linearity dynamic ranges, and interference minimization. In view of the simplicity, sensitivity and selectivity, the present method is recommendable for doping control.

## Acknowledgements

The financial support for this work from the Postgraduate Education and Research Program in Chemistry (PERCH) of Thailand is gratefully acknowledged. The authors thank Dr. N. Smith of King's College, University of London, for his helpful suggestions.

## References

1. United Nations, "Terminology and information on drugs", Scientific Section Laboratory, 1999.
2. V. Puthaviriyakorn, N. Siriviriyasomboon, J. Phorachata, W. Pan-ox, T. Sasaki, and K. Tanaka, "Identification of impurities and statistical classification of methamphetamine tablets (Ya-Ba) seized in Thailand", *Forensic. Sci. Int.,* 2002, *126*, 105-113.
3. K. Melbye, C. Khamboonruang, P. Kunawararak, D. D. Celentano, T. Prapamontol, K. E. Nelson, C. Natpratan, and C. Beyrer, "Lifetime correlates associated with amphetamine use among northern Thai men attending STD and HIV anonymous test sites", *Drug Alcohol Depend*, 2002, *68*, 245-253.
4. C. Casari and A. R. J. Andrews, "Application of solvent microextraction to analysis of amphetamine and phencyclidine in urine", *Forensic. Sci. Int.*, 2001, *120*, 165-171.
5. M. Pujadas, S. Pichini, S. Poudevida, E. Menoyo, P. Zuccaro, M. Farre, and R. Torre, "Development and validation of a gas chromatography-mass spectrometry assay for hair analysis of amphetamine, methamphetamine and methylenedioxy derivatives", *J. Chromatogr. B,* 2003, *798*, 249-255.
6. H. Schutz, J. C. Gotta, F. Erdmann, M. Ribe, and G. Weiler, "Simultaneous screening and detection of drugs in small blood samples and bloodstains", *Forensic. Sci. Int.*, 2002, *126*, 191-196.

7. K. Hara, S. Kashimura, Y. Hieda, and M. Kageura, "Simple extractive derivatization of methamphetamine and its metabolites in biological materials with Extrelut columns for their GC-MS determination", *J. Anal. Toxicol.*, 1997, *21*, 54 -58.
8. F. Centini, A. Masti, and B. Comparini, "Quantitative and qualitative analysis of MDMA, MDEA, MA and amphetamine in urine by headspace/solid phase micro-extraction (SPME) and GC/MS", *Forensic. Sci. Int.*, 1996, *83*, 161-166.
9. M. Yashiki, T. Kojima, T. Miyazaki, N. Nagasawa, Y. Iwasaki, and K. Hara, "Detection of amphetamines in urine using headspace-solid phase microextraction and chemical ionization selected ion monitoring", *Forensic Sci. Int.*, 1995, *76*, 169–177.
10. A. Ishii, H. Seno, T. Kumazawa, M. Nishikawa, K. Watanabe, H. Hattori, and O. Suzuki, "Simple clean-up of methamphetamine and amphetamine in human urine by direct-immersion solid phase microextraction (DI-SPME)", *Jpn. J. Forensic Toxicol.*,1996, *14*, 228–232.
11. N. Raikos, K. Christopoulou, G. Theodoridis, and H. Tsoukali, "Determination of amphetamines in human urine by headspace solid-phase microextraction and gas chromatography", *J. Chromatogr. B*, 2003, *789*, 59-63.
12. N. Snow, "Solid-phase micro-extraction of drugs from biological matrices", *J. Chromatogr. A.*, 2000, *885*, 445-455.
13. S. Gentili, M. Cornetta, and T. Macchia, "Rapid screening procedure based on headspace solid-phase microextraction and gas chromatography-mass spectrometry for the detection of many recreational drugs in hair", *J. Chromatogr. B.*, 2004, *801*, 289-296.
14. F. Musshoff, D. W. Lachenmeier, L. Kroener, and B. Madea, "Automated headspace solid-phase synamic extraction for the determination of amphetamines and synthetic designer drugs in hair samples", *J. Chromatogr. A.*, 2002, *958*, 231-238.
15. A. Namera, M. Yashiki, J. Liu, K. Okajima, K. Hara, T. Imamura, and T. Kojima, "Simple and simultaneous analysis of fenfluramine, amphetamine and methamphetamine in whole blood by gas chromatography-mass spectrometry after solid phase microextraction and derivatization", *Forensic Sci. Int.*, 2000, *109*, 215-223.
16. M. Yonamine, N. Tawil, R. L. de. M. Moreau, and O. A. Silva, "Solid-phase micro-extraction–gas chromatography–mass spectrometry and headspace-gas chromatography of tetrahydrocannabinol,
amphetamine, methamphetamine, cocaine and ethanol in saliva samples", *J. Chromatogr. B.*, 2003, *789*, 73-78.
17. K. J. Chia and S. D. Huang, "Simultaneous derivatization and extraction of amphetamine-like drugs in urine with headspace solid-phase microextraction followed by gas chromatography-mass spectrometry", *Anal. Chim. Acta*, 2005, *539*, 49-54.
18. J. Zhou and Z. Zeng, "Novel fiber coated with β-cyclodextrin derivatives used for headspace solid-phase microextraction of ephedrine and methamphetamine in human urine", *Anal. Chim. Acta*, 2006, *556*, 400-406.
19. S. Wercinski, "Solid phase microextraction: a practical guide", Marcel Dekker, New York, 1999.
20. H. Lord and J. Pawlisyn, "Evolution of solid-phase microextraction technology", *J. Chromatogr. A.*, 2000, *885*, 153-193.

21. M. R. Lee, Y. S. Song, B. H. Hwang, and C. C. Chou, “Determination of amphetamine and methamphetamine in serum via headspace derivatization solid-phase microextraction-gas chromatography-mass Spectrometry”, *J. Chromatogr. A.*, 2000, *896*, 265-273.
22. S. W. Myung, H. K. Min H.K, S. Kim, M. Kim, J. B. Chao, and T. J. Kim, “Determination of amphetamine, methamphetamine and dimethamphetamine in human urine by solid phase microextraction (SPME)-gas chromatography/mass spectrometry”, *J. Chromatogr. B.*, 1998, *716*, 359-365.
23. S. W. Myung, S. H. Yoon, and M. Kim, “Analysis of benzene ethylamine derivatives in urine using the programmable dynamic liquid-phase microextraction (LPME)”, *Analyst*, 2003, *128*, 1443-1446.
24. H. Fang, M. Liu, and Z. Zeng, “Solid-phase microextraction coupled with capillary electrophoresis to determine ephedrine derivatives in water and urine using a sol-gel derived butyl methacrylate/silicone fiber”, *Talanta*, 2006, *68*, 979-986.

*Mj. Int. J. Sci. Tech.* **2007**, *01(2)*, 157-165

***Maejo International***

***Journal of Science and Technology***

**ISSN 1905-7873**

Available online at www.mijst.mju.ac.th

*Review*

# The pyrido[1,2-*a*]azepine *Stemona* alkaloids

**Stephen G. Pyne,[1*] Alison T. Ung,[1] Araya Jatisatienr[2] and Pitchaya Mungkornasawakul[3]**

[1] Department of Chemistry, University of Wollongong, Wollongong, New South Wales, 2522, Australia.

[2] Department of Biology, Chiang Mai University, Chiang Mai, 50200, Thailand.

[3] Department of Chemistry, Chiang Mai University, Chiang Mai, 50200, Thailand.

*Corresponding author, e-mail: spyne@uow.edu.au

*Received:20 August 2007 / Accepted: 9 September 2007 / Published: 11 September 2007*

**Abstract:** This paper reviews the isolation, structure elucidation, proposed biosynthesis and biological activities of the small, but increasing, number of pyrido[1,2-*a*]azepine *Stemona* alkaloids.

**Keywords:** *Stemona*, alkaloids, pyrido[1,2-*a*]azepine, insecticide

## Introduction

This paper reviews the isolation, structure elucidation, proposed biosynthesis and biological activities of the small, but increasing, number of pyrido[1,2-*a*]azepine *Stemona* alkaloids.

The extracts of *Stemona* roots have been used in traditional medicine in South East Asia, China and Japan to treat the symptoms of bronchitis, pertussis and tuberculosis and have been used as anti-parasitics on humans and animals [1,2].The *Stemona* plant is known in the Thai, Chinese and Vietnamese vernacular as, “Non Tai Yak”, “Bai Bu” and “Bach Bo”, respectively [1,2]. Some of the pure alkaloids derived from the extracts of the leaves and roots of *Stemona* species have been shown to have significant antitussive activity in guinea pig after cough induction [3] as well as insect toxicity, antifeedant and repellent activities [4-6]. The *Stemona* group of alkaloids includes more than eighty different natural products that have been structurally classified by Pilli into eight different groups [1]. The pyrrolo[1,2-*a*]azepine nucleus (5,7-bicyclic A,B-ring system) is common to all compounds in six of these groups (as in croomine, Figure 1a, for example). Recently, Greger [2] has classified the *Stemona* alkaloids into three skeletal types based on their proposed biosynthetic origins. These are the croomine, stichoneurine (as typified by neotuberostemonine) and the protostemonine skeletal types

(Figure 1). Under Pilli's classification the pyrido[1,2-*a*]azepine *Stemona* alkaloids (Figure 2) fall under the stemocurtisine **1** structural group, while they are classified as of the protostemonine skeletal type under Greger's classification based on their proposed biosynthesis from protostemonine (see Proposed Biosynthesis section).

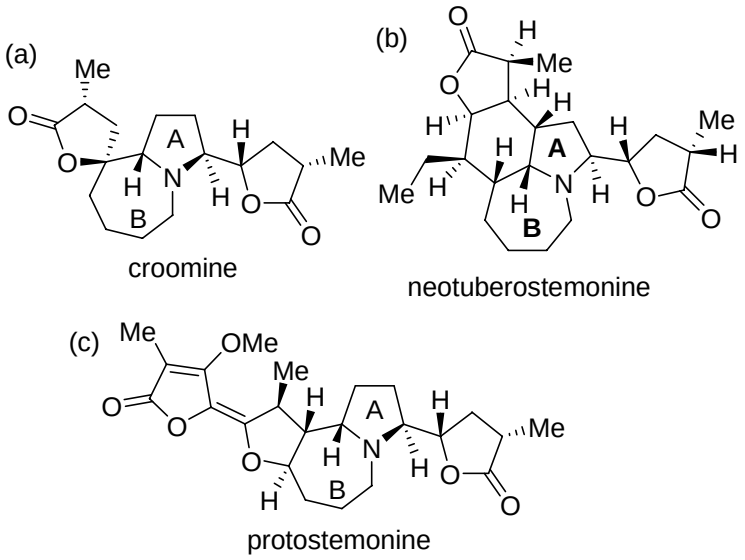


**Figure 1.** Skeletal types proposed by Greger [2]: (a) Croomine, from the croomine skeletal type; (b) neotuberostemonine, from the stichoneurine skeletal type; (c) protostemonine, from the protostemonine skeletal type.

**The pyrido[**1,2-***a*****]azepine *Stemona* alkaloids**

In 2003, we [7] and then Hofer and Greger [5] reported the first structures of *Stemona* alkaloids with a pyrido[1,2-*a*]azepine A,B-ring system. Our group reported the isolation of stemocurtisine **1** from the root extracts of *Stemona curtisii* growing in the northern part of Trang Province in Thailand [7]. The structure of stemocurtisine **1** was established by a single-crystal X-ray structural analysis, while Hofer and Greger reported the structures of stemocurtisine **1** (named pyridostemine in their paper), stemokerrin **2**, oxystemokerrin **3**, oxystemokerrin *N*-oxide **4** and methoxystemokerrin *N*-oxide **5** [5]. The structure of stemokerrin **2** was secured by a single-crystal X-ray structural analysis. These alkaloids were isolated from the root extracts of *S. kerri, S. curtisii* and an unknown species (*S. sp*.), designated as HG915. The *S. kerri* plant material grew in northern Thailand in Doi Sutep near Chiang Mai and in north-western Thailand in Khao Chomphu in Tak. The *S. curtisii* plant material came from southern Thailand in Satan Province while that from *S. sp* (HG 915) was from North-eastern Thailand in Udon Thani. The major alkaloid from the root extracts of both plant samples of *S. kerrii* was stemokerrin **2** with trace amounts of methoxystemokerrin **5** and oxystemokerrin *N*-oxide **4** also isolated, along with other pyrrido[1,2-*a*]azepine *Stemona* alkaloids. The *S. kerrii* species collected from Doi Sutep also provided oxystemokerrin **3** as a minor component. The root and leaf extracts of the *S. curtisii* plant material had trace amounts of oxystemokerrin **3** and its *N*-oxide **4** (in the leaves

*Mj. Int. J. Sci. Tech.* **2007**, *01(2)*, 157-165

only) along with other pyrrido[1,2-*a*]azepine *Stemona* alkaloids. The roots and leaves of *S. sp* (HG 915) contained trace amounts of stemocurtisine **1**, oxystemokerrin **3** and its *N*-oxide **4** (in the leaves only).

In 2004, our group reported the isolation of stemocurtisinol **6** and oxyprotostemonine **7** (Figure 3) from the same root extracts of *Stemona curtisii* that earlier provided us with stemocurtisine **1** as the major alkaloid [6]. The structure of stemocurtisinol **6** was also established from a single-crystal X-ray structural analysis (Figure 4a) while that of **7** was described earlier by Hofer and Greger [5].

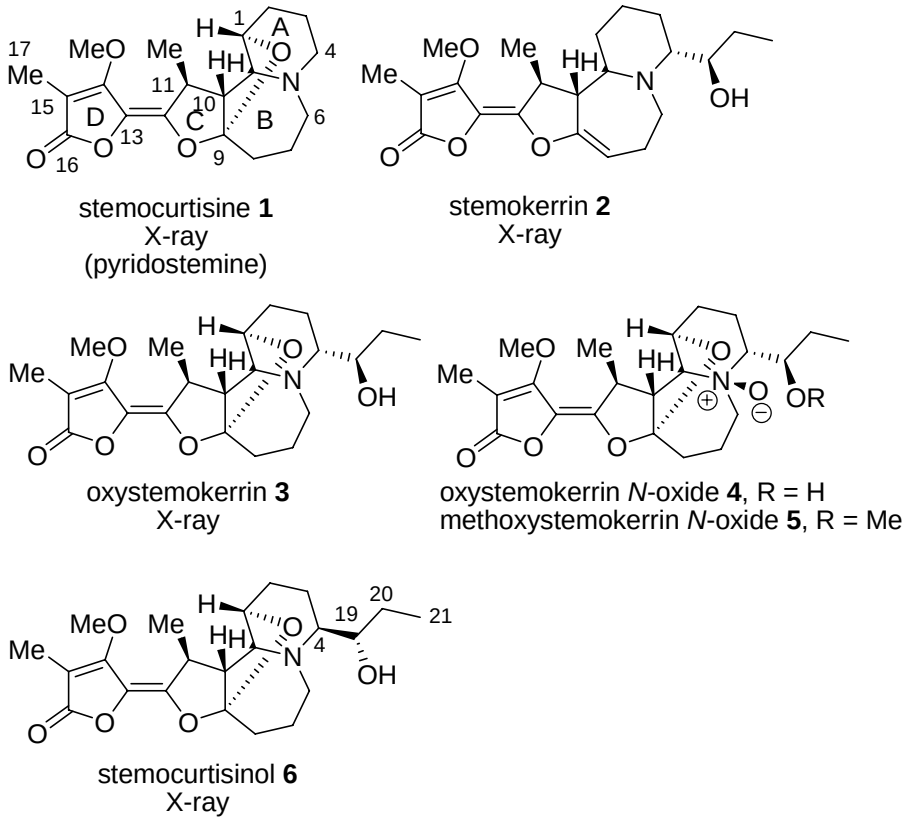


**Figure 2**. The first isolated pyrido[1,2-*a*]azepine *Stemona* alkaloids.

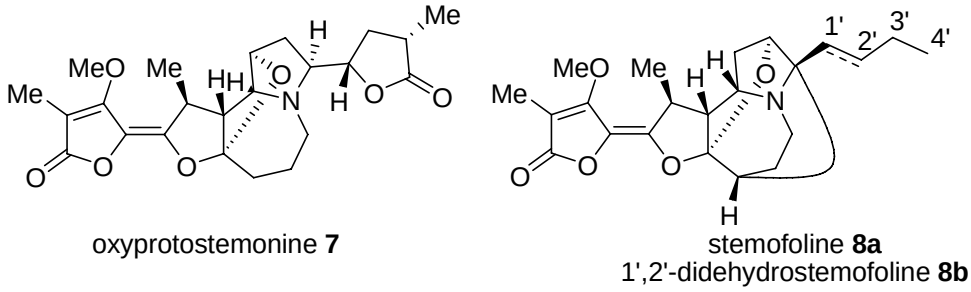


**Figure 3.** The structures of oxyprotostemonine **7**, stemofoline **8a**, and 1',2'-didehydrostemofoline **8b**.

Surprisingly, extracts of our *S. curtisii* plant sample and that of Hofer and Greger gave different pairs of pyrido[1,2-*a*]azepine *Stemona* alkaloids, **1** and **6,** and **3** and **4**, respectively. In our plant sample, the pyrido[1,2-*a*]azepine *Stemona* alkaloids **1** and **6** were the major alkaloid components [6,7].

In the case of Hofer and Greger [5], the pyrrolo[1,2-*a*]azepine *Stemona* alkaloids, stemofoline **8a** and 2'-hydroxystemofoline **8b** (Figure 3) were the major components. Interestingly, oxystemokerrin **3** and stemocurtisinol **6** were diastereomers at C-4 and C-19 (Figure 2). To further confirm the structure of **3** we isolated it from the root extracts of *S. kerrii* that were collected at Tambol Mae Hea, Amphur Muang, Chiang Mai, in August 2003. Fortunately we were able to grow crystals of this compound and verified its structure by a single-crystal X-ray structural analysis (Figure 4b) [8]. Figure 4 shows that the A-ring of both stemocurtisinol **6** [6] and oxystemokerrin **3** [8] adopts a chair conformation in which the C-4 1'-hydroxypropyl substituent is axially and equatorially positioned, respectively. Furthermore, it is clear that these compounds have the opposite configurations at the secondary carbinol carbon (C-19). In the solid state the C-19 hydroxyl group is intramolecularly H-bonded to the nitrogen atom in both alkaloids. Our X-ray analysis confirmed the structural assignments made for **3** by Hofer and Greger using 2D NMR spectroscopic methods.

(a)

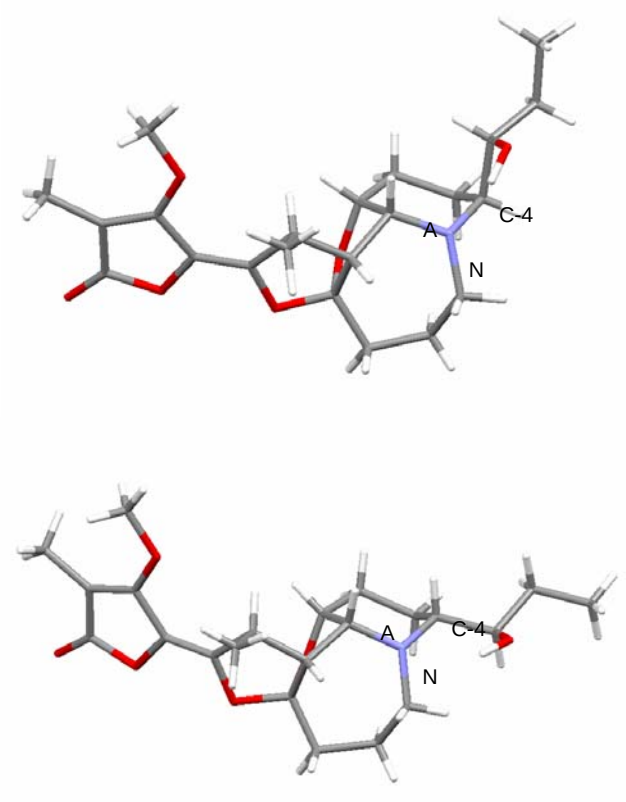


(b)

**Figure 4.** X-ray crystal structures of (a) stemocurtisinol **6** [6] and (b) oxystemokerrin **3** [8].

In a more recent study, Greger examined the alkaloid components of *S. curtisii* growing in different provinces in southern Thailand [9]. Plant collections from Krabi, Satun and Narathiwat showed stemofoline **8a** as the major alkaloid component with oxystemokerrin **3** and its *N*-oxide **4** present in varying amounts, while two different *S. cutisii* plant specimens from Chumphon were found to be rich in the pyrido[1,2-*a*]azepine *Stemona* alkaloids. One plant sample showed stemocurtisine **1** and stemocurtisinol **6** as the predominant alkaloid components, while the other showed oxystemokerrin **3**

*Mj. Int. J. Sci. Tech.* **2007**, *01(2)*, 157-165

and its *N*-oxide **4** as the major components and stemocurtisine **1** and stemocurtisinol **6** as more minor components. Interestingly, this latter plant contained both of the diastereomeric alkaloids, stemocurtisinol **6** and oxystemokerrin **3**. This study clearly indicated the variability of the alkaloid profiles of *S. curtisii* samples within different regions of southern Thailand. The phytochemical profile of the former *S. curtisii* plant sample from Chumphon is consistent with our sample of *S. curtisii* collected in the southern Thai province of Trang [6,7].

In work published in 2007, Ye [10,11] reported the isolation and identification of four new pyrido[1,2-*a*]azepine *Stemona* alkaloids from *S. sp.* from Vietnam (Figure 5). The root extracts of *S. cochinchinensis*, collected from the Sonla province of northern Vietnam, gave the alkaloid cochinchistemonine **9**, having a novel spirocyclic ring structure [10]. This structure was established by a single-crystal X-ray structural analysis. Meanwhile, the root extracts of *S. saxorum*, collected from the Hanam province of northern Vietnam, yielded the new alkaloids, cochinchistemoninone **10**, stemokerrin-*N*-oxide **11** and oxystemokerrilactone **12** along with oxystemokerrin **3**, its *N*-oxide **4** and stemokerrin **2** [11]. Other known pyrrolo[1,2-*a*]azepine *Stemona* alkaloids were also isolated. Cochinchistemonine **9** and cochinchistemoninone **10** and stemokerrin **2** and stemokerrin-*N*-oxide **11** are clearly related by oxidation-reduction chemical processes, while oxystemokerrilactone **12** is a truncated form of oxystemokerrin **3**.

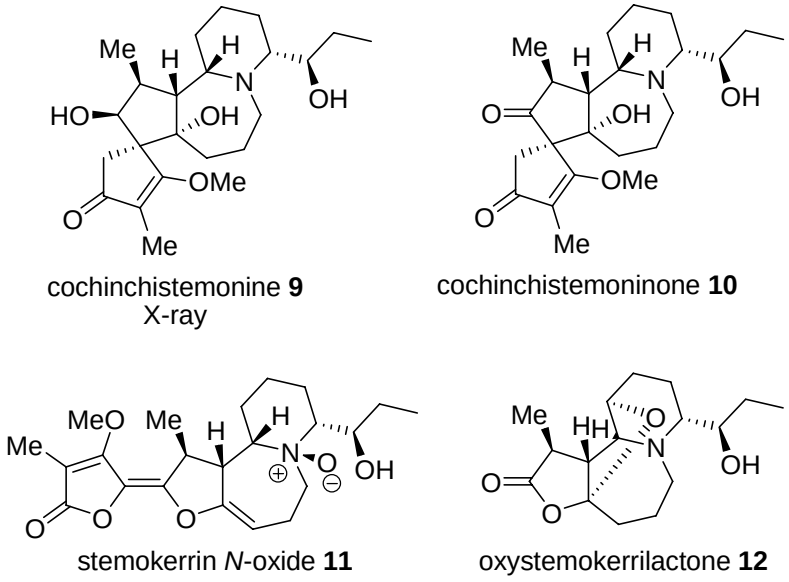


**Figure 5**. Pyrido[1,2-*a*]azepine *Stemona* alkaloids isolated from plants in Vietnam [10,11].

**Proposed Biosynthesis**

While biosynthetic studies on *Stemona* alkaloids have not been reported, a proposed biosynthetic pathway leading to the pyrrolo[1,2-*a*]azepine *Stemona* alkaloids has been made by Seger et al. [12]. The terpenoid origin of the C- and D-ring carbons (see Scheme 1 for ring numbering) has been postulated by Seger, while the A-ring of these alkaloids has been postulated to arise from spermidine. A ring expansion of the pyrrolidine ring (A-ring) of protostemonine to a piperidine ring has been proposed by Hofer and Greger to account for the biosynthesis of the pyrido[1,2-*a*]azepine *Stemona*

alkaloids (Scheme 1)[5]. This proposed mechanism does not account for the different stereochemistry at C-4 and C-19 in oxystemokerrin **2** and stemocurtisinol **6**.

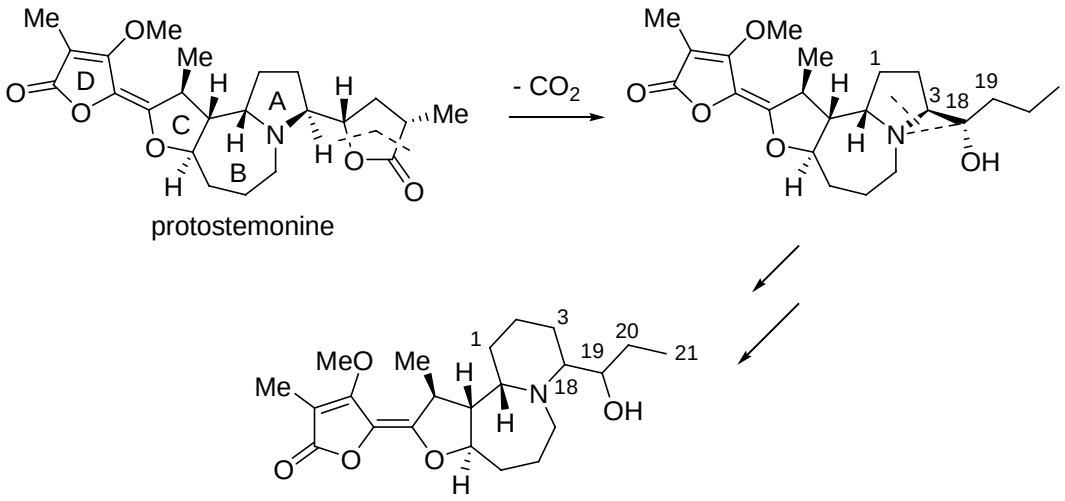


**Scheme 1.** Proposed biosynthesis of pyrido[1,2-*a*]azaepine alkaloids [5].

We have proposed an alternative biosynthesis as shown in Scheme 2 [8]. Our proposed biosynthesis of the A-ring of **2** and **6** is based on the known biosynthesis of the hemlock alkaloid (+)-conhydrine **13** from the acetate-derived polyketide derivative **14** [13,14]. Condensation of **14** with 1,4-diaminopropane, a biosynthetic product from the homospermidine synthase (HSS) production of homospermidine [15], could provide the piperidine A-ring precursor intermediate **15** (Scheme 2). A stereoselective reduction of the cyclic iminium ion intermediate **15** and a stereoselective oxidation at C-1 of the propyl side-chain of **15** may lead to intermediate iminium ion **16**. Coupling of **16** to a geranyl unit, as propsed by Seger et al. [12], could then provide alkaloids **3** or **6** (Scheme 2). Whatever

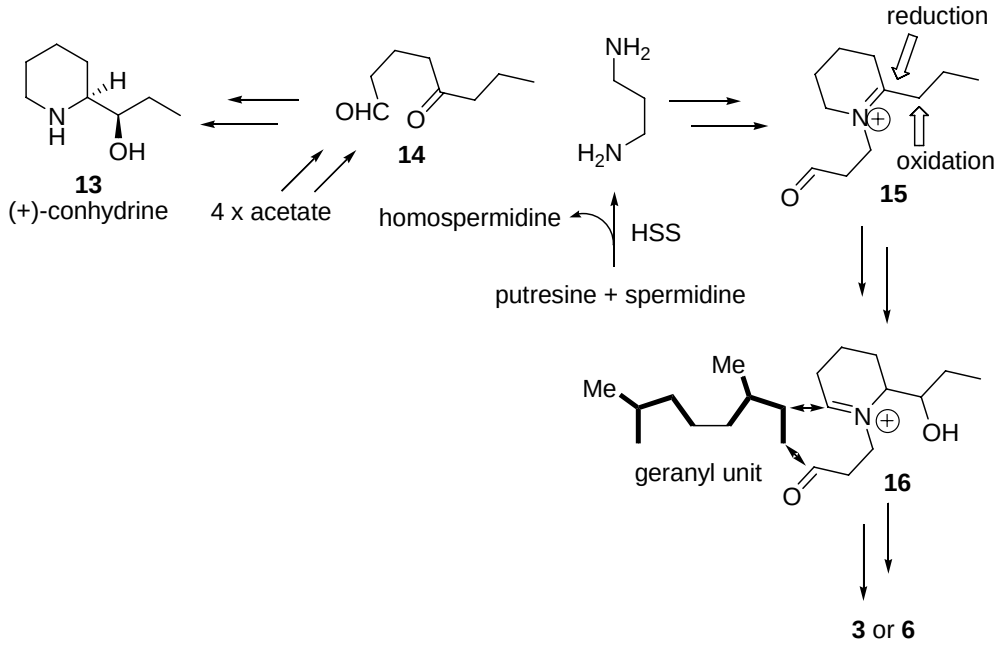

*Mj. Int. J. Sci. Tech.* **2007**, *01(2)*, 157-165

**Scheme 2.** Proposed biosynthesis of alkaloids **3** and **6** [8].

the biosynthetic pathway may be, however, it is clear that at least three *Stemona* species of plants have evolved to produce enzymes that give opposite stereochemical outcomes in their biosynthetic reactions, to produce stereoselectively either oxystemokerrin (**3**) or stemocurtisinol (**6**).

In the case of the spirocyclic ring structure types, Ye has proposed that cochinchistemonine **9** and cochinchistemoninone **10** are derived biosynthetically from stemokerrin **2** [10]. Hydrolysis of the enol ether group of stemokerrin **2** would be expected to give the diketone **17** which could undergo an intramolecular aldol reaction to give cochinchistemoninone **10**. A diastreoselective reduction of the ketone group of cochinchistemoninone **10** would then give cochinchistemonine **9** (Scheme 3).

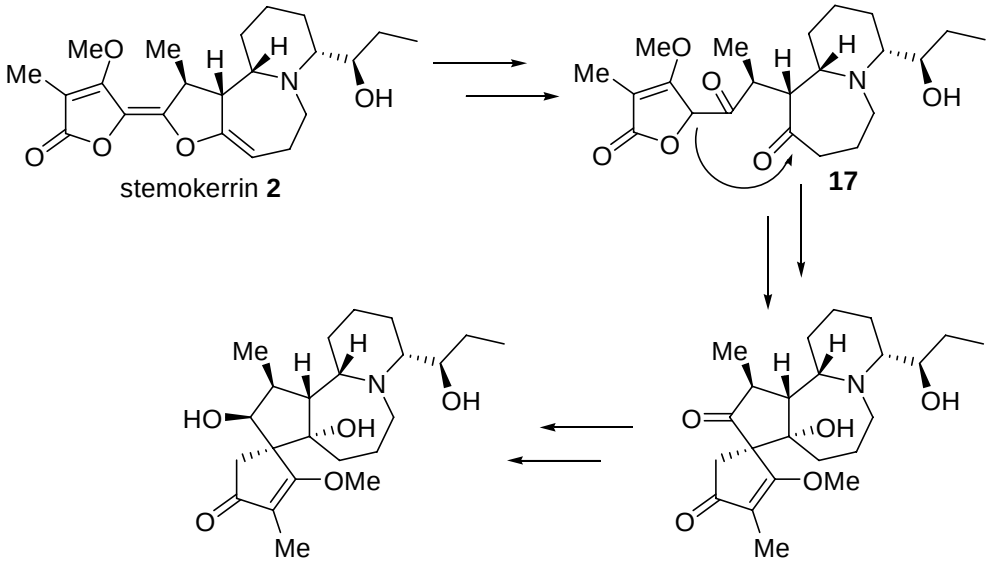


**Scheme 3.** Proposed biosynthesis of alkaloids **9** and **10** [10].

**Biological studies**

We have examined the larvicidal activity of our crude root extract of *S. curtisii* and that of compounds **1**, **6** and **7** on mosquito larvae (*Anopheles minimus*), using the WHO method to determine the $LC_{50}$ [6]. While the crude ethanol extract showed a $LC_{50}$ of 81 ppm, the individual alkaloid components were significantly more potent ($LC_{50}$ values of **1** and **6** were, 18 and 39 ppm, respectively). The most potent compound was oxyprotostemonine **7** having a $LC_{50}$ of 4 ppm. We have also demonstrated that the crude root extracts of *S. curtisii* shows strong insect antifeedant activities against third instar larvae of *Spodoptera littoralis* Boisduval [16]. The crude extract has been formulated into a "biopesticide" that shows great potential in agricultural field trials as an effective "natural pesticide" [16]. Hofer and Greger also demonstrated that their crude extract of *S. curtisii* had insecticidal activity against neonate larvae of *Spodoptera littoralis* with a $LC_{50}$ of 9 ppm [5], while their crude extracts of *S. kerrii* showed less insecticidal activity with $LC_{50}$ values of 48 (from Doi Sutep sample) and 89 (from Khao Chomphu sample) ppm. The individual alkaloids were also tested. Amongst the pyrido[1,2-*a*]azepine *Stemona* alkaloids tested (**1-5**) the most potent was oxystemokerrin **3** ($LC_{50}$ of 5.9 ppm), whereas stemocurtisine **1** was the least active ($LC_{50}$ of 149 ppm). Two of the

pyrrolo[1,2-*a*]azepine *Stemona* alkaloids also tested were much more potent, especially 1',2'-didehydrostemofoline **8b** ($LC_{50}$ of 0.8 ppm) and stemofoline **8a** ($LC_{50}$ of 2.0 ppm). These latter two compounds caused hyperactivity of the larvae resulting in their sudden death, whereas the pyrido[1,2-*a*]azepine *Stemona* alkaloids **1**-**5** only led to paralysis and the softening of the larval bodies [5].

A recent study by Limtrakul [17] showed that the crude root extract of *S. curtisii*, collected from Udon Thani in Thailand, inhibited the drug-efflux pump, P-glycoprotein. This study indicated the potential application of these extracts for the treatment of multidrug-resistant cancers. The alkaloid components of this extract were not determined. Future studies may involve the testing of the individual pure components.

## Conclusions

In conclusion, the pyrido[1,2-*a*]azepine *Stemona* alkaloids represent a small subset (about 10%) of the increasing number of *Stemona* alkaloids that have been discovered. In this paper the isolation, structure elucidation, proposed biosynthesis and biological activities of these alkaloids are reviewed from the time that they were first reported in 2003.

## Acknowledgments

We are grateful to the staff and students at the University of Wollongong and Chiang Mai University for their valuable contributions to this project. Their names are indicated in our publications. We are also grateful to the University of Wollongong, Chiang Mai University and the Department of Environmental Quality Promotion, Ministry of Natural Resources and Environment, Thailand for supporting this project.

## References

1. R. A. Pilli, G. B. Rosso, and M. C. F. de Oliveira, "The *Stemona* alkaloids", *The Alkaloids,* (Ed. G. A. Cordell), **2005**, Vol 62, Elsevier, Amsterdam , Ch. 2.
2. H. Greger, "Structural relationships, distribution and biological activities of *Stemona* alkaloids", *Planta Medica,* **2006**, *72*, 99-113.
3. H. S. Chung, P. M. Hon, G. Lin, P. P. H. But, and H. Dong, "Antitussive activity of *Stemona* alkaloids from *Stemona tuberosa*", *Planta Medica,* **2003**, *69*, 914-920.
4. B. Brem, C. Seger, T. Pacher, O. Hofer, S. Vajrodaya, and H. Greger, "Feeding deterrence and contact toxicity of *Stemona* Alkaloids - a source of potent natural insecticides", *J. Agric. Food Chem*., **2002**, *50*, 6383-6388.
5. E. Kaltenegger, B. Brem, K. Mereiter, H. Kalchhauser, H. Kahlig, O. Hofer, S.Vajrodaya, and H. Greger, "Insecticidal pyrido[1,2-*a*]azepine alkaloids and related derivatives from *Stemona* species", *Phytochemistry,* **2003**, *63*, 803-816.
6. P. Mungkornasawakul, S. G. Pyne, A. Jatisatienr, D. Supyen, C. Jatisatienr, W. Lie, A. T. Ung, B. W. Skelton, and A. H. White, "Phytochemical and larvicidal studies on *Stemona curtisii*: structure of a new pyrido[1,2-*a*]azepine *Stemona* alkaloid", *J. Nat. Prod*., **2004**, *67*, 675-677.

7. P. Mungkornasawakul, S. G. Pyne, A. Jatisatienr, D. Supyen, W. Lie, A. T. Ung, B. W. Skelton, and A. H. White, "Stemocurtisine, the first pyrido[1,2-*a*]azepine *Stemona* alkaloid", *J. Nat. Prod*., **2003**, *66*, 980-982.
8. P. Mungkornasawakul, H. Matthews, A. T. Ung, S. G. Pyne, A. Jatisatienr, W. Lie, B. W. Skelton, and A. H. White, "Confirmation of the structure of oxystemokerrin by single crystal X-ray structural analysis and a proposed biosynthesis", *ACGC Chem. Res. Comm.*, **2005**, *19*, 30-33.
9. J. Schinnerl, B. Brem, P. P. H. But, S. Vajrodaya, O. Hofer, and H. Greger, "Pyrrolo- and pyridoazepine alkaloids as chemical markers in *Stemona* species", *Phytochemistry*, **2007**, *68*, 1417-1427.
10. L. G. Lin, C. P. Tang, P. H. Dien, R. S. Xu, and Y. Ye, "Cochinchistemonine, a novel skeleton alkaloid from *Stemona cochinchinensis*", *Tetrahedron Lett.*, **2007**, *48*, 1559-1561.
11. Y. Z. Wang, C. P. Tang, P. H. Dien, and Y. Ye, "Alkaloids from the roots of *Stemona saxorum*", *J. Nat. Prod*., **2007**, *70*, 1356-1359.
12. C. Seger, K. Mereiter, E. Kaltenegger, T. Pacher, H. Greger, and O. Hofer, "Two pyrrolo[1,2-*a*]azipine type alkaloids from *Stemona collinsae* CRAIB: structure elucidations, relationships to asparagamine A, and a new biogenetic concept of their formation", *Chem. & Biodiversity*, **2004**, *1*, 265-279.
13. E. Leete, "Biosynthesis of the hemlock alkaloids: the incorporation of acetate-1-C14 into coniine and conhydrine", *J. Am. Chem. Soc*., **1964**, *86*, 2509-2513.
14. W. Steglich, B. Fugmann, and S. Lang-Fugmann (Ed.), "ROMPP Encyclopedia; Natural products", Georg Thieme Verlag, Stuttgart, **1997**, 285-286.
15. D. Ober and T. Hartmann, "Homospermidine synthase, the first pathway-specific enzyme of pyrrolizidine alkaloid biosynthesis, evolved from deoxyhypusine synthase", *Proc. Natl. Acad. Sci. U. S. A*., **1999**, *96*, 14777-14782.
16. T. Sastraruji, *PhD Thesis*, **2006,** Chiang Mai University, Thailand.
17. P. Limtrakul, S. Siwanon, S. Yodkeeree, and C. Duangrat, "Effect of *Stemona curtisii* root extract on p-glycoprotein and MRP-1 function in multidrug - resistant cancer cells", *Phytomedicine*, **2007**, *14*, 381-389.

*Mj. Int. J. Sci. Tech.* **2007**, *01(2)*, 166-177

***Maejo International***

***Journal of Science and Technology***

**ISSN 1905-7873**

Available online at www.mijst.mju.ac.th

*Full Paper*

# Physical mapping of *Bph3*, a brown planthopper resistance locus in rice

**Jirapong Jairin[1,*], Sa-nguan Teangdeerith[1], Phikul Leelagud[1], Kittiphong Phengrat[1], Apichart Vanavichit[2], and Theerayut Toojinda[2]**

[1] Ubon Ratchathani Rice Research Center, P.O. Box 65, Muang, Ubon Ratchathani 34000, Thailand,

2 Rice Gene Discovery Unit, Kasetsart University, Kamphaeng Saen, Nakhon Pathom 73140, Thailand

* Corresponding author; e-mail: (jirapong@ricethailand.go.th)

*Received: 23 August 2007 / Accepted: 6 September 2007 / Published: 24 September 2007*

**Abstract:** Resistance to brown planthopper (BPH), a destructive phloem feeding insect pest, is an important objective in rice breeding programs in Thailand. The broad-spectrum resistance gene *Bph3* is one of the major BPH resistance genes identified so far in cultivated rice and has been widely used in rice improvement programs. This resistance gene has been identified and mapped on the short arm of chromosome 6. In this study, physical mapping of *Bph3* was performed using a $BC_3F_3$ population derived from a cross between Rathu Heenati and KDML105. Recombinant $BC_3F_3$ individuals with the *Bph3* genotype were determined by phenotypic evaluation using modified mass tiller screening at the vegetative stage of rice plants. The recombination events surrounding the *Bph3* locus were used to identify the co-segregate markers. According to the genome sequence of Nipponbare, the *Bph3* locus was finally localized approximately in a 190 kb interval flanked by markers RM19291 and RM8072, which contain twenty-two putative genes. Additional phenotypic experiment revealed that the resistance in Rathu Heenati was decreased by increasing nitrogen content in rice plants through remobilization of nitrogen. This phenomenon should be helpful for identifying the *Bph3* gene.

**Keywords:** *Nilaparvata lugens*, BPH resistance gene, sequence information, *Oryza sativa*

*Mj. Int. J. Sci. Tech.* **2007**, *01(2)*, 166-177

## Introduction

The widespread damage caused by insect pests constitutes the most significant factors leading to substantial and unpredictable decrease in rice yield. Brown planthopper (BPH), *Nilaparvata lugens* Stål, a destructive monophagous insect pest, is one of the main biotic constraints in rice, causing huge yield losses in Asian rice-growing areas every year. The damage caused by BPH feeding has the greatest effect on the growth of rice plant [1]. In addition to feeding on the rice plant directly, BPH also causes indirect damage by transmitting viruses, which cause ragged and grassy stunt diseases [2].

Developing resistant rice cultivars is generally considered to be the most economic and effective way for controlling BPH. Rice plant resistance to BPH is recognized as a qualitative and quantitative trait. The genetic basis of the qualitative and quantitative BPH resistance has been well studied and at least 21 major resistance genes have been discovered from cultivated varieties and wild relatives [3-5]. Of these genes, 17 resistance genes have been assigned to rice chromosomes [3-14]. More than half of the discovered major resistance genes could not be used against some BPH populations found in Thailand [7]. Although BPH resistance genes have been intensively discovered and studied throughout the rice genome, until recently none of the BPH resistance gene has been cloned in rice and our current knowledge about insect resistance genes in rice plant is still limited.

Breeding a resistant cultivar with major resistance genes was highly successful. However, BPH itself also successfully adapts to feed on the resistant cultivars by changing their biotypes. The occurrence of new virulent biotypes has been a serious problem in breeding resistant rice cultivar against BPH. Identification and incorporation of new BPH resistance genes into rice cultivars are important breeding strategies to control the damage caused by new biotypes of BPH [4]. Therefore, selection of BPH resistance genes for improving resistant cultivars needs to be considered carefully.

A local rice cultivar of Sri Lanka, Rathu Heenati, was found to confer a strong and broad-spectrum resistance against BPH populations in Thailand [7]. The resistance in this cultivar was concluded to be controlled by a single dominant gene, *Bph3* [15-16]. The study of genetic analysis by classical genetic approach showed that f *Bph3* was closely linked to *bph4* in rice cultivar Babawee because no recombinants between these genes were observed among nearly 1,200 of $F_3$ progenies [17]. The chromosomal location of *Bph3* gene was first assigned to rice chromosome 10 based on trisomic analysis [18]. Later, it was suggested that *Bph3* was located on chromosome 4 and *bph4* was located on chromosome 6 [8, 13]. Recently, the chromosomal location of this locus has been confirmed on the short arm of chromosome 6 in two backcross populations derived from crosses of Rathu Heenati/KDML105 and PTB33/RD6. The locus is flanked by simple sequence repeat (SSR) markers RM589 and RM588 [7].

The publicly available rice genome sequence information has made map-based cloning in rice much more efficient in getting the target genes. Three BPH resistance genes, *Bph15*, *Bph18* and *bph19*, have been finely mapped on chromosome 3, 4 and 12, respectively [3-5]. *Bph15* was finely mapped to a genomic segment of approximately 47 kb long flanked by RFLP markers RG1 and RG2 [5]. The *bph19* locus was finely defined to an interval of about 60 kb flanked by SSR markers RM6308 and RM3134 [3]. The *Bph18* locus was also physically localized within an 843 kb physical interval that includes three BAC clones between the STS marker R10289S and SSR marker RM6869 [4]. In this study, the construction of a high-resolution linkage map with SSR markers is a crucial step in map-based cloning of *Bph3*. We report the fine mapping of the *Bph3* locus to an approximately 190 kb

target region on rice chromosome 6 using SSR markers. The region contains at least twenty-two putative functional annotation genes.

## Materials and Methods

### *Plant materials*

Two *indica* rice (*Oryza stiva* L.) cultivars were used as parents in this study. Rathu Heenati (acc. no. 11730), a landrace variety from Sri Lanka, carries a broad-spectrum resistance against four different BPH biotypes found in Thailand. KDML105, aromatic rice known as Jasmine rice, has a good cooking quality and adapts well in rainfed lowland areas in Thailand. The donor parent, Rathu Heenati, is highly resistant to BPH whereas the recurrent parent, KDML105, is extremely susceptible to BPH.

A backcross population $BC_3F_2$ consisting of 333 individuals was derived from the cross between Rathu Heenati and KDML105. The population was used to initially locate the *Bph3* in our previous study [7]. A $BC_3F_3$ population was developed from the $BC_3F_2$ resistant individual that shows heterozygous in the target region on chromosome 6. A total of 358 $BC_3F_3$ individuals derived from two families of $BC_3F_2$ were used to confirm the BPH resistance in the target region on the chromosome 6. From this population, two $BC_3F_3$ families consisting of 28 individuals were selected as material for physical mapping.

The parents and additional cultivars, TN1 and PTB33, were used in experiments for evaluating BPH resistance in vegetative and reproductive stages of rice plants.

### *Bioassay for BPH resistance*

A BPH population from a single colony of PBH was collected from Ubon Ratchathani province, Thailand, and was grown on a susceptible variety TN1 in a temperature-controlled rearing room. For evaluating the BPH resistance of parents, including resistant and susceptible lines at vegetative and flowering stages, three phenotypic experiments were conducted using standard seedbox screening (SSBS), modified mass tiller screening (MMTS) and semi-field screening (SMFS) methods. The SSBS was used to evaluate the BPH resistance of seedling plants. The pre-germinated seeds of the test lines were sown 5 cm apart in 20 cm rows in seedboxes. The susceptible control, TN1, was sown randomly in all the seedboxes. Seven days after sowing, the seedlings were infested with first to second nymphs of BPH at a number of twenty nymphs per seedling. Damage rating of the test lines was done when 90% of the plants in the susceptible control row were killed. The test lines were graded using the Standard Evaluation System (SES) for rice [19]. The MMTS was used to evaluate the BPH resistance of tillering-stage plants. The pre-germinated seeds of the test lines were individually sown (10×20 cm) in 7×24 $m^2$ plots. Twenty days after sowing, the seedlings were infested with 3rd-4th instar nymphs of BPH at a number of ten nymphs per seedling. Until TN1 and the susceptible recurrent parents died, we evaluated the severity scores of the test lines. The SMFS was used to evaluate rice plants at vegetative and reproductive stages in the rice field. Ten of twenty-day seedlings were transplanted (20×20 cm) in the rice field, and covered with a nylon net. Fifteen days after transplanting the rice plants were

*Mj. Int. J. Sci. Tech.* **2007**, *01(2)*, 166-177

infested with 3rd-4th nymphs of BPH at a number of five insects per hill. Then, we let the insect population increase for 1-2 generations. When all the TN1 had died, we scored the degree of damage undergone by the test seedlings. The scoring criteria were based on the SES. The remains of resistant lines were scored every ten days until flowering stage.

For evaluating the BPH resistance of $BC_3F_3$ progenies, the bioassay was done with the MMTS technique at the tillering stage of rice under greenhouse condition. In brief, the seeds of TN1, a susceptible cultivar, PTB33, RD6, parents and each $BC_3F_3$ progeny were separately sown in seedling plots. When the seedlings had 3-4 tillers (approximately 20-25 days), three similar growth-conditioned tillers were then separated and were transplanted in 7×24 $m^2$ plots. The leaves of each seedling were clipped for DNA extraction before transplanting. The leaf samples were stored frozen at -80°C prior to extraction. Genomic DNA samples were extracted using the method of Chen and Ronald [20]. Ten days after transplanting, the seedlings were infested with 3rd- 4th instar nymphs of the BPH at the density of 10 insects per tiller. Then, we let the insects feed, mate, lay eggs and hatch freely. Until TN1 and the susceptible recurrent parents died, we evaluated the severity scores of each $BC_3F_2$ individual on a scale of 1 (very slight damage) to 9 (all plants dead) according to the SES.

*Fine genetic mapping of the Bph3 locus*

Initial localization of the *Bph3* locus was based on the recent report of mapping on the short arm of rice chromosome 6 [7]. The linkage analysis was performed using 333 $BC_3F_2$ individuals from the cross between Rathu Heenati and KDML105. The resistance gene was located between the flanking markers RM589 and RM588. In this study, 16 additional SSR markers covering the BPH resistance gene region were used to screen Rathu Heenati and KDML105. The SSR markers were obtained from the public database released by Gramene (http://www.gramene.org/). PCR was performed in a 10 µl reaction mixture containing 25 ng of template DNA, 0.5 µM of each primer, 250 µM of each dNTP, 1.5 mM $MgCl_2$, 1 unit *Taq* polymerase and 2 µl of ×10 PCR reaction buffer. Amplification was performed for 35 cycles (1 min at 94°C, 1 min at 55°C and 2 min at 72°C) followed by 5 min at 72°C. The amplified product was electrophoresed on a 4.5% denaturing silver-stained polyacrylamide gel. The polymorphism between Rathu Heenati and KDML105 was screened using 16 SSR markers covering the target region. The polymorphic markers were used to assay 28 $BC_3F_3$ plants for the fine genetic and physical mapping of *Bph3*. The physical location of the *Bph3* locus in the *japonica* cultivar Nipponbare was determined. A physical map spanning the resistance gene locus was constructed *in silico*, based on the contig map. The prediction of candidate resistance genes with the conserved structures in the target region anchored by tightly linked markers was then analyzed according to the sequences of Nipponbare and was based on the TIGR prediction method (http://www.tigr.org).

## Results

*Evaluation of BPH resistance*

The resistance of the parents and the BPH resistant cultivar PTB33 was studied using SSBS, MMTS and SMFS methods. At the seedling and tillering stage, Rathu Heenati and PTB33 expressed

strong resistance to BPH in both the SSBS and MMTS (Table 1). Although Rathu Heenati and PTB33 showed high resistance to BPH in the vegetative stage (seedling to tillering stages) of heavy BPH infestation (Figure 1a, Table 1), they showed susceptibility during the reproductive stage (flowering to grain filling stage) when the remaining BPH in the field moved to feed on the panicles and panicle necks until plants died (Figure 1b,c, Table 2). Similar to Rathu Heenati, the resistant $BC_3F_2$ lines from a cross between Rathu Heenati and KDML105 were also susceptible to the BPH at flowering and grain filling stages (Figure 1d). The result indicated that Rathu Heenati and introgression lines were susceptible to BPH at the flowering stage and BPH can feed and grow well on the panicle of the resistant plants carrying *Bph3*.

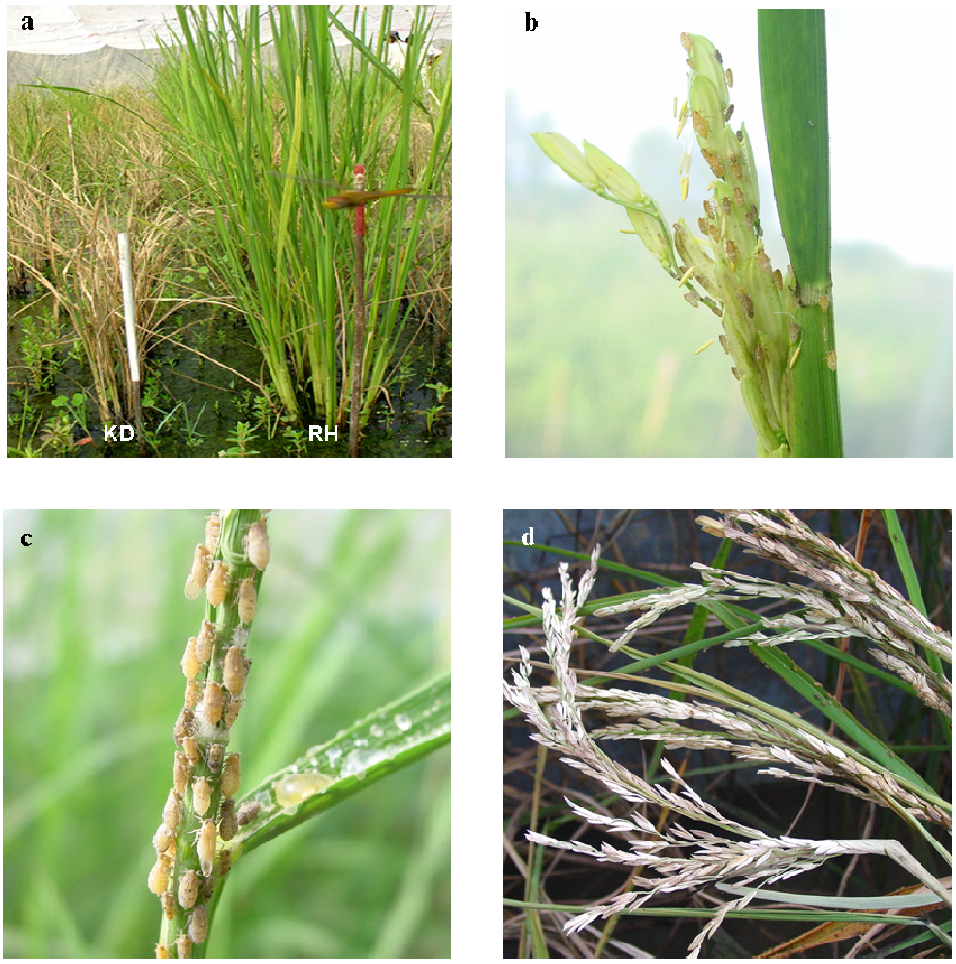


**Figure 1.** Evaluation of BPH resistance of Rathu Heenati in the rice field using semi-field screening **a** Rathu Heenati (RH) is highly resistant while KDML105 (KD) is susceptible to BPH at vegetative stage, **b** BPH nymphs can feed on the panicle at the flowering stage, **c** BPH feeding on the panicle neck at grain filling stage, **d** The feeding of BPH causes the unfilled grains before the rice plant dies.

*Mj. Int. J. Sci. Tech.* **2007**, *01(2)*, 166-177

**Table 1.** Average damage score of the parents and controls by BPH at the vegetative stage (seedling and tillering stages) of rice plants

| Cultivar | Seedling stage by SSBS | | | Tillering stage by MMTS | | |
|---|---|---|---|---|---|---|
| | 7 DAI | 10 DAI | 14 DAI | 7 DAI | 15 DAI | 23 DAI |
| Rathu Heenati | 1.0 | 2.2 | 2.4 | 1.0 | 1.0 | 1.0 |
| PTB33 | 1.0 | 2.4 | 3.5 | 1.0 | 1.0 | 1.0 |
| KDML105 | 6.5 | 8.9 | 9.0 | 5.0 | 9.0 | 9.0 |
| TN1 | 7.0 | 9.0 | 9.0 | 5.0 | 9.0 | 9.0 |

DAI=Days after infestation
Damage score: 1=very slight damage, 9=all plants dead

**Table 2.** Average damage score of the parents and controls by BPH. The evaluation was conducted in the rice field using semi-field screening method (SMFS)

| Cultivar | 30 DAI | 40 DAI | 50 DAI | Flowering stage |
|---|---|---|---|---|
| Rathu Heenati | 1.0 | 1.0 | 1.6 | 9.0 |
| PTB33 | 1.0 | 1.1 | 2.0 | 9.0 |
| KDML105 | 9.0 | 9.0 | 9.0 | 9.0 |
| TN1 | 9.0 | 9.0 | 9.0 | 9.0 |

DAI=Days after infestation
Damage score: 1=very slight damage, 9=all plants dead

In the previous study, we used a backcross population consisting of 2,343 $BC_3F_2$ plants derived from a cross between Rathu Heenati (donor parent) and KDML105 (recurrent parent), in which 333 random plants were used to evaluate and locate a major BPH resistance gene [7]. In this study, we selected two $BC_3F_2$ plants that were heterozygous on the short arm of chromosome 6 where *Bph3* is located. A total of 358 $BC_3F_3$ plants derived from the selected two $BC_3F_2$ were randomly selected and used to confirm the inheritance of BPH resistance in Rathu Heenati at the vegetative stage. Phenotypic evaluations of BPH resistance for the $BC_3F_3$ and the parents were conducted using the MMTS. Rathu Heenati expressed strong resistance to a Thai biotype of BPH whereas KDML105 was completely susceptible to BPH (Figure 2). Segregation of resistant and susceptible plants (265 resistant plants, 93 susceptible plants) fits in a 3:1 ratio in the 358 random $BC_3F_3$ plants ($\chi^2 = 0.18$, $p<0.67$) indicating the presence of a major dominant gene conferring resistance to BPH.

*Physical mapping of the Bph3 locus*

The published genetic mapping data from our previous study was used as a starting point for this study. Using a backcross population, $BC_3F_2$, derived from a cross between Rathu Heenati and KDML105, *Bph3* was mapped to about 1.4 cM interval between SSR markers RM588 and RM589 on the short arm of chromosome 6 [7]. The co-segregation marker RM589 explained 80.4% of the phenotypic variance of BPH resistance in the 358 random $BC_3F_3$ individuals.

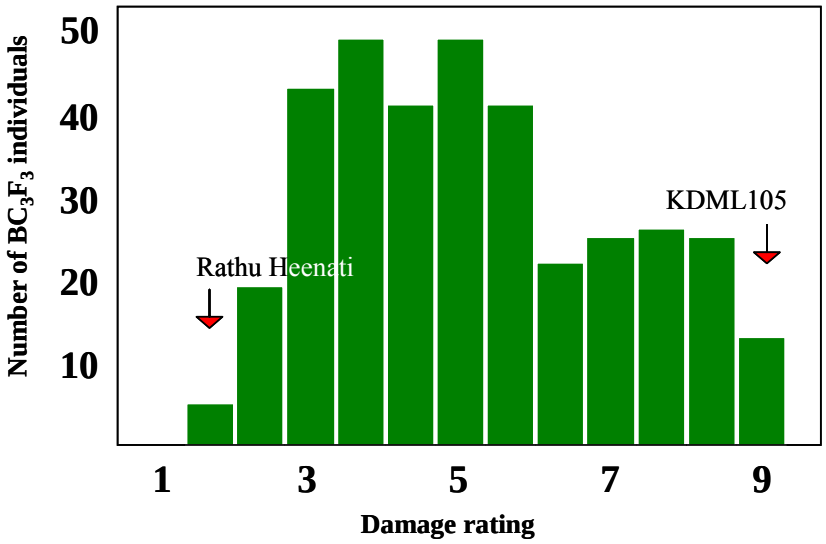


**Figure 2**. Frequency distribution of BPH resistance scores based on the overall average of four scoring periods from the modified mass tiller screening method at tillering stage of rice plants. The mean scores of Rathu Heenati and KDML105 are indicated by arrows

The location of the *Bph3* resistance gene on the map was determined on the basis of the resistance scores of the 28 recombinant plants. MMTS was employed to distinguish resistant plants from susceptible ones among the recombinant plants. A number of 16 SSR markers located around this genomic region were selected to screen polymorphism between Rathu Heenati and KDML105. Seven SSR markers (RM19291, RM19295, RM19296, RM8072, RM8074, RM19310, and RM19311) detected polymorphisms between the two parents. These seven markers were used to narrow down the region encompassing *Bph3* locus between the two flanking markers RM589 and RM588. The resulting high-resolution map of *Bph3* showed that RM19291 and RM8072 were flanking the *Bph3* resistance gene (Figure 3a). Twenty-eight plants were then identified with recombination break points between the SSR markers RM19291 and RM8072. Of these, three recombinant events were detected with marker RM19291, and five were found with marker RM8072. No recombinants were detected with the other three markers, RM19295, RM19296, and RM589. These three markers were identified to co-segregate with the *Bph3* locus. According to the genome sequence of a japonica rice cultivar Nipponbare, the *Bph3* locus was finally localized to approximately 190 kb interval flanked by markers RM19291 and RM8072 (Figure 3b).

*Putative genes in the 190 kb region*

Based on the available sequence annotation database of the *japonica* rice Nipponbare (http://www.rgp.dna.afrc.go.jp; http://www.tigr.org), there are twenty-two predicted putative genes in the 190 kb target region. Of these genes, seven had unknown functions, seven were hypothical proteins, and the functional annotation of the remaining eight genes encoded one NBS-LRR disease resistance protein (LOC_Os06g03500), two pentatricopeptides (LOC_Os06g03530 and LOC_Os06g03570), two oligopeptide transporters (LOC_Os06g03540 and LOC_Os06g03560), one

*Mj. Int. J. Sci. Tech.* **2007**, *01(2)*, 166-177

zinc finger, C3HC4 type family protein (LOC_Os06g03580), one transcriptional co-regulator family protein (LOC_Os06g03600), and one protein kinase family protein (LOC_Os06g03610).

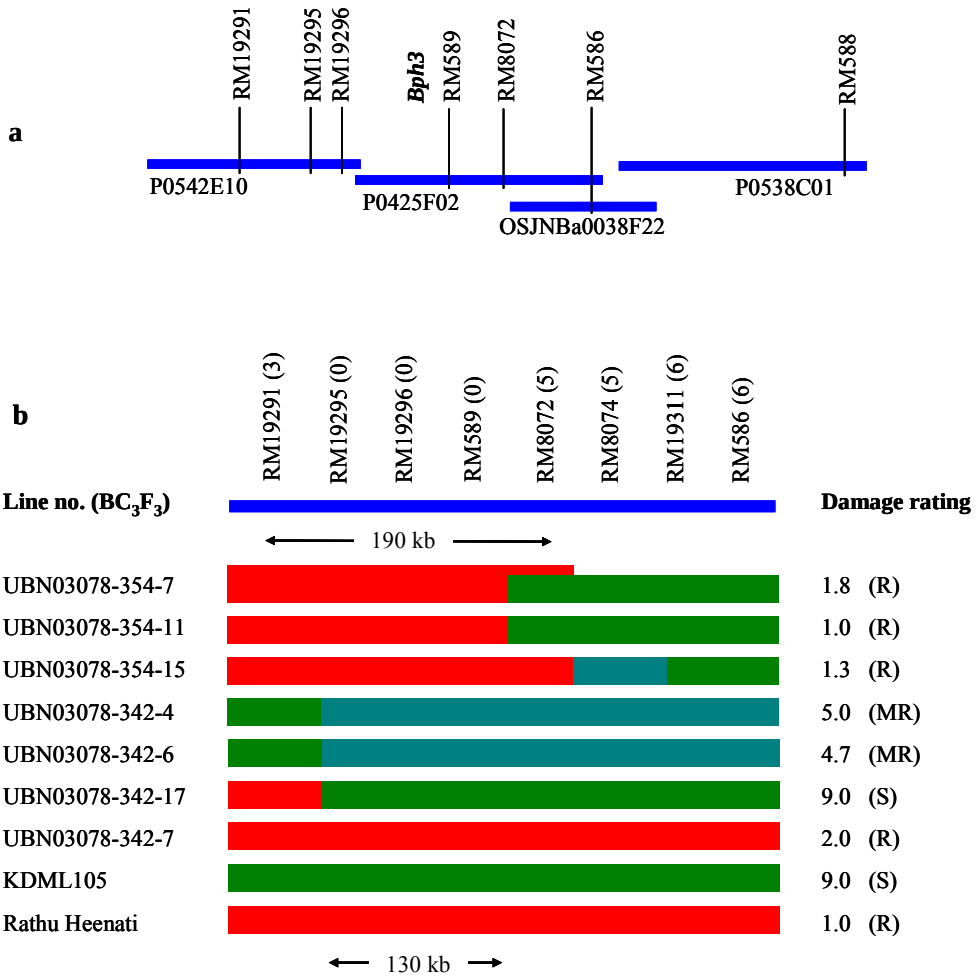


**Figure 3.** Physical map of the *Bph3* locus. **a** Physical mapping of *Bph3* locus showing four Nipponbare BAC clones interval delimited by RM19291 and RM588, **b** Genotypes and phenotypes of the recombinants between RM19291 and RM586. Red bars = homozygous Rathu Heenati allele; green bars = homozygous KDML105 allele; blue bars = heterozygous. The numerals in parentheses indicate the recombination events occurred at the corresponding marker loci. The BPH resistance score is on the right, R = resistant, MR = moderately resistant, and S = susceptible

## Discussion

In our earlier study, a major resistance gene *Bph3* was identified using two backcross populations, which were derived from crosses of Rathu Heenati/KDML105 and PTB33/RD6, at the vegetative stage of the rice plant with heavy infestation of the second generation of BPH. The broad-spectrum BPH resistance gene was mapped within a 1.4 cM interval between SSR markers RM589 and RM588 onto the short arm of rice chromosome 6. Starting from the flanking markers, we were able to locate the gene to a 190 kb segment of genomic DNA. The fragment contains twenty-two putative genes, which encode fourteen proteins (seven hypothetical and seven expressed) of unknown function, an NBS-LRR

disease resistance protein, two pentatricopeptides, two oligopeptide transporters, a zinc finger protein, a transcriptional co-regulator protein, and a protein kinase protein. This result should be helpful for cloning the *Bph3* gene, which is now in progress. The closely linked molecular markers found in this study should be also useful in the marker-assisted breeding programs against BPH.

According to previous studies, some of the major and minor BPH resistance genes tend to be clustered in particular regions of the rice chromosomes. There are four main clusters of BPH resistance genes on chromosomes 3, 4, 6 and 12. Of the twenty-one major BPH resistance genes reported to date, six resistance genes are derived from wild species of *Oryza* and the remaining fifteen are derived from native *indica* cultivars [5-14, 21-23]. Among the resistance genes from cultivated rice, *Bph3* has the most broad-spectrum resistance against BPH biotypes found in Thailand [7]. *Bph3* has been used extensively in rice breeding programs throughout Asia as well as in Thai breeding programs. Although breeding resistant cultivars with major resistance genes has been highly successful, BPH itself has also successfully adapted to feed on resistant cultivars. Therefore, understanding the gene function or mechanism of BPH resistance gene may provide information on how BPH can overcome the resistant cultivars. BPH resistance genes have been intensively studied but none of the gene has been cloned in rice. Until now, up to five resistance genes, *Bph1*, *bph2*, *Bph15*, *Bph18* and *bph19* have been finely mapped and were about to be cloned [3-5, 24].

BPH resistance in rice cultivars carrying *Bph3* was reported to govern an antixenotic reaction to BPH [25]. Rathu Heenati has no repellent chemical against planthoppers and only has common volatiles as released by susceptible cultivars. The feeding inhibition of this cultivar occurred when the insect started to ingest phloem sap [26]. In the present study, Rathu Heenati showed high resistance to BPH at the vegetative stage; only a few numbers of BPH could survive on the resistant plants. The surviving insects had light body weight, slow development and low fecundity (data not shown). On the other hand, Rathu Heenati was susceptible to BPH at the flowering and grain filling stages. BPH could feed and grow well on panicle necks and panicles of the resistant plants (Figure 1). This phenomenon may affect the expression of BPH resistance gene in Rathu Heenati. Further studies are needed to clarify this event especially the chemical analysis of the phloem sap from resistant and susceptible isogenic lines [27]. Comparison of phloem sap components by using a chemically defined diet [28] will also provide information to clarify the phenomenon.

The mechanism of plant resistance to phloem sap-feeding insects has been reported to involve the balance of the amino acid composition of the phloem sap [29-30]. Variation of phloem amino acid composition has been implicated in the nitrogen quality of the phloem sap for phloem feeders [29-31]. It plays a major role in the performance and fitness of insects [32]. The susceptibility of Rathu Heenati at the flowering stage observed in this study may probably involve in the nutritional quality of the phloem sap. In the rice panicles, the total nitrogen arises from remobilization of glutamine synthetase through the phloem from senescing organs [33-35]. The major forms of reduced nitrogen in the phloem sap of rice plants are glutamine and asparagine [36]. Application of a nitrogen fertilizer can dramatically increase the amount of total nitrogen and free amino acids available in the phloem sap [37], especially glutamine and asparagine [38-39]. Therefore, the remobilization of nitrogen in rice plants can increase the total free amino acids in the phloem sap, which may affect the BPH resistance in rice plants and insect performance. Currently, three possible hypotheses can explain how BPH resistance gene is involved in the phenomena: (i) a resistance gene(s) may be poorly expressed in the

upper internodes of heading rice plants, (ii) the amount of the reduced nitrogen forms or nitrogenous compounds in the phloem sap may affect the expression of the BPH resistance gene, and (iii) a resistance gene(s) may involve the phloem nitrogen quality, which affects the activities of symbiotic micro-organisms in BPH. However further studies are needed to investigate the mechanism of BPH resistance in Rathu Heenati and should elucidate which gene present in the 190 kb segment confers resistance against BPH when introduced into BPH-susceptible plants.

**Acknowledgements**

This study was supported in part by a grant from the Rockefeller Foundation.

**References**

1. T. Watanabe and H. Kitagawa, "Photosynthesis and translocation of assimilates in rice plants following phloem feeding by the planthopper *Nilaparvata lugens* (Homoptera: Delphacidae)", *J. Econ. Entomol.*, **2000**, *93*, 1192-8.
2. E. A. Heinrichs, in "Leafhopper vectors and planthopper disease agents" (Ed. K. Moramorosch and K. F. Arris), Academic Press, New York, **1979**.
3. J. W. Chen, L. Wang, X. F. Pang, and Q. H. Pan, "Genetic analysis and fine mapping of a rice brown planthopper (*Nilaparvata lugens* Stål) resistance gene *bph19*(t)", *Mol. Genet. Genomics*, **2006**, *275*, 321-9.
4. K. K. Jena, J. U. Jeung, J. H. Lee, H. C. Choi, and D. S. Brar, "High-resolution mapping of a new brown planthopper (BPH) resistance gene, *Bph18*(t), and marker-assisted selection for BPH resistance in rice (*Oryza sativa* L.)", *Theor. Appl. Genet.*, **2006**, *112*, 288-97.
5. H. Yang, A. You, Z. Yang, F. Zhang, R. He, L. Zhu, and G. He, "High-resolution genetic mapping at the *Bph15* locus for brown planthopper resistance in rice (*Oryza sativa* L.)", *Theor. Appl. Genet.*, **2004**, *110*, 182-91.
6. T. Ishii, D. S. Brar, D. S. Multani, and G. S. Khush, "Molecular tagging of genes for brown planthopper resistance and earliness introgressed from *Oryza australiensis* into cultivated rice, *O. sativa*", *Genome*, **1994**, *37*, 217-221.
7. J. Jairin, K. Phengrat, S. Teangdeerith, A. Vanavichit, and T. Toojinda, "Mapping of a broad-spectrum brown planthopper resistance gene, *Bph3*, on rice chromosome 6", *Mol. Breed.*, **2007**, *19*, 35-44.
8. M. Kawaguchi, K. Murata, T. Ishii, S. Takumi, N. Mori, and C. Nakamura "Assignment of a brown planthopper (*Nilaparvata lugens* Stål) resistance gene *bph4* to the rice chromosome 6", *Breed. Sci.*, **2001**, *51*, 13-8.
9. G. Liu, H. Yan, Q. Fu, Q. Qian, Z. Zhang, W. Zhai, and L. Zhu, "Mapping of a new gene for brown planthopper resistance in cultivated rice introgressed from *Oryza eichingeri*", *Chinese Sci. Bull.*, **2001**, *46*, 1459-62.
10. K. Murata, M. Fujiwara, C. Kaneda, S. Takumi, N. Mori, and C. Nakamura, "RFLP mapping of a brown planthopper (*Nilaparvata lugens* Stål) resistance gene *bph2* of indica rice introgressed into a japonica breeding line 'Norin-PL4", *Genes. Genet. Syst.*, **1998**, *73*, 359-64.

11. K. Murata, M. Fujiwara, H. Murai, S. Takumi, N. Mori, and C. Nakamura, "Mapping of a brown planthopper (*Nilaparvata lugens* Stål) resistance gene *Bph9* on the long arm of rice chromosome 12", *Cereal Res. Commun*., **2001**, *29*, 245-50.
12. K. Renganayaki, A. K. Fritz, S. Sadasivam, S. Pammi, S. E. Harrington, S. R. McCouch, S. M. Kumar, and A. S. Reddy, "Mapping and progress toward map-based cloning of brown planthopper biotype-4 resistance gene introgressed from *Oryza officinalis* into cultivated rice, *O. sativa*", *Crop Sci.*, **2002**, *42*, 2112-7.
13. L. Sun, Y. Liu, L. Jiang, C. Su, and J. Wan, "Identification of quantitative trait loci associated with resistance to brown planthopper in the *indica* rice cultivar Col.5 Thailand", *Hereditas*, **2006**, *144*, 48-52.
14. L. Sun, C. Su, C. Wang, H. Zhai, and J. Wan, "Mapping of a major resistance gene to the brown planthopper in the rice cultivar Rathu Heenati", *Breed. Sci.*, **2005**, *55*, 391-6.
15. R. Ikeda, "Studies on the inheritance of resistance to the rice brown planthopper (*Nilaparvata lugens* Stål) and the breeding of resistance rice cultivars", *Bull. Nat. Agri. Res. Cent.*, **1985**, *3*, 1-54.
16. A. Lakshminarayana and G. S. Khush, "New genes for resistance to the brown planthopper in rice", *Crop Sci*., **1977**, *17*, 96-100.
17. G. S. Sidhu and G. S. Khush, "Linkage relationships of some genes for disease and insect resistance and semidwarf stature in rice", *Euphytica*, **1979**, *28*, 233-7.
18. R. Ikeda and C. Kaneda, "Genetic analysis of resistance to brown planthopper, *Nilaparvata lugens* Stål, in rice", *Jpn. J. Breed.*, **1981**, *31*, 279-85.
19. IRRI, "Standard evaluation system for rice" International Rice Research Institute, Manila, **1996**.
20. D. H. Chen and P. C. Ronald, "A rapid DNA minipreparation method suitable for AFLP and other PCR applications", *Plant Mol. Biol. Rep.*, **1999**, *17*, 53-7.
21. H. Hirabayashi and T. Ogawa, "RFLP mapping of *Bph-1* (Brown planthopper resistance gene) in rice", *Jpn. J. Breed.*, **1995**, *45*, 369-71.
22. M. A. Kabir and G. S. Khush, "Genetic analysis of resistance to brown planthopper in rice (*O. Sativa* L.)", *Plant Breed.*, **1988**, *100*, 54-8.
23. H. Nemoto, R. Ikeda, and C. Kaneda, "New genes for resistance to brown planthopper, *Nilaparvata lugens* Stål, in rice", *Jpn. J. Breed.*, **1989**, *39*, 23-8.
24. H. Murai, Z. Hashimoto, P. N. Sharma, T. Shimizu, K. Murata, S. Takumi, N. Mori, S. Kawasaki, and C. Nakamura, "Construction of a high-resolution linkage map of rice brown planthopper (*Nilaparvata lugens* Stål) resistance gene *bph2*", *Theor. Appl. Genet.*, **2001**, *103*, 526-32.
25. R. C. Sexena and S. H. Okech, "Role of plant volatiles in resistance of selected rice varieties to brown planthopper, *Nilaparvata lugens* (Stål) (Homoptera: Delphacidae)", *J. Chem. Ecol.*, **1985**, *11*, 1601-16.
26. G. Liu, R. C. Saxena, and R. M. Wilkins, "Behavioral responses of the whitebacked planthopper *Sogatella furcifera* (Homoptera: Delphacidae) on rice plants whose odors have been masked", *J. lnsect Behavior*, **1994**, *7*, 343-53.
27. J. Q Chen, Y. Rahbé, B. Delobel, N. Sauvion, J. Guillard, and G. Febvay, "Melon resistance to the aphid *Aphis gossypii*: behavioural analysis and chemical correlations with nitrogenous compounds", *Entomol. Exp. Appl.*, **1997**, *85*, 33-44.

*Mj. Int. J. Sci. Tech.* **2007**, *01(2)*, 166-177

28. Q. Fu, Z. Zhang, C. Hu, F. Lai, and Z. Sun, "A chemically defined diet enables continuous rearing of the brown planthopper, *Nilaparvata lugens* (Stål) (Homoptera: Delphacidae)", *Appl. Entomol. Zool.*, **2001**, *36*, 111-6.
29. A. E. Douglas, "The nutritional quality of phloem sap utilised by natural aphid populations", *Ecol. Entomol.*, **1993**, *18*, 31-8.
30. J. Sandstrom. "Nutritional quality of phloem sap in relation to host plant-alternation in the bird cherry-oat aphid", *Chemoecology*, **2000**, *10*, 17-24
31. A. J. Karley, A. E. Douglas, and W. E. Parker, "Amino acid composition and nutritional quality of potato leaf phloem sap for aphids", *J. Exp. Biol.*, **2002**, *205*, 3009-18.
32. J. H. W. Weibull, "Free amino acids in the phloem sap from oats and barley resistant to *Rhopalosiphum padi*", *Phytochem.*, **1988**, *27*, 2069-72.
33. T. Hayakawa, T. Yamaya, T. Mae, and K. Ojima, "Changes in the content of two glutamate synthase proteins in spikelets of rice (*Oryza sativa*) plants during ripening", *Plant Physiol.*, **1993**, *101*, 1257-62.
34. T. Mae and K. Ohira, "The remobilization of nitrogen related to leaf growth and senescence in rice plants (*Oryza sativa* L.)", *Plant Cell Physiol.*, **1981**, *22*, 1067-74.
35. M. Tabuchi, T. Abiko, and T. Yamaya, "Assimilation of ammonium ions and reutilization of nitrogen in rice (*Oryza sativa* L.)", *J. Exp. Bot.*, **2007**, *58*, 2319-27.
36. T. Yamaya, M. Obara, H. Nakajima, S. Sasaki, T. Hayakawa, and T. Sato, "Genetic manipulation and quantitative-trait loci mapping for nitrogen recycling in rice", *J. Exp. Bot.*, **2002**, *53*, 917-25.
37. H. Hayashi, S. Nakamura, Y. Ishiwatari, S. Mori, and M. Chino, "Changes in the amino acid composition and protein modification in phloem sap of rice", *Plant Soil*, **1993**, *155/156*, 171-4.
38. A. K. Tobin and T. Yamaya, "Cellular compartmentation of ammonium assimilation in rice and barley", *J. Exp. Bot.*, **2001**, *52*, 591-604.
39. X. Q. Zhao and W. M. Shi, "Expression analysis of the glutamine synthetase and glutamate synthase gene families in young rice (*Oryza sativa*) seedlings", *Plant Sci.*, **2006**, *170*, 748-54.

*Mj. Int. J. Sci. Tech.* **2007**, *01(2)*, 178-183

***Maejo International***

***Journal of Science and Technology***

**ISSN 1905-7873**

Available online at www.mijst.mju.ac.th

*Short Communication*

# Some physical properties of chitosan in propionic acid solutions

**Esam. A. El-hefian, Rashid Atta Khan*, and Abdul Hamid Yahaya**

Department of Chemistry, University of Malaya, 50603 Kuala Lumpur, Malaysia

*Corresponding author, e-mail: dr_rashid@um.edu.my

*Received: 20 September 2007 / Accepted: 15 October 2007 / Published: 27 October 2007*

**Abstract:** Surface tensions, contact angles and conductivities of propionic acid solutions containing different amounts of chitosan were measured at a room temperature to a temperature accuracy of $\pm 0.20^{o}$. The value of critical coagulation concentration (CCC) was then obtained from the plots of contact angle and conductivity versus concentration. Viscosity of the solutions with different concentrations was also measured in this work at the same temperature and from the plot of viscosity against concentration, the intrinsic viscosity was determined by extrapolation.

**Keywords:** propionic acid, chitosan, intrinsic viscosity, critical coagulation concentration

## Introduction

Chitosan, $1 \rightarrow 4$ linked: 2 – amino-2-deoxy-$\beta$-D-glucan, is a modified carbohydrate polymer derived from chitin by deacetylation [1]. It is also known as soluble chitin. Due to the amino groups that chitosan possesses in its chain, it can be dissolved in dilute aqueous acid solutions such as acetic acid and propionic acid. Chitosan is described in terms of the average molecular weight and degree of deacetylation [2, 3]. Chitosan has been extensively used over a wide range of applications. As a matter of fact, many of chitosan's applications depend upon its unique properties such as biodegradability and non-toxicity. For instance, it can be used in wastewater treatment, medicine, food and cosmetics [4-9]. A lot of work has been done on chitosan. However, the literature is still relatively poor with respect to the physical properties of this polymer [10].

The objective of this work is to study some physical properties of chitosan in propionic acid solutions with a view to further explore the thin film properties and its applications.

*Mj. Int. J. Sci. Tech.* **2007**, *01(2)*, 178-183

## Materials and Methods

### *Materials*

Shrimp-source chitosan (95-97% deacetylation) was used in this work. It was provided by the chitin-chitosan laboratory of Universiti Kebangsaan Malaysia (UKM). Propionic acid used in this work was of 98% purity. Distilled water was used to prepare all solutions.

### *Methods*

The k122 processor tensiometer was used for the determination of surface tension. The surface tension was determined by the plate method. Calibration of the instrument was done with distilled water. The platinum wire was cleaned before every measurement by ethanol, then rinsed with distilled water and finally dried by momentarily heating in a luminous flame. Contact angle of the samples was measured using the contact angle measuring system G40 at 28$^{o}$C. The measurement was done on microscope slides (25.4 × 76.2 mm, 1-1.2 mm thick). Each slide was cleaned before use by soaking in ethanol overnight. The average contact angle of both sides of the drop was taken into consideration, the average value of which was 42$^{o}$. Volume of sample used was 1 $\mu$L and the measurement time was 1.5 minutes.

Conductivity measurements were carried out using the Orion Model 105 Conductivity meter. The actual conductivity reading is obtained by multiplying the observed conductance (observed reading) by the cell constant (K), which is equal to 1.0 cm$^{-1}$ in this case. Calibration was done with standard potassium chloride solution.

Ubbelohde type viscometer was used to measure the viscosity. Flow time was recorded automatically using a viscoclock (Schott ViscoClock). Each value was an average of about 4 measurements. The average values of the intrinsic viscosity was taken by extrapolating the graphs of the inherent viscosity, $\frac{\ln \eta_r}{C}$, and the reduced viscosity, $\frac{\eta_{sp}}{C}$, versus concentration to C=0.

In order to achieve maximum possible accuracy, all the values taken were repeated five times and then an average was taken.

## Results and Discussion

### *Surface tension of chitosan in 0.02M propionic acid solutions*

The values of surface tension at various concentrations of chitosan in 0.02M propionic acid do not show any significant change over a wide range (Figure 1). This suggests that chitosan is fully dissolved in 0.02M propionic acid solutions and that there are no chitosan molecules at air-solution interface (no interfacial activity). This behaviour of chitosan in propionic acid is different from that in acetic acid and formic acid [11].

*Mj. Int. J. Sci. Tech.* **2007**, *01(2)*, 178-183

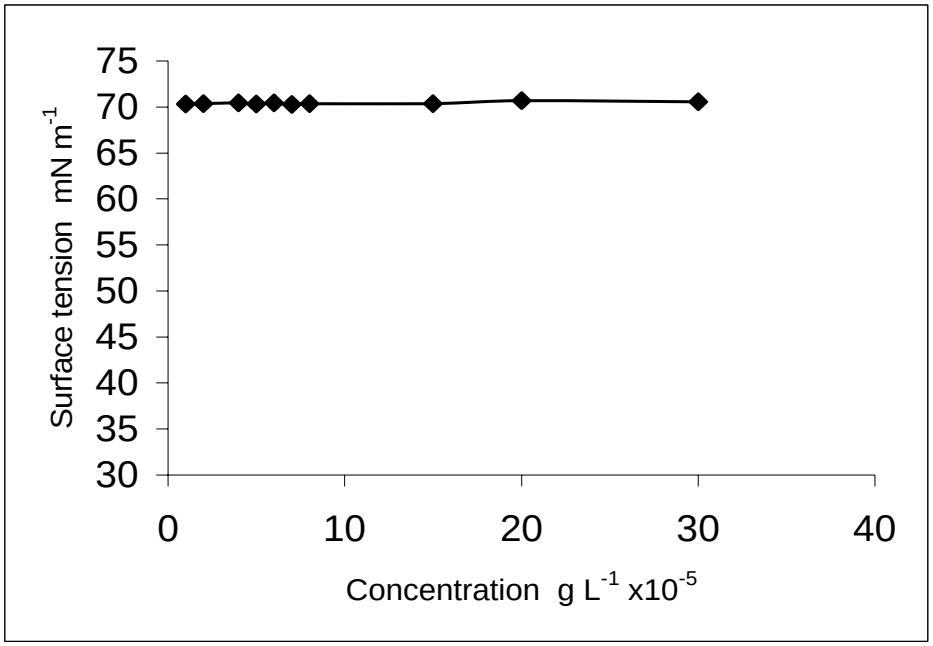


**Figure 1**. Plot of surface tension of chitosan in 0.02M propionic acid.

*Contact angle of chitosan in 0.02M propionic acid solutions*

The average contact angle is plotted as a function of concentration. As the concentration increases, the contact angle increases ($\cos\theta$ decreases) (Figures 2) until a critical coagulation concentration (CCC) is achieved and the contact angle becomes independent of concentration. The value of CCC is about $4.5\times10^{-5}$ g $L^{-1}$.This phenomenon of chitosan solution in propionic acid is similar to that in formic and acetic acid solutions [12].

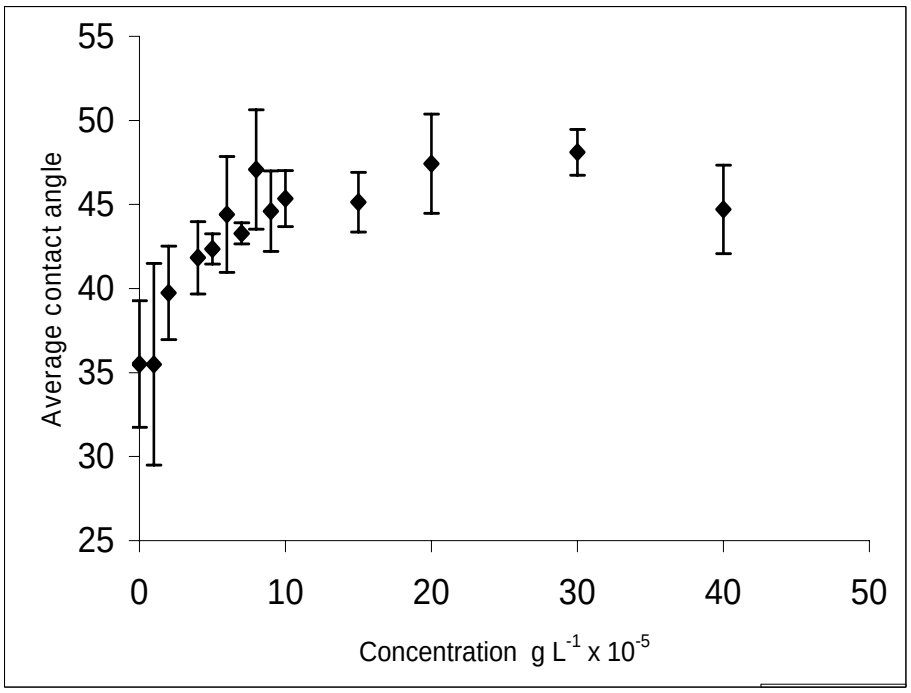


**Figure 2**. Average contact angle of chitosan in 0.02M propionic acid versus concentration.

*Mj. Int. J. Sci. Tech.* **2007**, *01(2)*, 178-183

*Conductivity of chitosan in 0.02M propionic acid solutions*

Figure 3 shows the correlation between equivalent conductivity and concentration. Equivalent conductivity decreases rapidly with increasing concentration until a critical coagulation concentration is obtained, from where it starts decreasing gradually (almost constant), which indicates that aggregation has occurred, but it is not that significant. From this profile, the CCC value estimated was $5\times10^{-5}$ g $L^{-1}$. Interestingly, this value closely corresponds to that estimated from the contact angle measurement.

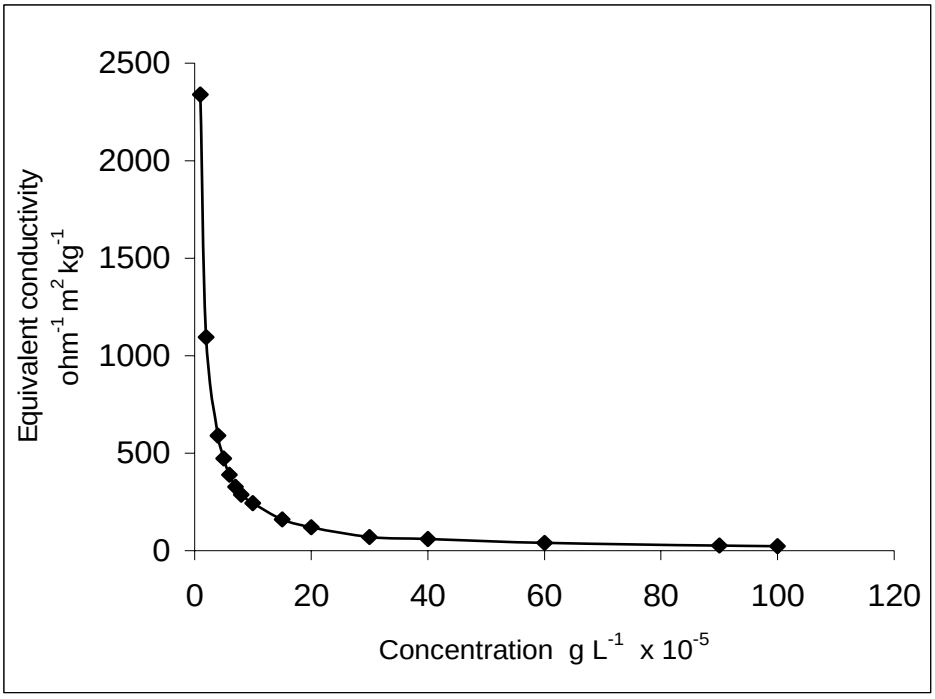


**Figure 3.** Equivalent conductivity of chitosan in 0.02M propionic acid versus concentration.

*Viscosity measurement*

The value of intrinsic viscosity, $\eta$, can be obtained by extrapolating the linear portion of the graph to $C$ = 0 (Figure 4). This gives the value of intrinsic viscosity of 3.7679 x $10^3$ $cm^3$ $g^{-1}$, which is higher than that found in other acids. Also, contrary to the normal behaviour, the viscosity of chitosan in propionic acid solutions decreases with concentration. Presumably, the interactions among the charge carriers could be the possible answer for this abnormal behaviour.

The values of coefficients $k_1$ and $k_1'$, which were calculated from the slopes, are 7.85 x $10^{-2}$ and 4.87 x $10^{-2}$ respectively. It is accepted that the difference ($k_1$- $k_1'$) can be higher or lower than 0.5 [13, 14].

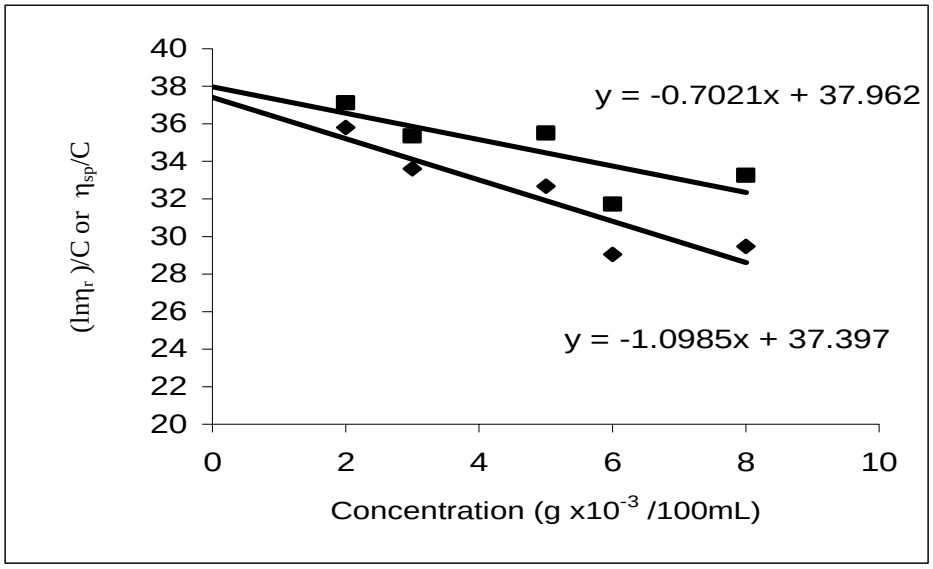


**Figure 4**. Inherent viscosities ( $\frac{\ln \eta_r}{C}$ ) and reduced viscosities ( $\frac{\eta_{sp}}{C}$ ) of chitosan in propionic acid solutions versus concentration.

## Conclusions

The following conclusions can be drawn from this study.

1. Unlike chitosan in formic and acetic acids, that in propionic acid solutions is fully dissolved and shows no surface activity. However, they all show similar behaviour with respect to contact angle and conductivity measurements.
2. The intrinsic viscosity of chitosan in propionic acid is quite high. In addition, the viscosity of chitosan in propionic acid solutions decreases as a function of concentration.
3. In the design of suitable experimental conditions, the predetermined physical properties and behaviour of the chitosan in above mentioned acids could play a significant role.

## References

1. R. A. A. Muzzarelli, “Natural chelating polymers”, Pergamon Press Ltd, London, **1973**, pp.83-95.
2. R. A. A. Muzzarelli, “Chitin”, Pergamon Press Ltd, Oxford, **1977**, pp.83-143.
3. S. E. Lower, “Polymers from the sea: chitin and chitosan", *Manufacturing Chemist*, **1984**, *55***,** 73-75.
4. S. Hirano and Y. J. Noishiki, “The blood compatibility of chitosan and N- acylchitosans”, *J. Biomed. Mater. Res.*, **1985**, *19*, 413-417.
5. Y. W. Cho, Y. N. Cho, S. H. Chung, and W. Ko, “Water-soluble chitin as a wound healing accelerator”, *Biomater.*, **1999**, *20*, 2139-2145.
6. O. Pillai and R. Panchagnula, “Polymers in drug delivery”, *Curr. Opin. Chem. Biol.*, **2001**, *5*, 447-451.
7. E. Khor and L. Y. Lim, “Implantable applications of chitin and chitosan”, *Biomater.*, **2003**, *24*, 2339-2349.

*Mj. Int. J. Sci. Tech.* **2007**, *01(2)*, 178-183

8. S. Yuan and T. J. Wei, "New contact lens based on chitosan/gelatin composites" *Bioact. Compat. Polym.*, **2004**, *19*, 467-479.
9. G. Crini, "Non-conventional low-cost adsorbents for dye removal: a review", *Bioresour. Technol.*, **2006,** *97*, 1061-1085.
10. A. Domard, "Some physicochemical and structural basis for applicabilty of chitin and chitosan", Paper presented at the Second Asia Pacific Symposium, Bangkok, Thailand, **1996**.
11. A. E. Esam, *MSc Thesis*, "Physicochemical characterization of chitosan interfacial properties in solution and films", **2002**, University of Malaya, Malaysia.
12. A. E. Esam, M. Misni, and A. H. Yahya, "Study of contact angles and conductivities of chitosan solutions", Paper presented at the $5^{th}$ International Conference of the European Chitin Society (EUCHIS'02), Trondheim, Norway, **2002**.
13. S. H. Maron and R. B. Reznik, "A new method for determination of intrinsic viscosity", *J. Polym. Sci. Ed., Part A-2: Polym. Phys*., **1969**, *7*, 309-324.
14. D. J. Streeter and F. F. Boyer, "Viscosities of extremely dilute polystyrene solutions", *J. Polym. Sci*., **1953**, *14*, 5-14.

*Mj. Int. J. Sci. Tech.* **2007**, *01(2)*, 184-193

***Maejo International***

***Journal of Science and Technology***

**ISSN 1905-7873**

Available online at www.mijst.mju.ac.th

*Full Paper*

# Effect of ethanol on the longevity and abscission of bougainvillea flower

**A. B. M. Sharif Hossain*, Amru Nasrulhaq Boyce, Haji Mohamed A. Majid, Somasundran Chandran, and Razali Zuliana**

Plant Physiology and Biotechnology Laboratory, Institute of Biological Science, Faculty of Science, University of Malaya, Kuala Lumpur 50603, Malaysia

*Corresponding author, email: sharif@um.edu.my

*Received: 27 July 2007 / Accepted: 26 October 2007 / Published: 31 October 2007*

**Abstract***:* The experiment was carried out to study the effect of different concentrations of ethanol on bougainvillea flower vase life and delayed abscission. Young and fresh flowers were harvested from 4-year-old bougainvillea trees randomly. Flower stems (petiole) were placed individually in an open solution containing different concentrations of ethanol immediately after harvesting. The solutions used for treatment were water (control), 2, 4, 8, 10, 20, 30, 40, 50 and 70% ethanol. Positive responses were found in the case of 8 and 10% ethanol after 5 days of treatment. Flower longevity was 2 days longer in 8 and 10% ethanol than in water control and other concentrations of ethanol. Petal wilting and abscission occurred 2 days later than water control. Perianth abscission was later in 8 and 10% ethanol than water control. Percent petal scar (color changing) was later in water control, 2, 4, 8 and 10 than 20, 30, 40, 50 and 70% ethanol The result showed that the flower vase life was significantly affected by ethanol concentrations and longevity was more in 8 and 10% ethanol than water control and other concentrations.

**Keywords:** bougainvillea flower, longevity, abscission

## Introduction

Bougainvilleas are popular ornamental plants and used as official flowers in most areas with warm climates, including Australia, India, Malaysia, the Mediterranean region, Mexico, South Africa, Taiwan, and the United States in Arizona, California, Florida, Hawaii, and southern Texas. It is used to

*Mj. Int. J. Sci. Tech.* **2007**, *01(2)*, 184-193

decorate fences and arbours with explosions of colour in the house corridor, office and play ground. A bougainvillea tree can be made guarding the entry or framing a window. It is a great vine for large containers to decorate hot patios and plazas. It is also used to create beautiful flowering bonsai specimens. Its flowers are usually dropped having a short vase life. Cameron et al. [1] reported that bougainvillea bracteoles were attractive at the end of 6-day observation period and dropped 32.2% when treated with silver thiosulfate [STS, (0.5 oz/gallon)], while 100% dropped in control tree.

In normal senescing, cut carnation flowers show irreversible wilting of the petals. Previous reports [2,6] showed that ethanol (4 and 6%) increased the vase life of carnation flowers and cultivars showed variable response to ethanol treatment with regard to vase life increment. Moreover, it was reported that treatment with 4% ethanol inhibited ethylene production as well as sensitivity to ethylene. Longevity of vase life is an important factor for consumer preference and considerable research has been carried out on the causes of carnation senescence [7, 8, 9]. Senescence of cut flowers is induced by several factors, e.g. water stress [10], carbohydrate depletion [11], microorganisms [12], and ethylene effects [13]. Ethanol has been found to be effective in increasing the vase life of carnation flowers by inhibiting ethylene biosynthesis [14,15] as well as its action [15]. The effective concentration of ethanol in increasing the vase life of carnation flowers ranges from 2% to 8% [14,15]. This variation in response could be due to differences in cultivar sensitivity to ethylene [16,17] or differences in age of the flowers used [15].

Podd and Staden [18] stated that ethanol, when applied at a low concentration in holding solutions, extended the vase life of cut carnation flowers. They also mentioned that a low concentration of either ethanol or acetaldehyde apparently decreased the formation of ethylene by inhibiting the action of 1-aminocyclopropane-1-carboxylic acid (ACC) synthase. Treatment of cut carnation flowers with low concentrations of ethanol increased their vase life significantly [15, 19, 20]. Podd and Staden [20] also reported that carnation flower senescense was delayed by ethanol.

The literature has not yet been available on similar work for bougainvillea flowers. Thus, our interest has grown to develop on the vase life of these flowers. The aim of this project is then to improve on their post-harvest qualities (color development, longevity extension and delayed senescence) by applying different ethanol concentrations, the result of which may have a positive effect on the use of this ornamental plant in social and occasional functions.

## Materials and Methods

### *Site*

The experimental site was University of Malaya campus, Kuala Lumpur, Malaysia.

### *Plant material*

Three four-year-old bougainvillea trees from nursery, University of Malaya campus were used in this experiment for collecting flower samples. Each tree was about 1.2 m high and canopy length was about 2.0 m. Each tree consisted of 6 branches. Flowers were harvested from each branch randomly. Weeding, irrigation and pesticide were applied as needed.

*Flower harvesting and measurement*

Flowers were harvested on January 18, 2007. They were weighed immediately after harvest and used in the following treatments.

*Design of experiment and treatment setting*

The experiment design was Randomized Completely Block Design (RCBD). A total of 40 flowers from 7 branches were used for 10 treatments. Mean separation was done by Duncan's multiple range test (DMRT). The treatments were set following completely blocked design. Each treatment was done in quadruplicate. The treatments were water (control), 2, 4, 8, 10, 20, 30, 40, 50 and 70% ethanol The flowers were put individually with the petiole dipping in different concentrations of ethanol (20 ml) in a vial bottle (25 ml) immediately after harvest with scissors and placed at room temperature (28 $^0$C ) (Figure 5).

*Response character determination*

Response characters were observed. Positive (+) indicates the freshness of flower just before wilting. Negative (-) indicates the onset of wilting of flower

*Vase life, petal wilting, scar (color change) and abscission evaluation*

Vase life was observed by counting day after treatment. Longevity was determined as the mean number of days after harvest until initial wilting or rolling-in of the petals [5]. Petal wilting was investigated. Percent petal wilting was calculated by dividing the wilted petal area by the total petal area and multiplying by100. Color changing (petal scar) was determined by visual observation. After wilting phase, petal abscission was evaluated by observing petal abscised position.

*Fresh and dry weight measurement*

Fresh weight of each flower was measured immediately after harvest. Dry weight was measured after all flowers were abscised.

*Chlorophyll content measurement*

Chlorophyll content was measured by Chlorophyll Meter SPAD-502, Minolta Co. Japan, and was represented by SPAD value. The petal was inserted into the meter and SPAD value was measured 5 times from different spots of a single petal, then averaged.*-

*Petal drop measurement*

Petals were forced to drop with blown air using a table electric fan at medium speed. The flowers were kept in front of the fan for 5 minutes. The number of petals dropped by air was observed and the percentage of dropping was calculated.

*Mj. Int. J. Sci. Tech.* **2007**, *01(2)*, 184-193

**Results and Discussion**

The response character to ethanol was seen to be positive (before wilting) from 12h-day 7 (D7) after treatment and afterwards negative for all treatments (Table 1). The highest positive response (D7) was found for 8 and 10% ethanol treated flowers and the lowest (D1) was found for 70% ethanol treated flowers. In case of water (control) wilting occurred on D6, while it was observed in D8 for 8 and 10% ethanol treated flowers (Figure 1). The wilting started from D1 for 70% ethanol, D2 for 40 and 50 % ethanol, D3 for 30 % ethanol, D4 for 20 % ethanol, D6 for 4, 2 % ethanol and water (control), D8 for 8 and 10 % ethanol treated flowers (Figure 1). In the case of water (control), 100% wilting occurred in D8, while it was found in D10 for 8 and 10% ethanol treated flowers. Percent petal abscission was earlier for water control, 2, 4 than 8 and 9% ethanol (Figure 2). The petal abscission duration was D2-12 in different concentrations of ethanol.

**Table 1.** Response character of bougainvillea flower at different concentrations of ethanol

| Treatments | Response Character | | | | | | | | | | | |
|---|---|---|---|---|---|---|---|---|---|---|---|---|
| | 12h | D1 | D2 | D3 | D4 | D5 | D6 | D7 | D8 | D9 | D10 | D11 |
| Water | + | + | + | + | + | + | -(W) | -(W) | -(W) | -(A) | -(A) | -(A) |
| 2% ethanol | + | + | + | + | + | + | -(W) | -(W) | -(W) | -(A) | -(A) | -(A) |
| 4% ethanol | + | + | + | + | + | + | -(W) | -(W) | -(W) | -(A) | -(A) | -(A) |
| 8% ethanol | + | + | + | + | + | + | + | + | -(W) | -(W) | -(W) | -(A) |
| 10% ethanol | + | + | + | + | + | + | + | + | -(W) | -(W) | -(W) | -(A) |
| 20% ethanol | + | + | + | + | -(W) | -(W) | -(W) | -(W) | -(A) | -(A) | -(A) | -(A) |
| 30% ethanol | + | + | + | -(W) | -(W) | -(W) | -(W) | -(A) | -(A) | -(A) | -(A) | -(A) |
| 40% ethanol | + | + | -(W) | -(W) | -(W) | -(A) | -(A) | -(A) | -(A) | -(A) | -(A) | -(A) |
| 50% ethanol | + | + | -(W) | -(W) | -(A) | -(A) | -(A) | -(A) | -(A) | -(A) | -(A) | -(A) |
| 70% ethanol | + | -(W) | -(W) | -(A) | -(A) | -(A) | -(A) | -(A) | -(A) | -(A) | -(A) | -(A) |

+ : positive, -: negative, W: wilting, A: abscission, D: day

The abscission order was 70< 50 < 40 < 30 < 20 <water control<8 and 10% ethanol. A similar trend was found for percent perianth abscission (Figure 3). However, the perianth abscission was 1 day later than petal abscission. The 100% perianth abscission was found for 8 and 10% ethanol on D13 while for water control, 2, 4 and 20% ethanol treated flowers, it was found on D11. Percent petal scar was earlier in water, 2, 4 20, 30, 40, 50 and 70 than 8 and 10% ethanol respectively (Figure 4). A similar increasing (day) trend was found in case of all ethanol treated flowers. Petal scar started in D4 for water control and peaked (100%) on D12, whereas it started in D6 and peaked (100%) in D12 for 8 and 10% ethanol treated flowers.

The vase life was 2 days longer for 8 and 10% ethanol than water, 2 and 4% ethanol treated flowers (Table 2). The vase life was gradually decreasing as 7, 5, 3, 2, 1 and <1 day following the order of 8 and 10> water control, 2 and 4> 20 >30 >40 and 50 >70% ethanol. Fresh weight (before wilting) was measured and there was no significant difference among all treatments (Table2). Dry weight was measured after abscission. It was significantly reduced for all treatments but much more so for 30, 40, 50 and 70% ethanol treated flowers. Fresh to dry weight ratio was lower for 2, 4, 8 and 10% ethanol

*Mj. Int. J. Sci. Tech.* **2007**, *01(2)*, 184-193

treated flowers than water, 20, 30, 40, 50 and 70% ethanol treated flowers (Table 2). Petal was shed 33% for 8 and 10% ethanol, 66% for water, 2, 4, 20 and 30% ethanol and 100% for 40, 50 and 70% ethanol treated flowers.

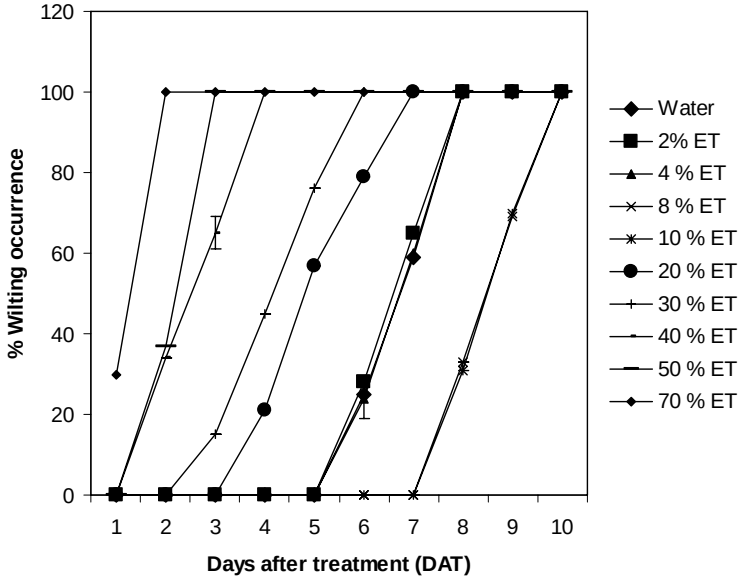


**Figure1.** Wilting occurrence followed at different concentrations of ethanol. Bars represent SE (n=4).

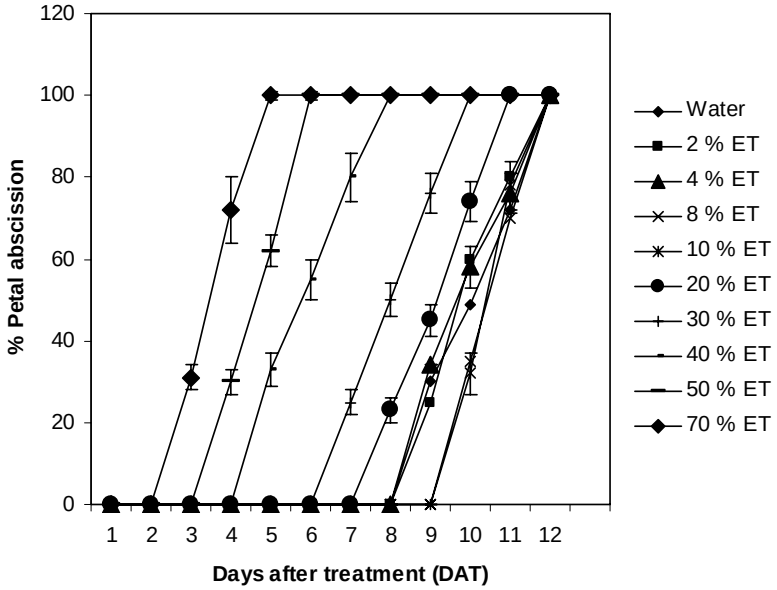


**Figure 2.** Petal abscission followed at different concentrations of ethanol. Bars represent SE (n=4).

*Mj. Int. J. Sci. Tech.* **2007**, *01(2)*, 184-193

**Table 2.** Fresh and dry weight of bougainvillea flowers at different concentrations of ethanol.

| Treatments | Fresh weight (Initial) g | Dry weight After abscsion (Final) g | Ratio (FW/DW) | Vase life (Day) | Petal shedding (%) | Chlorophyll content (SPAD value) Initial | Final |
|---|---|---|---|---|---|---|---|
| Water | 0.66±0.10a | 0.36±0.05b | 1.83±0.20a | 5.1±0.31c | 66±5.7b | 3.8±0.5a | 0.4±0.02b |
| 2 % ethanol | 0.72±0.11a | 0.45±0.06c | 1.61±0.11a | 5.3±0.35c | 66± 5.7b | 3.7±0.4a | 0.4±0.02b |
| 4 % ethanol | 0.56±0.09a | 0.31±0.05b | 1.80±0.13a | 5.2±0.34c | 66±5.7b | 3.6±0.4a | 0.3±0.01a |
| 8 % ethanol | 0.65±0.08a | 0.37±0.06c | 1.73±0.12a | 7.2±0.45d | 33±3.3a | 3.8±0.3a | 0.6±0.03b |
| 10% ethanol | 0.61±0.12a | 0.40±0.05c | 1.51±0.15a | 7.3±0.38d | 33±3.3a | 3.8±0.3a | 0.7±0.03b |
| 20% ethanol | 0.52±0.07a | 0.32±0.04b | 1.65±0.16a | 3.0±0.27b | 66± 00b | 3.6±0.4a | 0.3 ±0.01a |
| 30% ethanol | 0.70±0.11a | 0.30±0.04b | 2.33±0.23b | 2.0±0.25b | 66± 00b | 3.7±0.5a | 0.2±0.01a |
| 40% ethanol | 0.68±0.10a | 0.19±0.03a | 3.56±0.28c | 1.1±0.12a | 100±00c | 3.5±0.4a | 0.2±0.01a |
| 50% ethanol | 0.53±0.08a | 0.12±0.03a | 4.20±0.37c | 1.0±0.05a | 100±00c | 3.8±0.5a | 0.1±0. 005a |
| 70% ethanol | 0.62±0.09a | 0.09±0.02a | 7.12±0.51d | <1.0±0.05a | 100±00c | 3.8±0.5a | 0.1±0.005a |

Mean±SE (n =4). FW: Fresh weight, DW: Dry weight, Means followed by the common letters in column are not significantly different at the 5% level by Duncan`s multiple range test (DMRT).

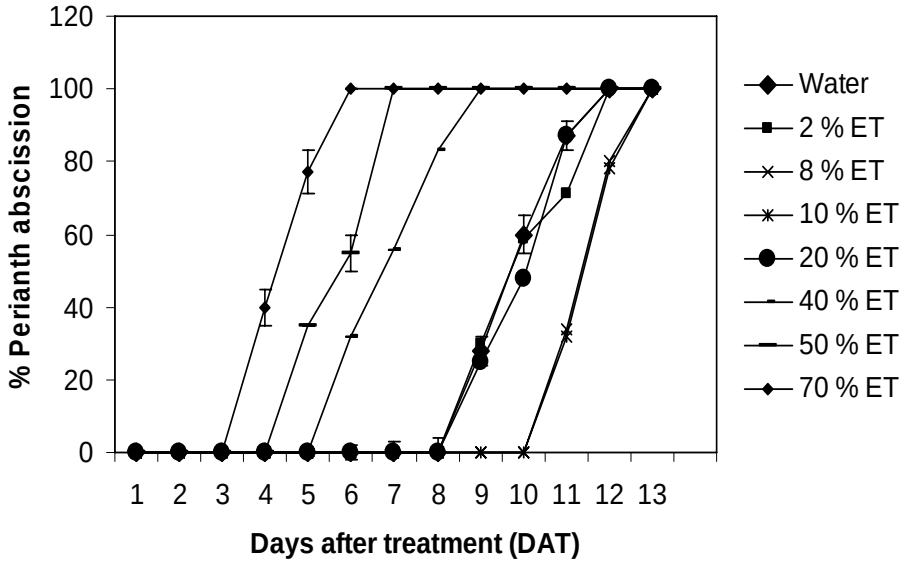


**Figure 3**. Perianth abscission monitored at different concentrations of ethanol. Bars represent SE (n=4).

Initially chlorophyll content (SPAD value) was higher for water, 8, 10, 50, 70 than 2, 4 20, 30 and 40% ethanol treated flowers. Finally, however, it was higher for 8 and 10% ethanol than all other treatments. Figure 5 shows the different flower structures and colour changing after various treatments at different stages.

The results showed that ethanol was effective as an ethylene inhibiting component in bougainvillea flower. It was found that the more effective concentrations of ethanol were 8 and 10%. The results seemed to indicate that sensitivity to ethylene developed several days after flower opening such that ethanol had only a limited capacity to delay vase life as well as petal abscission. It was reported that ethylene was the major coordinator for senescence in many flowers [2]. Podd and Staden [16] stated that ethanol, when applied as low concentration holding solutions, could extend the vase life of cut carnation flowers. They also mentioned that a low concentration of ethanol apparently decreased the formation of ethylene by inhibiting the action of ACC synthase. The vase life of carnation flowers has been increased using ethanol by inhibiting ethylene biosynthesis [14, 15] as well as its action [15].

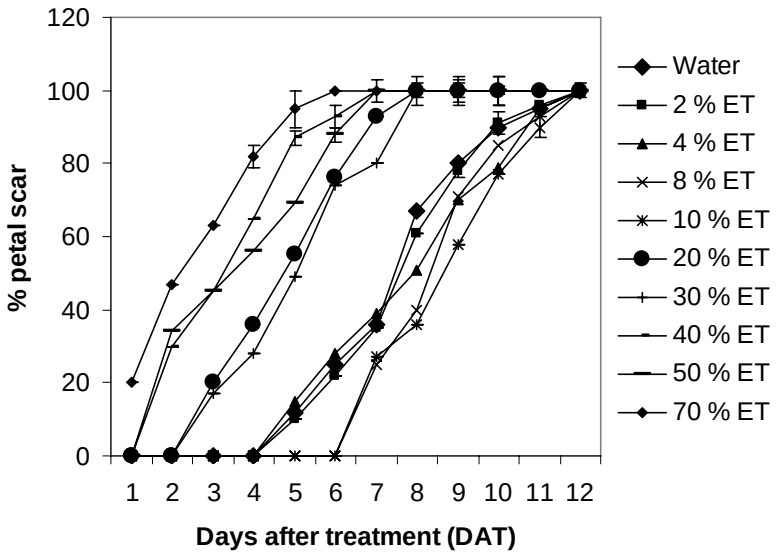


**Figure 4**. Petal scar monitored at different concentrations of ethanol. Bars represent SE (n=4).

Similar results have been reported by other researchers. The concentration of ethanol effective in increasing the vase life of carnation flowers ranges from 2% [14] to 8% [15] for the different cultivars. This variation in response could be due to differences in cultivar sensitivity to ethylene [16, 17]. Treatment of cut carnation flowers with low concentrations of ethanol increased their vase life significantly [15, 19, 20].

*Mj. Int. J. Sci. Tech.* **2007**, *01(2)*, 184-193

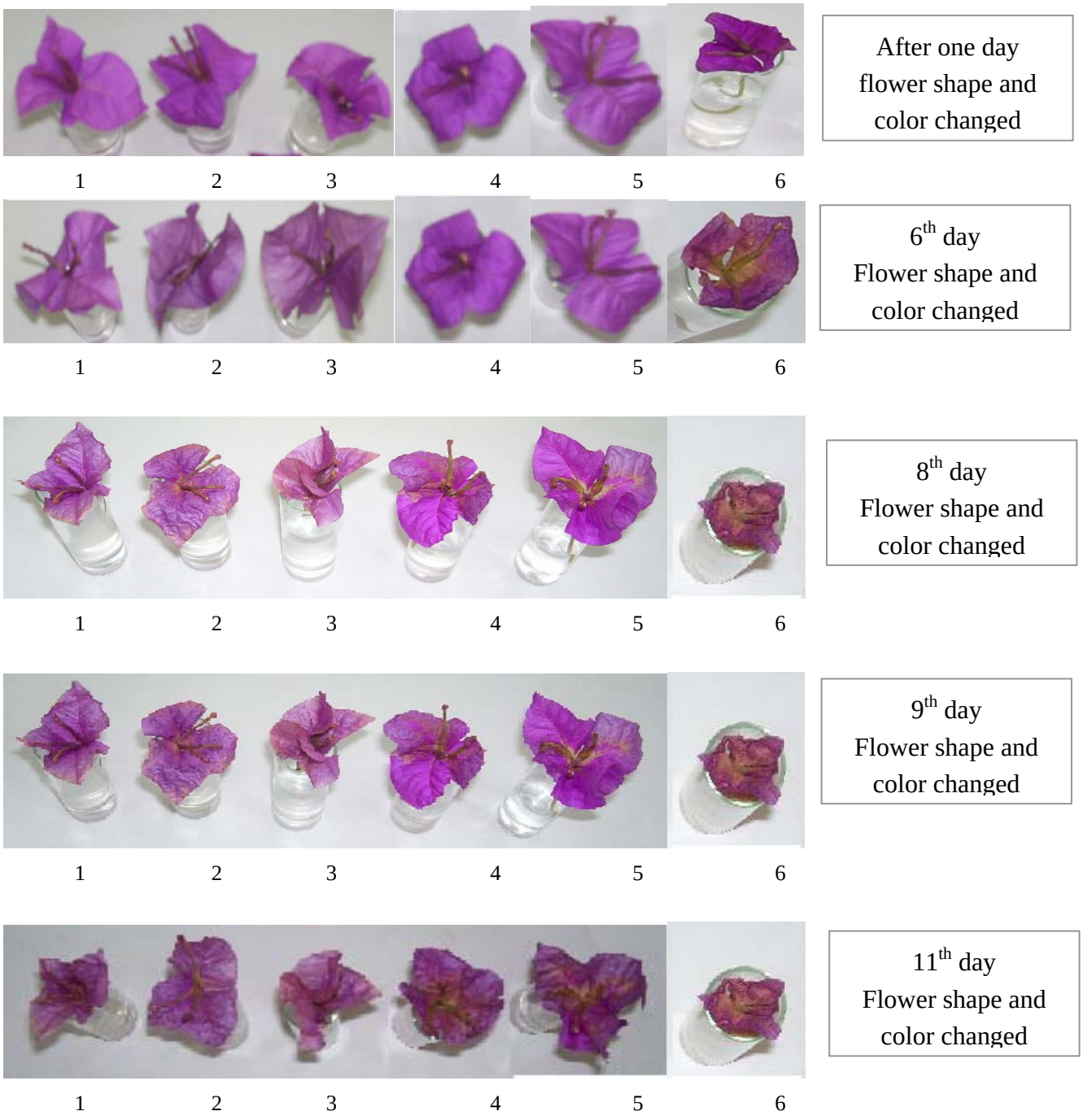


**Figure 5.** Petal and perianth wilting and abscission (shape and colour) after treatment;
1: water control, 2: 2%ethanol, 3: 4% ethanol, 4: 8% ethanol, 5: 10% ethanol, 6: 70% ethanol

**Conclusion**

It is possible to extend the vase life of bougainvillea flowers using 8% and 10% ethanol by causing delayed senescence. A low concentration of ethanol presumably decreased the formation of ethylene by inhibiting the action of ACC synthase. While low concentrations of ethanol (2-8%) had been found to be effective in extending the vase life of cut carnation flowers, the results of the present experiment also showed similar effects in bougainvillea flowers.

*Mj. Int. J. Sci. Tech.* **2007**, *01(2)*, 184-193

**Acknowledgements**

The authors are grateful to Musammath Maimuna Akter for assistance in sample preparation and computing data in this research.

**References**

1. C. A. Cameron, M. S. Reid, and G. W. Hickman, "Using STS to prevent flower shattering in potted flowering plants—progress report. Flower and nursery report for commercial grower", Cooperative Extension, University of California, **1981**, p.6.
2. R. Nichols, "The response of carnation (*Dianthus caryophyllus*) to ethylene", *J. Hort. Sci.* **1968**, *43*, 335–349.
3. E. L. Cook and J. V. Staden, "Senescence of cut carnation flowers: ovary development and $CO_2$ fixation", *Plant Growth Regul.,* **1983**, *1*, 221–232.
4. E. L. Cook and J. V. Staden, "The ovary as a sink in the senescence of cut carnation flowers", *Acta Hort.,* **1986**, *181*, 345–352.
5. A. H. Halevy and A. M. Kofranek, "Silver treatment of carnation flowers for reducing ethylene damage and extending longevity", *J. Amer. Soc. Hort. Sci.*, **1977,** *102*, 76-77.
6. U. K. Pun, R. N. Rowe, J. S. Rowarth, M. F. Barnes, C. Dawson, and J. A. Oheyes, "Influence of ethanol on climacteric senescence in five cultivars of carnation", *New Zealand J. Crop Hort. Sci.,* **1999**, *27*, 69-77.
7. M. S. Reid, J. L. Paul, M. B. Farhoomand, A. M. Kofranek, and G. L. Staby, "Pulse treatments with the silver thiosulphate complex extend the vase life of cut carnations", *J. Amer. Soc. Hort. Sci.*, **1980**, *105*, 25-27.
8. M. S. Reid, A. M. Kofranek, and S. T. Besemer, "Postharvest handling of carnations", *Acta Hort.,* **1983**, *141*, 235-238.
9. A. Menguc and E. Usta, "Research on the effects of silver thiosulphate plus sucrose pretreatment on the cold storage period and post storage vase life of cut flowers of carnation cv. Astor havested at different maturities", *Acta Hort.,* **1994**, *368,* 802- 807.
10. C. K. Sankat and S. Mujaffar, "Water balance in cut anthurium flowers in storage and its effect on quality", *Acta Hort.*, **1994**, *368*, 723-732.
11. S. Ketsa, "Vase life characteristics of inflorescences of dendrobium 'Pompadour'", *J. Hort. Sci.*, **1989**, *64*, 611-615.
12. Y. De Witte and W. G. Van Doom, "The mode of action of bacteria in the vascular occlusion of cut rose flowers", *Acta Hort.*, **1991**, *298*, 165-167.
13. M. J. Wu, W. G. Van Doom, and M. S. Reid, "Variation in the senescence of carnation *(Dianthus caryophyllus L.)* cultivars. II. Comparison of sensitivity to exogenous ethylene and of ethylene binding", *Scientia Hort.*, **1991**, *48*, 109-116.
14. R. D. Heins and N. Blakely, "Influence of ethanol on ethylene biosynthesis and flower senescence of cut carnation", *Scientia Hort.*, **1980**, *13*, 361-369.
15. M. J. Wu, Z. Lorenzo, M. E. Saltveit, and M. S. Reid, "Alcohols and carnation senescence", *Hort. Sci.*, **1992,** *27*, 136-138.

*Mj. Int. J. Sci. Tech.* **2007**, *01(2)*, 184-193

16. M. Serrano, F. Romojaro, J. L Casas, and M. Acosta, “Ethylene and polyamine metabolism in climacteric and non-climacteric carnation flowers”, *Hort. Sci.*, **1991**, *26*, 894-896.
17. S. Mayak and T. Triosh, “Unusual ethylene-related behaviour in senescing flowers of the carnation Sandrosa”, *Physiol. Plantarum*, **1993**, *88* ,420-426.
18. L. A. Podd and J. V. Staden, “The role of ethanol and acetaldehyde in flower senescence and fruit ripening”, *J. Plant Growth Regul.*, **2004,** *26*, 183-189.
19. R. D. Heins, “Inhibition of ethylene synthesis and senescence in carnation by ethanol”, *J. Amer. Soc. Hort. Sci.*, **1980,** *105*, 141–144.
20. L. A. Podd and J. V. Staden, “The role of ethanol and acetaldehyde in flower senescence and fruit ripening - a review”, *Plant Growth Regul.*, **1998,** *26*, 183–189.

*Mj. Int. J. Sci. Tech.* **2007**, *01(2)*, 194-207

***Maejo International***

***Journal of Science and Technology***

**ISSN 1905-7873**

Available online at www.mijst.mju.ac.th

*Full Paper*

# Modification and tuning of diesel bus engine for biogas electricity production

**Sittiboon Siripornakarachai* and Thawan Sucharitakul**

Department of Mechanical Engineering, Faculty of Engineering, Chiang Mai University, Chiang Mai 50200, Thailand

* Corresponding author, e-mail : siripornakarachai@yahoo.com and thawan@dome.eng.cmu.ac.th

*Received: 19 September 2007 / Accepted: 2 November 2007 / Published: 9 November 2007*

**Abstract:** This study is to convert and tune a bus diesel engine for electricity production in a farm using biogas as fuel. The engine under study was a Hino K-13CTI 13,000cc 24 valve turbocharged engine coupled to a 3-phase 4-pole induction motor to produce electricity at 50 Hz. Modifications included an addition of biogas carburettor for air-fuel mixing, replacing the fuel injection system with spark ignition system, reduction of compression ratio from the original 16:1 to 8:1 using a cylinder head spacer, and modification of the turbocharger waste gate so the boost pressure can be adjusted. When the induction motor was synchronised to the power grid, the running speed of the engine was 1,500 rpm. Optimal engine efficiency was achieved at 28.6% by setting the lambda factor at 1.097, ignition timing at 54$^{o}$ before top dead center, and the turbocharger boost at 56 kPa. With this setting, the generator power output was 134.20 kilowatt with emission of CO and $NO_X$ being 1,154 and 896 ppm respectively.

**Keywords:** modification engine, engine for electricity, biogas engine, engine for biogas, gas engines

## Introduction

Biogas is a by-product of waste treatment in animal farms and can be used to replace fossil fuel to produce electrical energy. Biogas is formed by digestion of animal waste by anaerobic bacteria and the approximate composition is 60-80% methane, 20-40% carbon dioxide, and about 1% hydrogen sulfide

*Mj. Int. J. Sci. Tech.* **2007**, *01(2)*, 194-207

and other trace gases. Biogas has a liquefying pressure of 200-300 bar and a heating value of about 23,400 kJ/$m^3$ [1,2]. The gas density is 1.2 kg/$m^3$ and has research octane number (RON) of about 130 [2,3]. From the above properties, it can be seen that it is difficult to liquefy biogas for storage or transport and it is quite suitable to be used as fuel in an internal combustion engine [4,5]. Statistics as of 2006 shows that in Thailand there are pig farms which have biogas waste treatment system that can produce biogas totalling 35,000,000 cubic metres per year. If all are used to produce electricity, the total energy of 35,000,000 kilowatt-hour can be produced per year [6]. With an increase in biogas production towards larger quantities, such technical utilisation as the transformation into mechanical energy becomes an issue to be researched on. While larger engines specifically designed for gas are on the market, smaller engines modified from standard Otto or diesel engines are seen to fill the gap for small-to-medium and decentralised applications. Indian [7,8], Chinese [9], and French [10] publications mainly dealt with the modification of small stationary diesel engines for dual fuel operation. Others went on to modify medium-sized diesel engines including their governors [11], or researched on the performance parameters of dual fuel biogas engines in more detail [12].

In Thailand, the bus is an expensive commodity compared to per capita income. As a result, buses are kept running long beyond its life expectancy set by the manufacturer. To keep these buses running, skilled mechanics as well as used engine markets and spare parts are well developed in Thailand. A used bus engine imported from Japan in a reasonably good condition can be had for about 5,500 US dollars. The cost for engine overhaul after about 1,000,000 kilometers of use is about 1,400 US dollars. With a used bus engine coupled to an electrical generator, a farm owner can make a 130 kilowatt power generator fueled by biogas for about 23,100 US dollars and the break-even of the investment can be as short as one year. These engines do not use a proper gas carburettor and are seldom tuned for best efficiency or low pollution [13]. This project is to investigate the proper adaptation of engine for durability and tune it for high efficiency and low emission.

Just about any engine can be converted to run on biogas and produce electricity in a farm. Smaller engines (under 5,000 cc capacity) are normally designed to perform best at higher engine speed and are normally not designed for full capacity output like those required in electrical power production [14]. On the other hand, larger engines like those found in heavy trucks or large buses are designed to carry a full load for most of its operating cycle and are also designed to run at lower engine speed. As a result, car engines will last about 150,000 kilometers between overhauls while buses and large trucks engines are expected to last more than 1,000,000 kilometers between overhauls. The long operating life of large engine makes it more suitable for electricity production in a farm and will probably cost less in the long run to operate [13].

Few variables need to be considered before the attempted adaptation of a diesel engine for electricity production. First consideration is given to the overall engine design itself. The engine will need to run at the generator synchronization speed to work as a generator. In this case, the generator requires the engine speed of 1,500 rpm for a four-pole generator and 3,000 rpm for a two-pole generator. The bus engine under consideration provides maximum torque at 1,500 rpm so it is suitable for the 1,500 rpm running speed. Another variable to be considered is the feasibility of reducing the compression ratio down to the spark ignition range. An overhead camshaft engine would be easy to adapt but the engine under consideration can also be adapted if the valve pushrod can be extended to accommodate the additional distance between the camshaft and the rocker arm, due to the thickness of

the cylinder head spacer. The space issue when replacing the fuel injectors with spark plugs also needs to be considered before the adaptation.

This study aims to adapt a large diesel engine to run on biogas only and the adaptation involves an addition of biogas carburettor for air-fuel mixing, replacing the fuel injection system with spark ignition system, reducing the compression ratio to suit biogas fuel using a cylinder head spacer, and modification of the turbocharger waste gate so the boost pressure can be adjusted. The test rig used a Hino K-13CTI 13,000cc 24 valve turbocharged engine coupled to a 3-phase 4-pole induction motor to produce electricity at 50 Hz. The engine was then tuned by changing air/fuel ratio, ignition timing, and turbocharger boost pressure to obtain the optimal running condition.

## Materials and Methods

The Hino K-13CTI engine being studied was a turbocharged bus diesel engine that came with a fuel injection system as well as a high compression ratio of 16:1 and a fixed waste gate boost control. For biogas fuel adaptation, a biogas carburettor was designed, manufactured, and installed. The fuel injection system was replaced with a spark ignition system, the compression ratio was reduced to 8:1, and the waste gate was modified so the boost pressure could be adjusted. Each of these modifications is discussed in turn in the following section of the paper.

### *Carburettor design*

The biogas carburettor designed and installed in this study is shown in Figure 1. A literature survey shows that a suitable carburettor for a biogas engine should be a venturi with the accelerator cone being tapered as a curve of 40 mm radius and the diffuser cone angle of $10^{o}$. The biogas is fed into the venturi through multiple circular ports around the throat area and the throat air velocity should be between 100 to 150 meters/second [2]. With this information, a carburettor designed for the 13,00cc engine operating at 1,500 rpm should have the throat diameter of 7.5 mm. The metering needle for the gas inlet was fabricated with a square root profile to provide some linearity between the needle position and the gas flow rate. The venturi was machined from aluminum stock and the carburettor body was fabricated from PVC pipe parts.

### *Spark ignition*

The distributor and ignition coil was adapted from the one used in 6-cylinder Toyota 5-ME engine. The vacuum and centrifugal advance was disabled because the engine would run at a constant speed and a full load when used to drive the generator. The distributor was driven by the original fuel injection distributor mechanism. The fuel injection nozzle in the cylinder head was removed and replaced with a spark plug and an appropriate guide tube. The spark plug modification detail is shown in Figure 2.

*Mj. Int. J. Sci. Tech.* **2007**, *01(2)*, 194-207

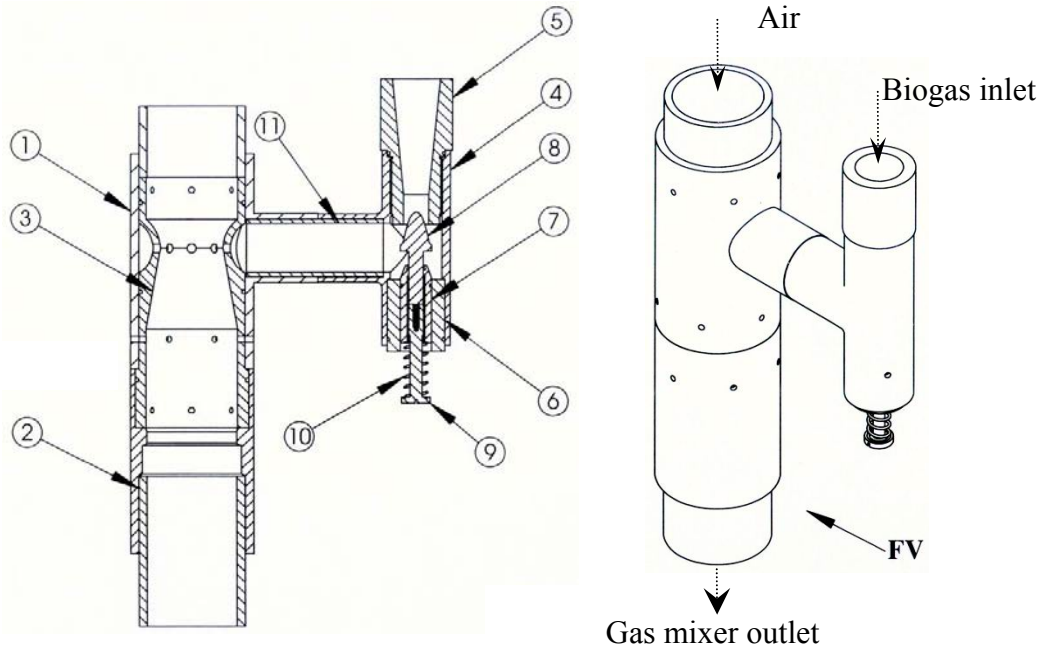


**Figure 1**. Biogas carburettor design: (1) Venturi housing, (2) Venturi base, (3) Venturi mixer, (4) Metering housing, (5) Main jet, (6) Metering adjusting nut spacer, (7) Metering adjusting nut, (8) Metering needle, (9) Metering adjusting screw, (10) Return spring, and (11) Pipe junction

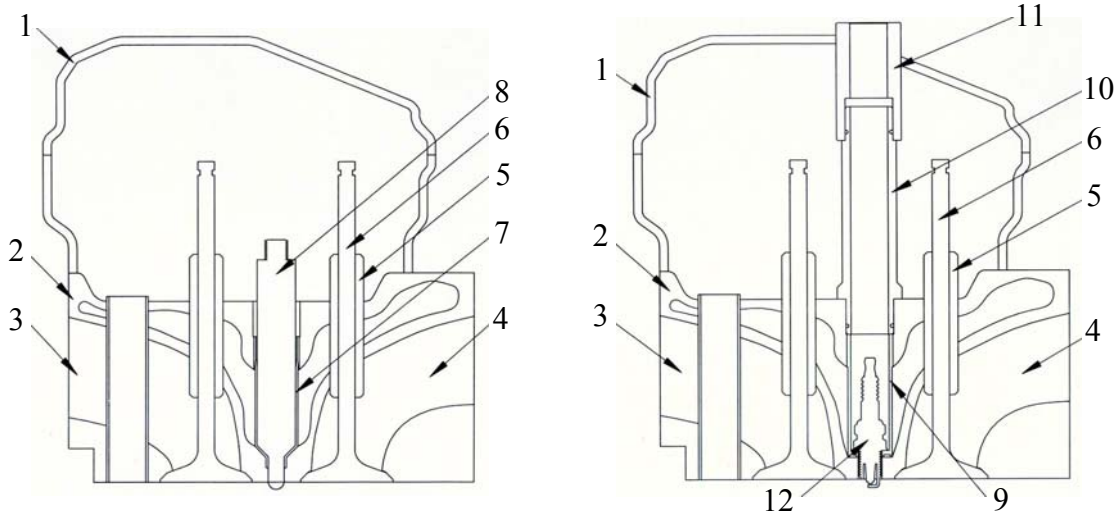

**(A) Before modification** **(B) After modification**

**Figure 2.** Cutaway view of the modified cylinder head: (1) Valve cover, (2) Cylinder head, (3) Intake port, (4) Exhaust port, (5) Valve guide, (6) Exhaust valve, (7) Diesel injection nozzle guide, (8) Diesel injection nozzle, (9) Spark plug guide, (10) Middle spark plug rod guide, (11) Upper spark plug rod guide, and (12) Spark plug

*Mj. Int. J. Sci. Tech.* **2007**, *01(2)*, 194-207

*Compression ratio*

For proper biogas operation, the compression ratio needs to be brought down from the original 16:1 to some lower value to avoid engine knock. Literature suggests that the compression ratio should be between 10:1 and 12:1 for biogas operation [2]. Since a turbocharger would be used, the compression ratio was further lowered to 8:1. To achieve this, a steel spacer 10 mm thick was fabricated for this purpose.

*Turbocharger boost pressure*

The turbocharger pressure is another parameter to be optimised. Too low pressure will cause loss of efficiency while too much boost will cause knocking, which can damage the engine in the long run. The boost pressure in the experimental engine was varied by modifying the waste gate spring housing so it could be adjusted to vary the turbocharger pressure. After the modification, the turbocharger boost could be adjusted between 40 kPa and 80 kPa. Details of the modification are in Figure 3.

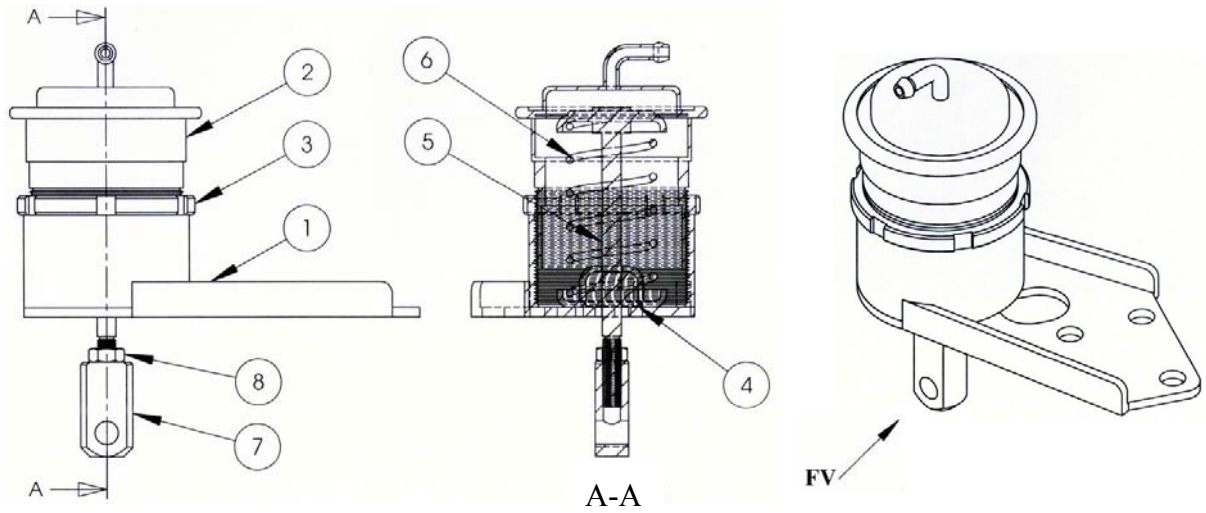


**Figure 3.** Modified waste gate from standard waste gate for adjustable turbocharger pressure: (1) Waste gate base, (2) Waste gate spring housing, (3) Waste gate adjustment lock nut, (4) Push rod bushing, (5) Waste gate push rod, (6) Return spring, (7) Adjustable push rod joint, and (8) Lock nut

Test Rig Description

The purpose of this experiment is to find an optimal tuning condition when a bus diesel engine is modified and converted to a spark ignition engine which will be fueled by biogas to drive an electrical generator to produce electricity. Inlet air and biogas were monitored so air/fuel ratio could be calculated. Exhaust gas was also checked for carbon monoxide and oxide of nitrogen emission at various engine settings. Each component of the test rig is briefly described in the following section. The overall block diagram of the test rig is shown in Figure 4.

*Mj. Int. J. Sci. Tech.* **2007**, *01(2)*, 194-207

*Test engine*

The test engine was a Hino 13,000cc diesel engine with 4 valves per cylinder, modified for biogas fuel as described above. The engine model was K-13CTI and was normally installed in buses in Thailand. This engine was chosen because of used engine availability and commonly available spare parts. It was overhauled to new engine specification before testing and is currently undergoing endurance test at 4T farm, Chiang Mai, Thailand.

*Electrical generator unit*

The generator used was a 3-phase 4-pole 132-kW generator with an induction motor made by HASCON, model number 200L2-2. The generator was directly coupled by a clutch mechanism to the test engine and was synchronised to the power grid when in operation. The nominal operating speed was 1,500 rpm.

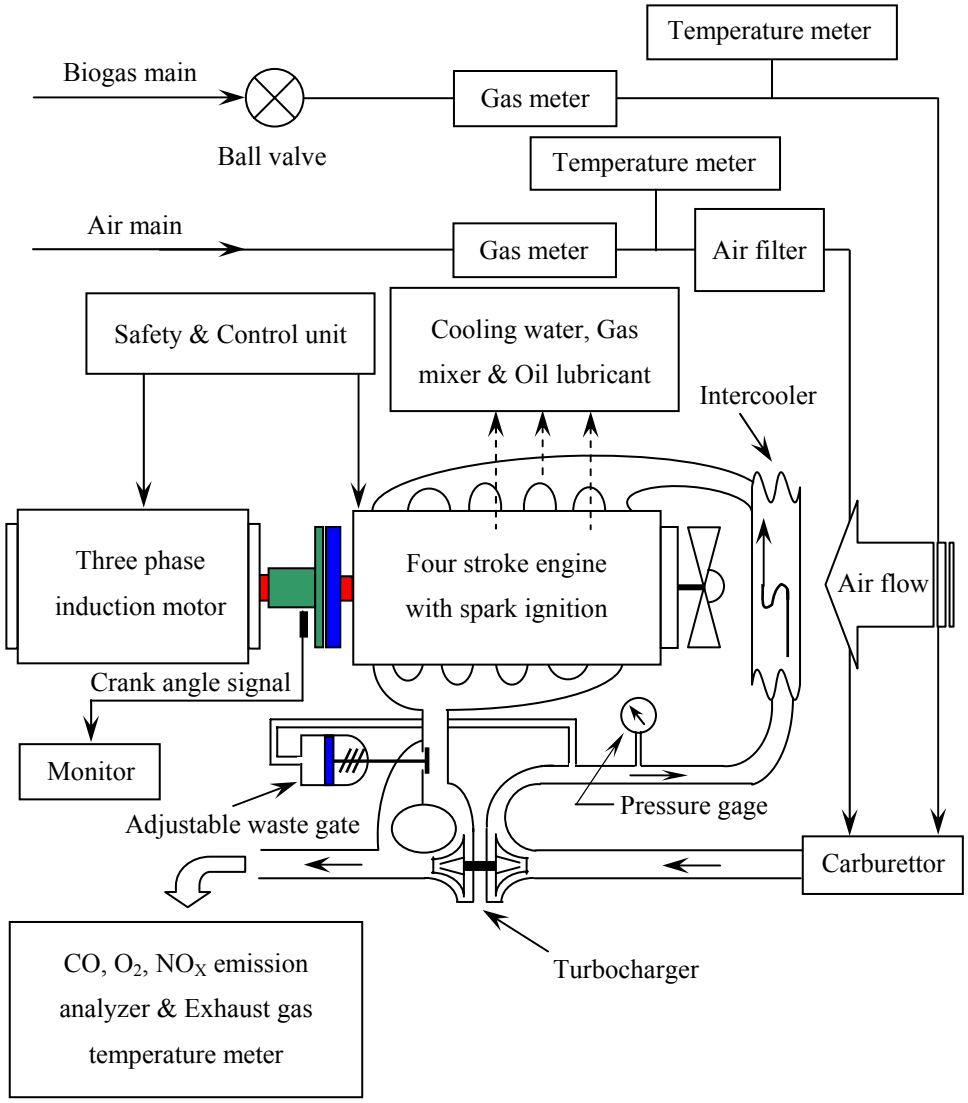


**Figure 4.** Block diagram of the test rig

*Control unit*

Biogas Advisory Unit, Chiang Mai University, designed the control unit and the blueprint was available to the public at no cost. It was used to start the test engine, synchronise the generator with the power grid, as well as monitor safety function in the case of gas supply shortage, short circuit, overloading in power grid, engine overheating, loss of oil pressure in the engine, or power grid failure.

*Intake air measurement*

Intake air flow rate was measured using a Kobold gas flow meter model GVPA-303-GDR.

*Intake biogas measurement*

The composition of inlet biogas varies with the type of animal waste used to produce the gas as well as the ambient temperature in which the fermentation occurs. In general, biogas contains carbon dioxide, methane and one percent of other trace gases. The methane content of biogas can be determined by finding the amount of carbon dioxide, adding 1 percent to the amount and subtracting this from 100, thus yielding the percentage by volume of methane. The amount of carbon dioxide in the biogas was determined by using the Brigon IND 60 gas analyser. The volume flow rate of biogas was measured using a Kobold gas flow meter model GVPA-303-GDR.

*Exhaust gas measurement*

A flue gas analyser (Testo 300XL-1) was used to monitor the quantity of $O_2$, CO, and $NO_X$ in the exhaust gas. The probe attached could also measure the exhaust gas temperature as well.

*Ignition timing measurement*

Ignition timing was measured by a timing light (Sincro model DG86) with trigger signal from the high tension wire from the distributor to cylinder number one spark plug.

*Power output measurement*

The power output from the generator was monitored by Curcutor model AR5 supply network analyser.

Experimental Procedure

The experiment was carried out using the following steps to collect data for analysis.

*Turbocharger pressure adjustment*

The engine was run on biogas with RON of about 130. To get the most benefit from the higher RON, higher compression ratio was used for higher thermal efficiency [15-18]. The proper compression ratio for the spark ignition engine to be run on biogas fuel was between 10 to 12:1 [2].

*Mj. Int. J. Sci. Tech.* **2007**, *01(2)*, 194-207

While a naturally aspirated spark ignition engine may have sufficient margin of safety relative to knock to allow modest inlet-air boost, any substantial air compression prior to cylinder entry will require changes in engine design and/or operating variables to offset the negative impact on knock. The variables which were adjusted to control knock in a turbocharged SI engine were: compression ratio, spark retard from optimum, charge air temperature, and air/fuel equivalence ratio [18]. Therefore the cylinder head was installed with a spacer to increase the combustion chamber volume and produce lower compression ratio. The experiment would start at the compression ratio of 8:1 and the turbocharger pressure was adjusted by the waste gate at 40 kPa and increased at an increment of 4 kPa until engine efficiency began to decrease.

*Initial air/fuel mixture adjustment*

The engine was started, the ignition timing was set at about mid range ($55^o$ BTDC) and the air/fuel mixture screw (metering adjustment screw in the carburetor) was adjusted to the position that the engine just ran smoothly (lean mixture).

*Initial ignition timing adjustment*

The ignition timing was set at $50^o$ BTDC at the beginning of a data collection.

*Data collection*

The recording of the following set of data was performed: air temperature, biogas temperature before and after boost by turbocharger and after cooling by intercooler, engine coolant temperature, lubricating oil temperature, exhaust gas temperature, air and biogas consumption rate, ignition timing, generator power output, oxygen remaining after combustion, carbon monoxide and oxide of nitrogen in the exhaust gas.

*Ignition timing increment*

The ignition timing was advanced $2^o$ and the data above were again collected. The process was repeated until the ignition timing reached $60^o$ BTDC or excessive pre-ignition was observed.

*Air/fuel mixture increment*

After a set of data was collected, the air/fuel mixture screw was turned half a revolution in the rich direction. Another set of data was collected and the process was repeated until the mixture was too rich for the engine to run smoothly.

**Results**

The collected data were processed into excess air ratio ($\lambda$), engine efficiency, and then the system efficiency (overall efficiency), power output, exhaust gas temperature, specific biogas consumption,

oxygen quantity in exhaust gas, carbon monoxide and oxide of nitrogen emission were plotted against the ignition timing, excess air ratio, and turbocharger pressure. The resulting graphs are shown in Figures 5-7.

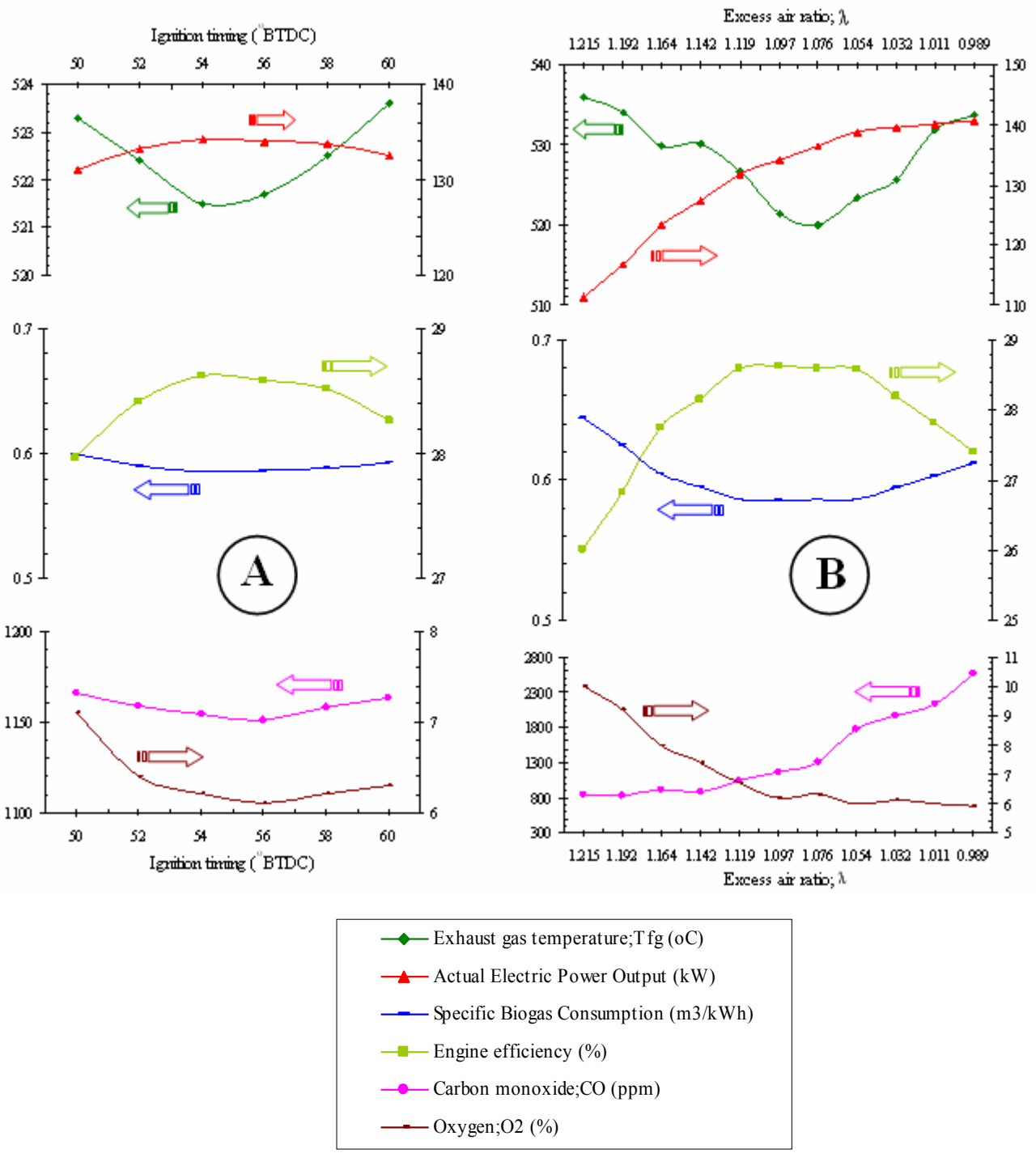


**Figure 5.** Exhaust gas temperature, electric power output, specific biogas consumption, engine efficiency, carbon monoxide, and oxygen for compression ratio of 8:1 and turbocharger pressure setting at 56 kPa plotted against: (A) Ignition timing, and (B) Excess air ratio.

*Mj. Int. J. Sci. Tech.* **2007**, *01(2)*, 194-207

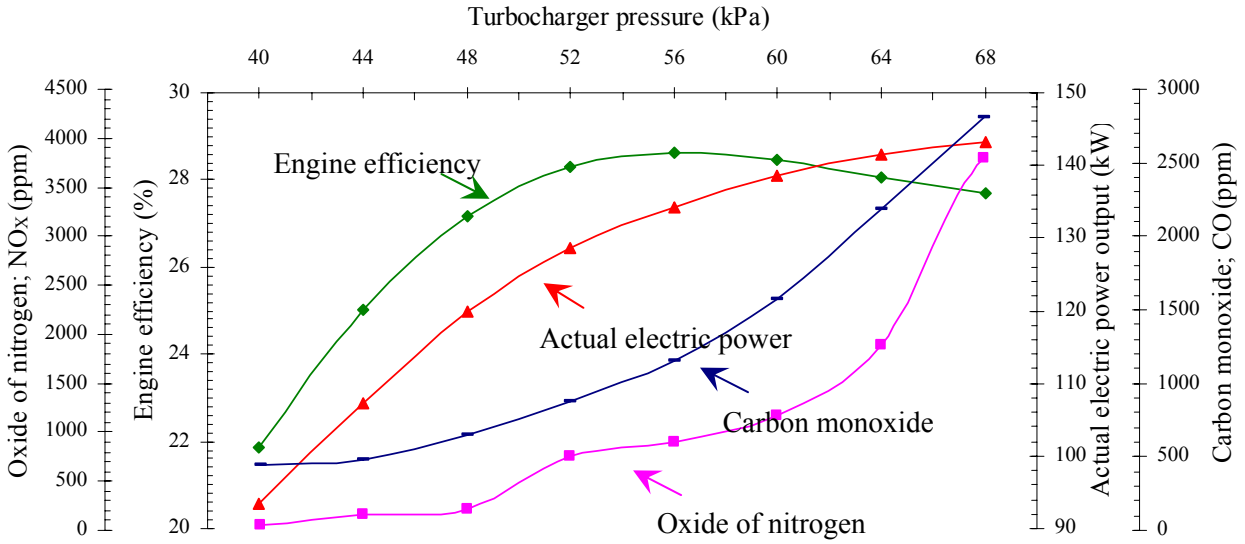


**Figure 6.** Output power, engine efficiency, carbon monoxide and oxide of nitrogen plotted against turbocharger boost pressure.

## Discussion

### *Effect of Ignition Timing on Engine Performance*

From Figure 5(A) it can be seen that the maximum engine efficiency and maximum output power can be achieved at 54° BTDC ignition timing. When the timing is retarded from the optimal setting, the combustion process is completed after the bottom dead center position of the crankshaft and the thermal energy transferred to shaft power is reduced. The result is higher exhaust gas temperature as shown in the graph. If the ignition timing is advanced beyond the optimal point, knocking occurs, resulting in excessive combustion temperature and increase in $NO_X$ and CO emission.

### *Effect of Air/Fuel Mixture on Engine Performance*

Figure 5(B) shows that the optimal excess air ratio for this engine is 1.097. Leaner mixture results in lower flame speed and incomplete combustion, which leads to high exhaust gas temperature. Rich mixture can lead to engine knock and results in higher $NO_X$ and CO emission as well as high exhaust temperature.

### *Effect of Turbocharger Boost Pressure on Engine Performance*

Figures 6 and 7 show that the increase in turbocharger boost pressure can increase the engine output even though the engine efficiency has dropped off at higher boost pressure. Increasing the boost pressure beyond the maximum efficiency point results in high CO and $NO_X$ emission as well as excessive engine vibration and it appears that the increased engine output is not worth the increased pollution and shortened engine life due to vibration.

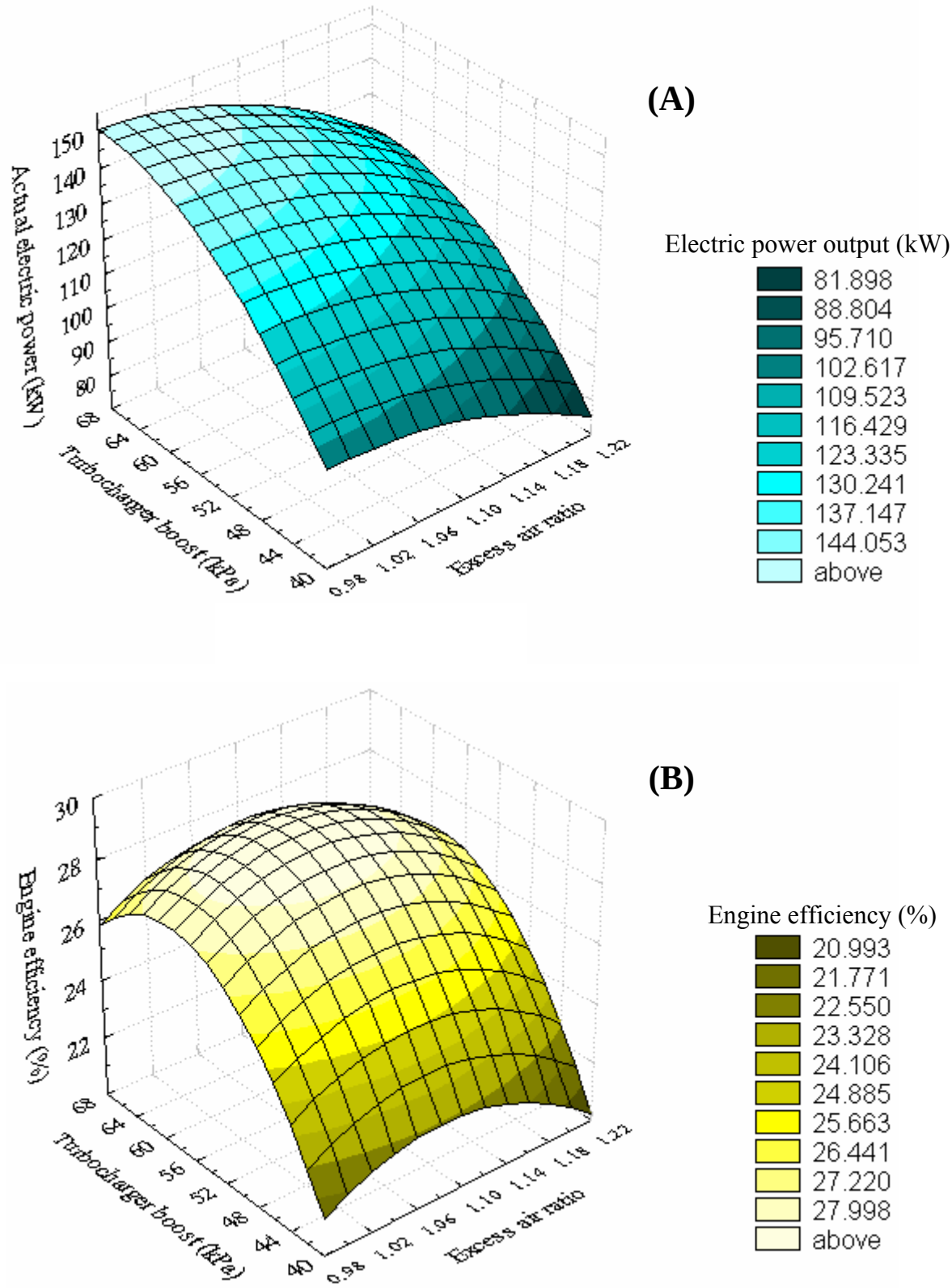


**Figure 7.** Power output (A) and engine efficiency (B) plotted against excess air ratio and turbocharger pressure at compression ratio of 8:1

*Mj. Int. J. Sci. Tech.* **2007**, *01(2)*, 194-207

Three categories of tuning optimisation were done. The categories are lowest CO emission, highest engine efficiency, and highest power output. The tuning parameters and collected data for the three categories are presented in Table 1.

With the presented data, it can be shown that a large diesel engine can be economically adapted for power generation in a farm. The payback period is less than one year and when properly tuned, the engine passes the internationally accepted pollution control standard of carbon monoxide of a vehicle engine [19, 20].

**Table 1.** Summarised data of fine tuning of biogas engine for optimum operation when compression ratio is 8:1 and turbocharger boost pressure is 56 kPa

| Item | Lowest CO emission | Highest engine efficiency | Highest power output |
|---|---|---|---|
| 1. Optimum ignition timing ($^o$ BTDC) | 57 | 54 | 52 |
| 2. Excess air ratio; $\lambda$ | 1.215 | 1.097 | 0.989 |
| 3. Fuel consumption; $\dot{f}_C$ ($m^3$/hr) | 71.80 | 78.60 | 86.10 |
| 4. Specific fuel consumption; sfc ($m^3$/kWh) | 0.64 | 0.59 | 0.61 |
| 5. Actual electric power output; $P_{EL}$ (kW) | 111.40 | 134.20 | 140.70 |
| 6. Engine efficiency; $\eta_{eng}$ (%) | 26.01 | 28.63 | 27.40 |
| 7. Overall efficiency; $\eta_{tot}$ (%) | 23.41 | 25.76 | 24.66 |
| 8. Oxide of nitrogen emission; $NO_X$ (ppm) | 511 | 896 | 843 |
| 9. Carbon monoxide emission; CO (ppm) | 854 | 1,154 | 2,576 |
| 10. Oxygen in exhaust gas; $O_2$ (%) | 10.00 | 6.20 | 5.90 |
| 11. Engine coolant temperature; $T_{eng}$ ($^o$C) | 88.2 | 88.7 | 89.0 |
| 12. Lubricating oil temperature; $T_{oil}$ ($^o$C) | 87.8 | 87.2 | 87.6 |
| 13. Exhaust gas temperature; $T_{fg}$ ($^o$C) | 536.0 | 521.5 | 533.8 |
| 14. Payback period (year) | 0.78 | 0.52 | 0.49 |

## Conclusion

In this study, engine performance and pollution figures are recorded for a range of engine tuning parameters, viz. turbocharger boost, ignition timing and excess air ratio. The compression ratio was set at 8:1 and the turbocharger boost was varied by adjusting the waste gate. When the system was operating at 1,500 rpm, the range of engine setting was as follows: excess air ratio between 0.9 to 1.2, ignition timing between 50$^o$ to 60$^o$ before top dead center, and turbocharger pressure setting between 40 to 68 kPa. Under these operating conditions, the engine efficiency increased as the boost was increased from 40 to 56 kPa and there was a slight increase of $NO_X$ and CO as the boost went up. As the boost was increased from 56 kPa to 68 kPa, the engine efficiency began to decrease and the amount of pollution was increased. Increase in engine vibration was also noted in this turbocharger boost range. Oxide of nitrogen ($NO_X$) was high when high pressure and temperature occurred in the combustion. A test showed that more power can be generated if the engine is operated with rich excess

air ratio and high turbocharger boost. Higher engine output will yield shorter payback period for the investment but increasing the boost pressure beyond 56 kPa will cause excessive pollution emission and engine vibration, which will probably shorten the engine life. It can be concluded that the boost pressure of 56 kPa yields the highest efficiency with acceptable pollution level for this engine.

**Acknowledgements**

The work presented in this research would not have been possible without the invaluable support from many people. First and foremost, the authors would like to gratefully acknowledge material assistance from the Mechanical Engineering Department of Chiang Mai University and also from Biogas Technology Center (BTC). 4T Farm Chiang Mai is cordially thanked for permission to use the location and biogas to finish the research.

Last and most importantly, we would like to thank the Energy Policy and Planning Office (EPPO), Thailand for financial support.

**References**

1. U. Werner, U. Stoehr, and N. Hees, "A Handbook of Biogas Plants in Animal Husbandry; A Practical Guid in Deutsche Gesellschaft fuer Technische Zusammenarbeit (GTZ)", Friedr. Vieweg & Sohn, Verlagsgesellschaft mbH, **1988**.
2. K. von Mitzlaff, "A Handbook of Engine for Biogas; Theory, Modification, Econum, Operation", Friedr. Vieweg & Sohn, Verlagsgesellschaft mbH, **1988**.
3. G. Sridhar, P. J. Paul, and H. S. Mukunda, "Biomass derived producer gas as a reciprocating engine fuel, an experimental analysis", *J. Biomass and Bioenergy*, **2001**, *21*, 61−72.
4. J. L. King and T. Mintner, "Biogas-driven generator set", *US Patent*, Patent Number: 5,724,948, Mar. 10, **1998.**
5. S. Siripornakarachai and T. Sucharitakul, "Adapting gasoline engine to biogas engine for electrical power generation", *J. Energy Word*, **2007,** *37*, 34-36.
6. N. Potikanond, "Use of animals dung from biogas reactor as fertilizer", Project for Promotion of Biogas Production in Animals Farm (Handbook), Biogas Advisory Unit (BAU), Chiang Mai, **1995**.
7. M. K. K. Publ, "Kirloskar Dual Fuel Biogas Engines", Commonwealth Regional (Asia/Pacific) Rural Technology Programme, Bombay, **1980**.
8. A. Henhem and M. K. Makkar, "Combustion of simulated biogas in a diesel-fuel diesel engine", *J. Sci.*, **1998**, *39*, 2001-2009.
9. S. P. E. Persson and H. D. Bartlett, "Biogas engines for agricultural motor-generators", *J. Amer. Soc. Agric. Eng. (ASAE)*, **1981**, Paper Number: 811211.
10. A. Bilican, O. L. Corre, and A. Delebarre, "Thermal efficiency and environmental performances of a biogas-diesel stationary engine", *J. Environ. Tech.*, **2003,** *24*, 1165-1173.
11. J. O. Canavate, D. J. Hills, and W. J. Chancellor, "Diesel engine modification to operate on biogas.", Transactions of the American Society of Agricultural Engineers (ASAE), **1981**.

*Mj. Int. J. Sci. Tech.* **2007**, *01(2)*, 194-207

12. K. V. Mitzlaff and M. H. Mkumbwa, "Use of biogas as an alternative fuel in stationary diesel engines.", Technical Report, University of Dar-es-Salaam, Tanzania, **1985**.
13. S. Siripornakarachai and T. Sucharitakul, "Modification of diesel engine for electricity production fueled by biogas", The 6th Asia Pacific Conference on Sustainable Energy and Environmental Technologies (APCSEET 2007*)*, 7 - 11 May **2007**, Bangkok, Thailand.
14. S. Siripornakarachai and T. Sucharitakul, "Tuning of multi-valve automotive engine for electricity production fueled by biogas.", International Conference on Green and Sustainable Innovation (ICGSI 2006*)*, 29 November - 1 December **2006**, Chiang Mai, Thailand.
15. S. Siripornakarachai, "The result of worked as velocity of electrical power generator used by biogas", *J. Energy Word*, **2007,** *36*, 32-35.
16. Hino Motors, Ltd., "A Handbook of Industrial Engines", Tokyo, **2005**.
17. J. Huang and R. J. Crookes, "Assessment of simulated biogas as a fuel for the spark ignition engine", *J. Sci.*, **1998**, *77*, 1793−1801.
18. J. B. Heywood, "A Textbook of Internal Combustion Engine Fundamentals", Int. Edn., McGraw-Hill, New York, **1988**.
19. Pollution Control Department in Ministry of Natural Resources and Environment, Bangkok, Thailand, "Law & Regulations of Air Quality and Noise Standard", *http//www.pcd.go.th/info_serv/ reg_std_airsnd02.html*, 1 November, **2007**.
20. United States Environmental Protection Agency (USEPA), "Law & Regulations of Air Pollution", *http//www.epa.gov/ebtpages/air.html*, 1 November, **2007**.

*Mj. Int. J. Sci. Tech.* **2007**, *01(02)*, 208-215

***Maejo International***

***Journal of Science and Technology***

**ISSN 1905-7873**

Available online at www.mijst.mju.ac.th

*Full Paper*

# Growth inhibition of *Penicillium digitatum* by antagonistic microorganisms isolated from various parts of orange tree

**Kreuawan Thonglem, Abhinya Plikomol, and Wasu Pathom-aree***

Microbiology Section, Department of Biology, Faculty of Science, Chiang Mai University, Chiang Mai 50200, Thailand

*Corresponding author, e-mail: wasu@chiangmai.ac.th

*Received: 3 October 2007 / Accepted: 4 November 2007 / Published: 10 November 2007*

**Abstract:** *Penicillium digitatum* (Pers.:Fr) Sacc. is the major cause of green mold disease in orange trees grown for orange production industry in Thailand. In this study, antagonistic microorganisms were isolated from various parts of healthy orange trees. A total of 121 microbial isolates were recovered from which 15 isolates showed inhibitory effect against *P. digitatum* by spot test technique. The inhibitory effect of these 15 isolates was also tested by agar disc diffusion method using culture filtrate from nutrient broth. It was found that isolate W1L1, D1L2 and W1L9 gave the best inhibition with a clear zone of 21, 15 and 14 mm in diameter, respectively. The effect of culture filtrate on spore germination was also investigated. The result showed that isolate W1L1 gave the highest inhibition after 8 hours of incubation with the lowest germination rate of 2.4%. Morphological and biochemical characterizations revealed that these isolates were members of the genus *Bacillus* and identified as *B. pumilus*.

**Keywords:** *Penicillium digitatum*, antagonistic microorganisms, oranges, *Bacillus*, biological control

*Mj. Int. J. Sci. Tech.* **2007**, *01(02)*, 208-215

## Introduction

Orange (*Citrus sinensis*) is one of the economic fruits in Thailand. Most production areas are in the northern part of the country especially Chiang Mai. In 2004, Thailand exported 2,189 tons of oranges to Asian countries with a value of 50.8 million Baht [1]. Fungal diseases are one of the major problems facing the citrus production in all areas of the world and resulted in enormous economic losses [2]. Green mold is the most important postharvest disease of citrus in many Asian countries including Thailand. The responsible agent is the fungus, *Penicillium digitatum* (Pers.:Fr) Sacc. [3]. This fungus survives in the orchard from season to season mainly in the form of conidia and causes infection by airborne spores where there are injuries or blemishes [4]. The disease is generally controlled by fungicides such as imazalil, sodium ortho-phenyl phenate, or thiabendazole [5,6]. The use of these chemical agents has been applied for many years with few or limited success due to the development of resistance by the fungus [7,8]. In addition, the accumulation of hazardous chemicals in the environment raises public concern about their effect on human health. There is an urgent demand for new methods to supplement the existing regimes to achieve better disease control. Biological control offers an environment-friendly alternative to the use of chemicals for controlling plant diseases [2,9,10]. The increasing interest in the development of such control has led to our investigation of microorganisms associated with orange trees as potential microbial agents for the control of *P. digitatum*. In this study, we reported the isolation of antagonistic microorganisms from various parts of healthy orange trees and their inhibitory effect on growth and spore germination of *P. digitatum* in vitro.

## Materials and Methods

### *Isolation of antagonistic microorganisms*

Samples of branches, flowers, leaves, and young fruits of healthy orange trees were collected from 4 orange plantations in Chiang Mai and antagonistic microorganisms were isolated from these samples. Approximately 25 g of each sample were added to 225 ml of sterile distilled water in a 500 ml conical flask and incubated in an ultrasonic bath for 10 minutes. The resultant suspension (0.1 ml) was used to inoculate nutrient agar plates. All plates were incubated at room temperature and microbial colonies appearing after 24 hours were picked and restreaked until pure cultures were obtained. The isolates were maintained on nutrient agar slant for routine use and in 20% glycerol at -20$^{o}$C for long term preservation.

### *Pathogen*

*P. digitatum* was isolated from an infected orange and cultured on a potato dextrose agar (PDA). The spore suspensions were prepared from a 5 day old culture by adding sterile distilled water on the surface of the agar slant and scraping the growth off the surface using sterile cotton swab.

Tween 20 (0.04%) was added to the resultant spore suspension to help dispersion. The concentration of spores was determined by direct count using a haemacytometer and adjusted as required.

*Preliminary screening for antifungal activity*

The antagonistic potential of isolated microorganisms against *P. digitatum* was determined in triplicate by spot test technique [11] on PDA for each isolate. The tested isolates were grown on nutrient agar for 24 hours and used to inoculate at the periphery of PDA plates seeded with *P. digitatum* spore suspension. Five isolates were inoculated on each plate. All plates were incubated for 3 days at room temperature before recording of the inhibition zone. Isolates that showed inhibitory effect against *P. digitatum* were selected for further screening using agar diffusion method.

*Screening of antifungal activity by agar disc diffusion method*

Subsequent screening of promising isolates from preliminary study was performed using Kirby-Bauer method [12]. For this purpose, the antagonistic isolates were grown on nutrient agar and incubated for 24 hours at room temperature. Two loops were taken from the resulting colonies from each isolate and transferred to 50 ml of nutrient broth. The cultures were incubated on a rotary shaker (150 rpm) for 24 hours at 28$^{o}$C. The bacterial cells were harvested by centrifugation (6000 rpm for 20 min) at 4$^{o}$C and the supernatant collected. The supernatant was filtered through a 0.22 μm-pore cellulose acetate filter and stored at 4$^{o}$C until use. Three 5-mm sterile paper discs were placed on PDA plates seeded with *P. Digitatum* spore suspension and 25 μl of supernatant were applied to each disc. Antifungal activity was determined on PDA after 4 days incubation at room temperature and expressed as diameter (mm) of the inhibition zone.

*Inhibitory effect of culture filtrate on the spore germination of P. digitatum*

An equal volume of *P. digitatum* spore suspension ($3x10^{6}$ spores/ml) was mixed with the culture filtrate of isolates D1L2, W1L1 and W1L9 in sterile test tubes. The germination of spore was observed microscopically at 0, 4 and 8 hours. The spore was considered to be germinated only when the length of the germ tube was twice that of the diameter [12], and the results were presented as percentage of germination. In addition, another set of experiment was prepared by incubating the mixture of spore suspension and culture filtrate (1:1, v/v) at room temperature for 7 days and spore germination observed. A control set using nutrient broth in place of culture filtrate was included in all experiments.

*Mj. Int. J. Sci. Tech.* **2007**, *01(02)*, 208-215

*Identification of bacterial isolates*

Identification of the three most effective isolates was carried out according to Bergey's Manual of Systematic Bacteriology volume 2 [14]. The dichotomous key of Guerra-Cantera and Raymundo [15] was used to assist in the assignment of these isolates to the species level.

## Results and Discussion

A total of 121 microorganisms were isolated from various parts of healthy orange trees. Among these, 68 isolates were recovered from branches, 38 isolates from leaves, 9 isolates from fruits and 6 isolates from flowers. Preliminary screening of these isolates by spot test technique showed that 15 isolates were inhibitory to *P. digitatum* on PDA with the diameter of clear zone ranging between 12.5-28 mm (Table 1). Further screening by agar disc diffusion method showed that only 7 isolates gave positive results when their culture filtrates were tested. Among these, isolates W1L1, W1L9 and D1L2 gave the largest clear zones on the test media (Table 2). In addition, the culture filtrates of these three isolates were found to inhibit the germination of *P. digitatum*'s spores (Table 3). No growth was

Table 1. Antagonism of bacterial isolates against P. digitatum by spot test assay

| **Bacterial isolate** | **Zone of inhibition ( mm )** |
|---|---|
| D1L2 | 26 |
| D2S2 | 12.5 |
| K4L3 | 28 |
| K6L1 | 22 |
| WC2 | 16.5 |
| W1L1 | 21 |
| W1L2 | 22 |
| W1L4 | 19 |
| W1L7 | 15 |
| W1L8 | 26 |
| W1L9 | 27.5 |
| W2F3 | 18 |
| W3L2 | 28 |
| W3L4 | 15 |
| W3S1 | 21.5 |

*Mj. Int. J. Sci. Tech.* **2007**, *01(02)*, 208-215

observed in the tube containing a mixture of the spore suspension ($3x10^6$ spores/ml) and the culture filtrate (1:1, v/v) after incubation at room temperature for 7 days. On the contrary, the fungal hyphae were clearly visible in the control set. Identification tests showed that these isolates were Gram positive, rod shaped and produced endospores. They were catalase and oxidase positive and did not grow under anaerobic condition, thus belonging to the genus *Bacillus*. According to the identification key of Guerra-Cantera and Raymundo [15], these isolates were assigned to *B. pumilus* species.

**Table 2**. Antagonism of bacterial isolates against *P. digitatum* by agar disc diffusion method

| **Bacterial isolate** | **Zone of inhibition ( mm )** |
|---|---|
| D1L2 | 15 |
| WC2 | 10 |
| W1L1 | 21 |
| W1L4 | 12 |
| W1L8 | 12 |
| W1L9 | 14 |
| W3S1 | 7.5 |

**Table 3.** Germination rate (%) of *P. digitatum* spore in culture filtrate of antagonistic microorganisms

| **Time (hr)** | **Germination rate (%)** | | | |
|---|---|---|---|---|
| | **control** | **W1L1** | **W1L9** | **D1L2** |
| 0 | 0 | 0 | 0 | 0 |
| 4 | 1.5 | 0 | 1.9 | 1.9 |
| 8 | 17.0 | 2.4 | 3.0 | 4.3 |

Several antagonistic microorganisms have been shown to suppress decay of citrus by green mold [8,16-19]. Moreover, a commercial biocontrol product containing the yeast *Candida oleophila* has been available under the name Aspire (Ecogen Corporation, Langhorne, PA) in the United States and Israel for use against postharvest decay of citrus [20]. However, Aspire alone was found to be insufficient to reduce the decay to commercially acceptable levels. Later, Brown et al. [3] reported that the efficacy of Aspire was also affected by the type of injury, and cells of *C. oleophila* were sensitive to volatiles of orange peel oil. They also showed that citrus oil and its volatiles not only exhibited no activity against *P. digitatum* but also stimulated the germination of the fungus.

The use of *Bacillus* occurring naturally on the surface of fruits or vegetables as biocontrol of postharvest diseases has also been reported previously. Many surveys of antagonistic bacteria support the potential of *Bacillus* for controlling various plant pathogenic fungi [21-26]. Members of the genus

*Mj. Int. J. Sci. Tech.* **2007**, *01(02)*, 208-215

*Bacillus* have a natural advantage over Gram negative bacteria for use as biocontrol agents. Particularly, this is their ability to produce heat- and dessication-resistant spores, which offers an ease of formulation and storage of the products [9]. The formulation and application methods play key issues for the efficacy and successful outcome of the commercial products [10]. In addition, there are currently 2 biological control products approved by U.S. Environmental Protection Agency that contain *B. pumilus* as an active ingredient and currently available in the market, namely GB34 concentrate or technical biological fungicide (Bayer Cropscience LP, NC) and Sonata ASO or QST2808 technical (Agraquest Inc., OR) [27].

## Conclusion

In conclusion we have demonstrated that strains assigned as *Bacillus pumilus* isolated from healthy orange trees can inhibit the growth of *Penicillium digitatum* in vitro, thus contributing to the literature on biological control of *P. digitatum.* The results of the present study also provide further evidence that antagonistic microorganisms are good sources of potential biocontrol agents against plant pathogenic fungi.

## Acknowledgements

This work was supported by Chiang Mai University research fund. The authors would also like to thank the Department of Biology (Faculty of Science, Chiang Mai University) for all facilities provided, and Mr Patipan Nantakwang for the *P. digitatum* isolate used in this study.

## References

1. Office of Agricultural Economics, available from http://www.oae.go.th/statistic/export/QVExp.xls
2. W. J. Janisiewicz and L. Korsten, “Biological control of postharvest diseases of fruits”, *Annu. Rev. Phytopathol*., **2002**, *40*, 411-441.
3. G. E. Brown, C. Davis, and M. Chambers, “Control of citrus green mold with Aspire is impacted by the type of injury”, *Postharvest Biol. Technol*., **2000**, *18*, 57-65.
4. W. N. Chang and J. B. Petersen, “Citrus production: a manual for Asian farmers”, The Food and Fertilizer Technology Center for the Asian and Pacific Region, Taipei, 2003.
5. F. Yildiz, P. Kinay, M. Yildiz, F. Sen, and I. Karacali, “Effects of preharvest applications of $CaCl_2$, 2,4-D and benomyl and postharvest hot water, yeast and fungicide treatments on development of decay on *Satsuma mandarins*”, *J. Phytopathol*., **2005**, *153*, 94-98.
6. R.Torres, C. Nunes, J. S. Garcia, M. Abadias, I. Vinas, T. Manso, M. Olmo, and J. Usall, “Application of *Pantoea agglomerans* CPA-2 in combination with heated sodium bicarbonate solutions to control the major postharvest diseases affecting citrus fruit at several mediterranean locations”, *Eur. J. Plant Pathol*., **2007**, *118*, 73-83.

7. G. J. Holmes and J. W. Eckert, "Sensitivity of *Penicillium digitatum* and *P. italicum* to postharvest citrus fungicides in California", *Phytopathol*., **1999**, *89*, 716-721.
8. M. Zamani, A. S. Tehrani, M. Ahmadzadeh, and A. A. Abadi, "Effect of fluorescent pseudomonades and *Trichoderma* sp. and their combination with two chemicals on *Penicillium digitatum* caused agent of citrus green mold", *Commun. Agric. Appl. Biol. Sci*., **2006**, *71(3 Pt B)*, 1301-1310.
9. E. A. B. Emmert and J. Handelsman, "Biocontrol of plant disease: a (Gram-) positive perspective", *FEMS Microbiol. Lett.*, **1999**, *171*, 1-9.
10. D. Spadaro and M. L. Gullino, "State of the art and future prospects of the biological control of postharvest fruit diseases", *Int. J. Food Microbiol*., **2004**, *91*, 185-194.
11. R. K. S. Wood, "The control of diseases of lettuce by use of antagonistic organisms. I: The control of *Botrytis cinerea* Pers", *Ann. Appl. Biol*., **1951**, *38*, 203-216.
12. A. W. Bauer, W. M. Kirby, J. C. Sherris, and M. Turk, "Antibiotic susceptibility testing by a standardized single disk method", *Am. J. Clin. Pathol*., **1966,** *45*, 493-496.
13. Y. Kou, P. F. Molitor, and S. J. Schmidt, "Mobility and stability characterization of model food systems using NMR, DSC and conidia germination techniques", *J. Food Sci*., **1999**, *64*, 950-959.
14. P. H. A. Sneath, "Bergey's manual of systematic bacteriology", Vol. 2, Williams & Wilkins, Baltimore, **1986**, p. 1104-1139.
15. M. A. R. V. Guerra-Cantera and A. K. Raymundo, "Utilization of a polyphasic approach in the taxonomic reassessment of antibiotic- and enzyme-producing *Bacillus* spp. isolated from the Philippines", *World J. Microbiol. Biotechnol*., **2005**, *21*, 635-644.
16. G. Arras, "Mode of action of an isolate of *Candida famata* in biological control of *Penicillium digitatum* in orange fruits", *Postharvest Biol. Technol*., **1996**, *8*, 191-198.
17. G. Arras, B. Scherm, and Q. Migheli, "Improving biocontrol activity of *Pichia guillermondii* against post-harvest decay of oranges in commercial packing houses by reduced concentrations of fungicides", *Biocontrol Sci. Technol*., **2002**, *12*, 547-553.
18. C. G. Eayre, M. Skaria, C. T. Bull, and B. Mackey, "An avirulent *Galactomyces* species that controls green mold of citrus caused by *Penicillium digitatum*", *Subtropical Plant Sci*., **2003**, *55*, 46-50.
19. X. D. Zheng, H. Y. Zhang, and P. Sun, "Biological control of postharvest green mold decay of oranges by *Rhodotorula glutinis*", *Eur. Food Res. Technol*., **2005**, *220*, 353-357.
20. D. R. Fravel, "Commercialization and implementation of biocontrol", *Annu. Rev. Phytopathol.*, **2005**, *43*, 337-359.
21. M. Mari, M. Guizzardi, M. Brunelli, and A. Folchi, "Postharvest biological control of grey mould (*Botrytis cinerea* Pers.:Fr.) on fresh-market tomatoes with *Bacillus amyloliquefaciens*", *Crop Prot.*, **1996**, *15*, 699-705.
22. M. Mari, M. Guizzardi, and C. Pratella, "Biological control of gray mold in pears by antagonistic bacteria", *Biol. Control*, **1996**, *7*, 30-37.

*Mj. Int. J. Sci. Tech.* **2007**, *01(02)*, 208-215

23. T. W. Chen and W. S. Wu, “Biological control of carrot black rot”, *J. Phytopathol.*, **1999**, *147*, 99-104.
24. C. S. Schmidt, D. Lorenze, and G. A. Wolf, “Biological control of the grapevine dieback fungus *Eutypa lata*. I: screening of bacterial antagonists”, *J. Phytopathol.*, **2001**, *149*, 427-435.
25. A. L. Chiou and W. S. Wu, “Isolation, identification and evaluation of bacterial antagonists against *Botrytis elliptica* on lily”, *J. Phytopathol.*, **2001**, *149*, 319-324.
26. J. Obagwu and L. Korsten, “Integrated control of citrus green and blue molds using *Bacillus subtilis* in combination with sodium bicarbonate or hot water”, *Postharvest Biol. Technol.*, **2003**, *28*, 187-194.
27. available from www.epa.gov/pesticides/biopesticides

*Mj. Int. J. Sci. Tech.* **2007**, *01(02)*, 216-221

***Maejo International***

***Journal of Science and Technology***

**ISSN 1905-7873**

Available online at www.mijst.mju.ac.th

*Full Paper*

# Effect of culture season and stocking density on growth and production of giant freshwater prawn (*Macrobrachium rosenbergii* de Ma) raised in northern Thailand

**Rodrigo P. Baysa[*] and Niwooti Whangchai**

Faculty of Fisheries Technology and Aquatic Resources, Maejo University, Chiang Mai, 50290. Thailand

Corresponding author, e-mail: ogrids_baysa@yahoo.com

*Received: 1 October 2007 / Accepted: 31 October 2007 / Published: 2 December 2007*

**Abstract:** This study evaluated the effects of culture season and stocking density on productivity of freshwater prawns that were raised in northern Thailand. The first experiment investigated the effect of climatic condition on the culture and production of freshwater prawn post larvae (PL 10; mean weight of 0.02 g) stocked in 400m$^2$ ponds. Results of the first experiment revealed that freshwater prawns raised during the dry season to summer had higher growth rate (0.19 g and 0.15 g/day) and survival rate (34.27% and 24.49%) than those raised during summer to rainy season ($p<0.05$). The second experiment investigated the effect of 2 different stocking densities (25 and 50 individuals/m$^2$) on the production survival of freshwater prawns. Results showed that the rate of growth, survival rate, and production were much higher at a stocking density of 25 individuals/m$^2$ ($p<0.05$) in contrast to 50 individuals/m$^2$.

**Keywords:** seasons, stocking density, freshwater prawn

## Introduction

In recent years, aquaculture has been the fastest growing primary production industry worldwide, amounting to 39.4 million tons in 1998 [1]. The success of the industry is based on the selection of

*Mj. Int. J. Sci. Tech.* **2007**, *01(02)*, 216-221

species with adequate characteristics for commercial production. For example, an Australian redclaw crayfish species (*Cherax quadricarinatus*) is a species with considerable potential for commercial culture [2]. High growth and tolerance to wide variations in water quality parameters are important attributes, making the species suitable for cultivation [3].

Stocking density is a major factor affecting production parameters, such as growth, survival, and yield of culture species [4]. Several studies have been conducted to evaluate the effect of density on these production parameters in crayfish species. Lutz and Wolters [5], for example, developed model equations for prediction of pond harvest of red swamp crawfish (*Procambarus clarkii*) as a function of density. Jones and Ruscoe [6] conducted an experiment in earthen ponds to evaluate the effect of the stocking density (1, 3, and 5/$m^2$) on the production parameters for grow-out of red claw crayfish in Alabama. Morrisey [7] working with the same species in cages within the earthen ponds, determined stocking size (4.6-17.01 g) and density (3-15 individuals/m2) with optimum yields.

Pito and Rouse [8] proposed a management strategy for aquaculture in Ecuador, incorporating a mixed-sex nursery stage not exceeding 70-80 days, to obtain a minimum target size of 25 g. The individuals would subsequently be stocked at 6 individuals/$m^2$ for monosex grow-out for periods necessary to complete a 180-210 day cycle. In this study, an experiment was carried out using high stocking densities for the nursery stage to obtain the specified target size within 70-80 days and to evaluate the effect of those densities on survival and yields of the redclaw crayfish. Facilities of a commercial farm in gravel–lined ponds in Ecuador were used to conduct this investigation.

However, few researches about interactive effects of stocking density on prawn growth performance were reported. The experiment described here was conducted to determine the effect of culture season and stocking density on the growth, survival rate, and production of freshwater prawns (*Macrobrachium rosenbergii*).

## Materials and methods

### *Experimental protocol*

The study consisted of two experiments, in which the first evaluated of the effect of season on the growth and survival or production of freshwater prawns, while the second experiment evaluated the effect of stocking density on the same things. Two treatments (T1 and T2), each done in triplicate, were initiated in each experiment in a 400-$m^2$ experimental pond.

### *Experiment 1: Evaluation of the effect of culture season on the growth and production of freshwater prawns*

The experiment was conducted from the dry season to summer (treatment 1) and the second phase was conducted from summer to rainy season (treatment 2). Mixed sexes (male and female) were stocked with post lavae (PL 10) with a mean weight of 5 g at a density of 25 PL/$m^2$ and cultured for a seven-month period (October 2004 to April 2005 and February 2006 to September 2006) for each trial. Commercial feeds (36% crude protein content) were fed (Table 1) four times daily (0800, 1000, 1200, and 1600 hr) from 0 to 90 days (at the rates of 30, 20, 12, 8.0, and 6.0 percent of the total biomass per

day) and three times daily from 91 to 210 days (at the rates of 4.0, 3.0, and 2.5 percent of the total biomass per day).

**Table1.** Feeding rate and feeding frequency

| Age (day) | Feeding rate (%BW/day) | Feeding frequency (no.of time/day) |
|---|---|---|
| 0-15 | 30 | 4 |
| 15-45 | 20 | 4 |
| 45-60 | 12 | 4 |
| 60-75 | 8.0 | 4 |
| 75-90 | 6.0 | 4 |
| 91-120 | 4.0 | 3 |
| 120-150 | 3.0 | 3 |
| 150 to harvest (210) | 2.5 | 3 |

*Experiment 2: Evaluation of the effect of stocking density in growth and production of freshwater prawns*

Juvenile freshwater prawns were used. They were stocked into the experimental pond at 25 and 50 individuals/$m^2$ (T1 and T2 respectively). Commercial feeds (as above) were used and fed three times per day at an amount of 3 % of their total biomass/day.

*Sample collection*

The prawn sample was group-weighed (drained weight), counted, and returned to the pond. On the last sampling dates prior to harvest, prawns were also individually weighed.

*Water quality management and monitoring*

Water changes were made to all treatments at the same time. One-half volume of water was changed 3 times per week to maintain water quality. Aeration was contiunuous and DO concentrations were maintained to the experimental levels by control of aerating quantity. An on-site check for DO and temperature was done weekly (at 0900 hr) using a YSI Model 57 oxygen metre. Levels of total ammonia-nitrogen (TAN) and nitrite-nitrogen were determined weekly at approximately 0900 hr according to outlined procedures. The pH was determined weekly at 1300 hr using an electronic pH metre. Other variables measured (biweekly) were orthophosphate, nitrate, BOD, and turbidity. Data were compiled into monthly means for analysis.

*Mj. Int. J. Sci. Tech.* **2007**, *01(02)*, 216-221

*Data analysis*

Water quality data, prawn growth, survival rate, total production and feed conversion ration (FCR) data were analysed by Analysis of Variance (ANOVA) using SPSS 11.0 statistical software. Significant differences among the treatments were compared by Duncan's Multiple Range Test (DMRT). Differences were considered significant at the level of 0.05.

## Results and Discussion

*Experiment 1*

There were no major differences in measured water quality parameters between treatments. Each variable was within an acceptable limit for freshwater prawn culture. Water temperatures in ponds ranged from a average of 25.2°C (for treatment 1) to 31.0°C (for treatment 2). Dissolved oxygen ranged from 6.1 to 7.4 mg/L (mean of 6.8mg/L) and pH was maintained at 8.0.

There were significant differences ($P$<0.05) in prawn growth and survival between treatments (Table 2). Based on the result of this study, prawns raised in dry season have higher survival rate (34.3% vs. 24.5%) and growth rate (0.19g/day vs. 0.15 g/day) as well as higher production (392 kg/rai vs. 208 kg/rai) compared to those raised in the rainy season, possibly because the abundance of natural food is much higher in the dry season than during the rainy season. Treatment 1 also resulted in statistically higher individual weights (47.8 ± 3.7 g) compared with those in treatment 2 (34.8 ± 1.7 g), although the feed conversion ratio in treatment 1 (2.43 $\pm$ 0.16) was slightly lower than that in treatment 2 (2.50 $\pm$ 0.83).

**Table 2**. Mean (±S.D.) harvest weight, production, survival, growth, and feed conversion ratio (FCR) of prawns cultured in ponds for 104 days after being stocked

| | Treatment | |
|---|---|---|
| | T1 (Oct 2004-Apr.2005) | T2 (Feb 2006-Sep 2006) |
| Individual weight (g) | 47.8 ± 3.7[a] | 34.8 ± 1.7[a] |
| Total production (kg/rai[*]) | 392.7 ± 27.2[a] | 208.27 ± 83.0[a] |
| Survival rate (%) | 34.3 ± 3.9[a] | 24.5 ± 13.1[b] |
| Growth rate (g/day) | 0.19 ± 0.01[a] | 0.15 ± 0.07[b] |
| FCR | 2.43 ± 0.16[a] | 2.50 ± 0.83[a] |

[*] 1 rai = 0.4 acre

N.B. Values are means of three replicates. Means within a row with different superscripts are significantly different ($P$≤0.05) by ANOVA.

*Mj. Int. J. Sci. Tech.* **2007**, *01(02)*, 216-221

The lives of crustaceans are affected by various environmental factors and therefore it is difficult to separate the effect of each factor. However, prawn growth seems to be strongly affected by temperature. Water temperature significantly effects the growth and metabolism of prawns. Temperature has an especially pronounced effect on feed consumption and growth. Feed consumption is optimal when water temperatures ranges from 27-31ºC. Feed consumption decreases both above and below this temperature range. However, results show that although the animal's initial body weight had a close linear relationship with food consumption and growth, and oxygen and food consumption and growth increased with temperature, temperature showed no effect on growth efficiency. Average temperature in treatment 1 (25.2˚C) was much lower compared to treatment 2 (31.0˚C). It has also been reported that the total yield of prawns increases with decreasing temperature [9,10].

*Experiment 2*

There were no major differences in measured water quality parameters for the two treatments. All the measured variables were within acceptable limits for freshwater prawn culture. In this study, water temperature ranged from 23.8° C to 28.3° C. Dissolved oxygen ranged from 6.7 to 7.4 mg/L (mean of 7.1 mg/L) and pH varied from 7.5 to 8.5 (mean of 8.0).

There were significant differences ($P<0.05$) in results obtained for the two treatments (Table 3). Final mean weight (34.8 $\pm$ 1.7 g), average weight gain (0.19 ± 0.01 g/day), total biomass (392 kg), and survival (34.3%) were all much higher for T1 (25 prawns/$m^2$) than those for T2 (50 prawn/$m^2$), regardless of individual sizes.

**Table 3.** Mean (± S.E.) harvest weight, production, survival, growth rate, and feed conversion ratio (FCR), of prawns cultured in ponds for 104 days after being stocked

| | T1 (25 prawns/$m^2$) | T2 (50 prawns/$m^2$) |
|---|---|---|
| Individual weight (g) | $34.8 \pm 1.7^a$ | $13.6 \pm 2.2^b$ |
| Total production (kg) | $392.7 \pm 27.22^a$ | $340 \pm 91.7^b$ |
| Survival rate (%) | $34.3^a$ | $11.9^b$ |
| Growth rate (g/day) | $0.19 \pm 0.01^a$ | $0.09 \pm 0.01^b$ |
| FCR | $2.43^a$ | $2.53^a$ |

N.B. Values are means of three replicates. Means within a row with different superscripts are significantly different ($P\leq0.05$) by ANOVA.

Thus, it is clear that density affects growth and production of freshwater prawns and that prawns are negatively affected by inadequate space. For giant freshwater prawns to grow properly certain optimal space is required, and high stocking density does not give a positive impact in the production of giant freshwater prawns.

*Mj. Int. J. Sci. Tech.* **2007**, *01(02)*, 216-221

## Conclusion

Raising of freshwater prawns during dry season to summer and at lower stocking density resulted in superior growth of freshwater prawns.

## Acknowledgement

This research was funded by National Research Council of Thailand (NRCT) under Grant number 04113681-0005.

## References

1. A.G. Tacon and I. P. Forster, "Trends and challenges to aquaculture and aquafeed development in the new millennium", *Avances en Nutrición Acuícola, Memorias del V Simposium Internacional de Nutrición Acuícola, Mérida, Yucatán, México*, **2000**, pp. 1–12.
2. J. N. Páramo, A. Llamas, and H. Villarreal, "Effect of stocking density on growth, survival and yield of juvenile redclaw crayfish *Cherax quadricarinatus* (Decapoda: Parastacidae) in gravel-lined commercial nursery ponds", *Aquaculture*, **2004**, *242*, 197-206.
3. K. J. Anson and D. B. Rouse, "Effects of salinity on hatching and post-hatch survival of the Australian red claw crayfish *Cherax quadricarinatus*", *J. World Aquac. Soc.*, **1994**, *25*, 277–280. |
4. R.W. Hutching and H. Villarreal, "Biología y cultivo de la langosta de agua dulce (redclaw) *Cherax quadricarinatus*. Manual de Producción, Navimar, Guayaquil", Ecuador, **1996**, 400 pp.
5. C. G. Lutz and W. R. Wolters, "The effect of five stocking densities on growth and yield of red swamp crawfish Procambarus clarkii", *J. World Aquac. Soc.*, **1986**, *17*, 33–36.
6. C. M. Jones and I. M. Ruscoe, "Assessment of stocking size and density in the production of redclaw crayfish, *Cherax quadricarinatus* (von Martens) (Decapoda: Parastacidae), cultured under earthen pond conditions", *Aquaculture*, **2000**, *189*, 63–71.
7. N. M. Morrisey, "Density-dependent pond growout of single year-class cohorts of a freshwater crayfish *Cherax tenuimanus* (Smith) to two years of age", *J. World Aquac. Soc.*, **1992**, *232*, 154–168.
8. G. F. Pito and D. B. Rouse, "Growth and survival of the Australian red claw crayfish *Cherax quadricarinatus* at three densities in earthen ponds", *J. World Aquac. Soc.*, **1996**, *272*,192–197.
9. J. H. Tidwell, S. Coyle, C. Weibel,. and J. Evans, "Effects and interactions of stoking densities and added substrate on production and population structure of freshwater prawns *Macrobrachium rosenbergii*", *J. World Aquac. Soc.*, **1999**, *302*, 174–179.
10. E. R. Villagram, "Effects of stocking density and supplemental feeding on production of red swamp crawfish in pools", *Master's Thesis*, **1993**, Louisiana State University, USA.

*Mj. Int. J. Sci. Tech.*, **2007**, *01(02)*, 222-228

***Maejo International***

***Journal of Science and Technology***

**ISSN 1905-7873**

Available online at www.mijst.mju.ac.th

*Short Communication*

# Fatty acid content and antioxidant activity of Thai bananas

**Rungnapa Meechaona [1], Waya Sengpracha [2], Jirawan Banditpuritat [1*] Rungthip Kawaree [1*], and Weerachai Phutdhawong [1]**

[1]Department of Chemistry, Faculty of Science, Maejo University, Sansai, Chiang Mai 50290, Thailand

[2]Department of Chemistry, Silpakorn University, Nakornpathom 73000, Thailand

*Author to whom correspondence should be addressed, e-mail: liew_64@hotmail.com and t_chem@hotmail.com

*Received: 17 October 2007 / Accepted: 6 December 2007 / Published: 7 December 2007*

**Abstract:** The aril extracts of three Thai banana varieties, namely "Kluai Khai"(KK), "Kluai Namwa"(KN) and "Kluai Hom"(KH) were analysed by gas chromatography and mass spectrometry (GC-MS). GC-MS data were used to identify 5 methyl esters of each banana extract after transesterification. The most prominent components found in KK, KN and KH were hexadecanoic acid methyl ester (43.17, 29.18, 30.57 % respectively), 9, 12, 15-octadecatrienoic acid methyl ester (35.93, 30.46, 39.68 % respectively), 9, 12-octadecadienoic acid methyl ester (14.35, 36.10, 21.82 % respectively), 9-hexadecanoic acid methyl ester (3.76, 3.34, 3.32 % respectively) and octadecanoic acid methyl ester (2.79, 0.92, 4.60 % respectively). The antioxidant activity of the crude oils was evaluated using DPPH method.

**Key words:** banana, fatty acids, antioxidant

*Mj. Int. J. Sci. Tech.*, **2007**, *01(02)*, 222-228

## Introduction

The banana is one of the most popular fruits in the world. A member of the genus *Musa* (part of the family *Musaceae*), they are considered to be derived from the wild species *Musa acuminata* and *Musa balbisiana* [1]. It is believed that there are almost 1000 varieties of bananas in the world, subdivided into 50 groups [2]. The origin of bananas is placed in South-east Asia, in the jungles of Malaysia, Indonesia and Philippines, where so many varieties of wild bananas still grow at present. In Thailand, there are three most popular varieties (among several to choose from), viz. "Kluai Khai" (KK), "Kluai Namwa" (KN) and "Kluai Hom" (KH). Bananas have many beneficial nutritional properties. They are a good source of vitamins C, B6 and A [3]. Bananas have a high content of carbohydrates and fibre, while they are low in protein [4]. They are also rich in potassium [5]. Several papers have reported the chemical content of volatiles of banana [6-9]. However, so far as we know, only one study has been carried out on the fatty acid composition of the fixed oils obtained from dried and fresh bananas [10]. Moreover, no study has been carried out on Thai banana varieties, especially the "Kluai Khai" (KK), "Kluai Namwa" (KN) and "Kluai Hom" (KH). We thus report here the fatty acid analysis result of "Kluai Khai" (KK), "Kluai Namwa" (KN) and "Kluai Hom" (KH) bananas by GC–MS and also the antioxidant activity of the obtained crude oil using DPPH method.

## Materials and Methods

### *Fruits*

"Kluai Khai" (KK), "Kluai Namwa" (KN) and "Kluai Hom" (KH) bananas were obtained from a local market in the provinces of Kampangpech (for KK), Chiang Mai (for KN) and Nakornpratom (for KH), Thailand, in May 2007.

### *Extraction*

The aril (700 g each) of the bananas (KK, KN and KH) was separately extracted with hexane (2×250 ml). The extract was dried over $Na_2SO_4$ and evaporated to give 1.27 % (KK), 1.31 % (KN) and 1.24 % (KH) yield of an oil.

*Transesterification* [11]

One g of each oil in benzene (20 ml) and methanol (20 ml) was added with a small amount of sodium (~0.05 g) and left overnight. The solution was extracted by dichloromethane, which was washed with water several times. The dichloromethane layer was evaporated to give ~ 2 ml of oil which was a mixture of the methyl esters. The FT-IR spectra (run with a Perkin Elmer System 2000) were used to confirm the ester functional group of the oils.

*GC-MS Analysis*

The oils obtained from the transesterification reaction were analysed by GC–MS [performed on a Agilent 6890(GC)/HP 5975(MS)]. Separation was achieved using $H_2$ as carrier gas (ca.1 ml/min) with a fused silica capillary column (DB-5) 30 m long, with 0.25 mm i.d. and 0.25 μm film thickness. Injector and detector temperatures were 250 °C and 260 °C, respectively; with oven temperature programme: 1 min isothermal at 40 °C, then at 10 °C/min to 260 °C (5 min isothermal). The MS instrument was operated in full scan and electron impact ionization mode (70 eV).

*Antioxidant activity, DPPH method* [12]

The oil was dissolved in methanol to give a solution of 100 ppm concentration. This sample was further diluted to 7 concentrations (two-fold dilutions). Each concentration was tested in triplicate. A portion of sample solution (1 ml) was mixed with an equal volume of 0.2 mM DPPH (1,1-diphenyl-2-picrylhydrazyl) in absolute methanol and allowed to stand at room temperature for 30 min. The absorbance (A) was then measured at 514.5 nm (Hitachi U-2001 UV-spectrophotometer). Vitamin E was tested in the same system as a positive control. The results were expressed as percent inhibition calculated from the equation: % inhibition = $[(A_{control} - A_{sample})/ A_{control}] \times 100$. $IC_{50}$ value (inhibition concentration of sample required to scavenge DPPH radical by 50 %) was obtained by linear regression analysis of the dose-response curve plot (% inhibition versus concentration).

**Results and Discussion**

A typical analysis result of the transesterified oils of KK, KN and KH bananas are shown in Figure 1. Compounds corresponding to the peaks are listed in Table 1.

*Mj. Int. J. Sci. Tech.*, **2007**, *01(02)*, 222-228

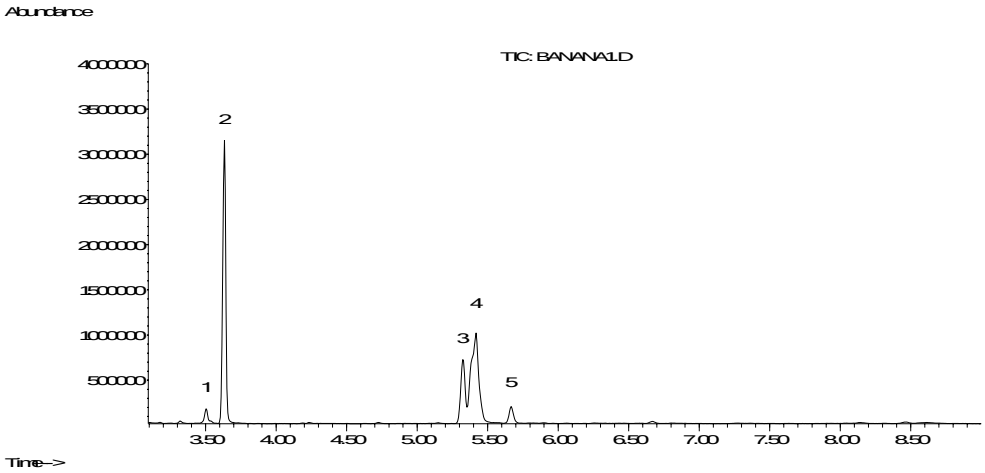


KK

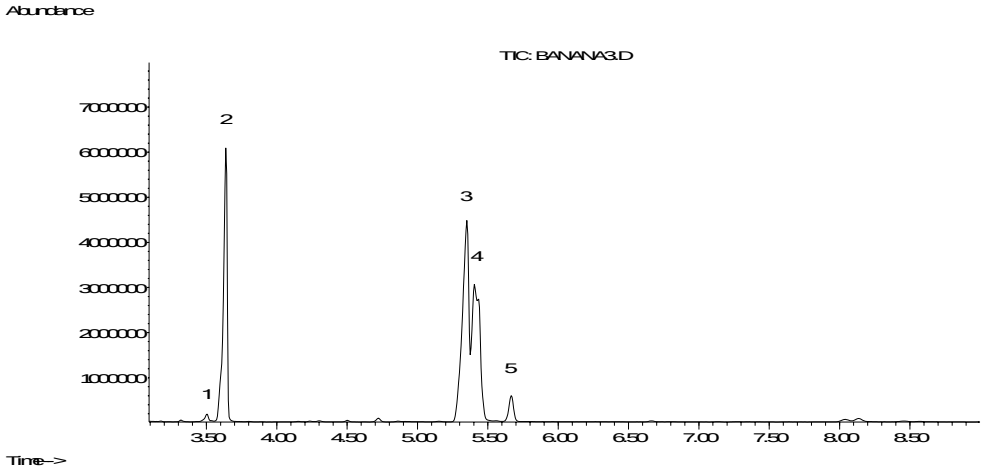


KN

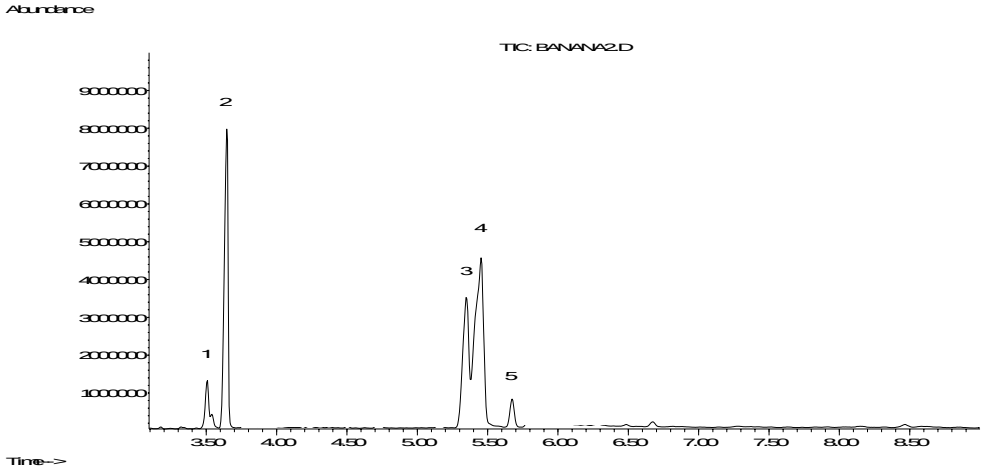


KH

**Figure 1**. Gas chromatograms of the transesterified oils of Thai bananas (KK, KN and KH)

*Mj. Int. J. Sci. Tech.*, **2007**, *01(02)*, 222-228

**Table 1**. Components in the transesterified oils of aril of Thai bananas (KK, KN and KH)

| Peak No. | Compounds | RA[a] % | | | MW[b] | Quality %[c] | Identification[d] |
|---|---|---|---|---|---|---|---|
| | | KK | KN | KH | | | |
| 1 | 9-Hexadecenoic acid methyl ester (palmitoleic acid methyl ester) | 2.79 | 0.92 | 4.60 | 268 | 99 | 1, 2 |
| 2 | Hexadecanoic acid methyl ester (palmitic acid methyl ester) | 43.17 | 29.18 | 30.57 | 270 | 99 | 1, 2 |
| 3 | 9, 12-Octadecadienoic acid methyl ester (linoleic acid methyl ester) | 14.35 | 36.10 | 21.82 | 294 | 99 | 1, 2 |
| 4 | 9, 12, 15-Octadecatrienoic acid methyl ester (linolenic acid methyl ester) | 35.93 | 30.46 | 39.68 | 292 | 99 | 1, 2 |
| 5 | Octadecanoic acid methyl ester (stearic acid methyl ester) | 3.76 | 3.34 | 3.32 | 298 | 99 | 1, 2 |

[a] RA: relative area (peak area relative to total peak area)

[b] molecular weight from GC-MS (EI) data

[c] MS quality compared with database

[d] 1, based on comparison of mass spectra from NIST library; 2, based on comparison of mass spectra from Wiley library

It is clear from Table 1 that in each of the banana oils after transesterification, five prominent peaks of methyl esters are identified. In these, there appears the presence of two saturated methyl esters (peaks No. 2 and 5) and three unsaturated methyl esters (peaks No. 1, 3 and 4). Thus, the major fatty acid components found in KK, KN and KH are hexadecanoic (palmitic) acid (43.17, 29.18, 30.57 % respectively), 9, 12, 15-octadecatrienoic (linolenic) acid (35.93, 30.46, 39.68 % respectively), and 9, 12-octadecadienoic (linoleic) acid (14.35, 36.10, 21.82 % respectively), and the minor fatty acids are octadecanoic (stearic) acid (3.76, 3.34, 3.32 % respectively) and 9-hexadecenoic (palmitoleic) acid (2.79, 0.92, 4.60 % respectively). These results were similar to those found in the previous study [10]. It was found therefore that KK, KN and KH bananas contain more unsaturated fatty acids than saturated ones and also each variety provides different amounts of each fatty acid, although their amounts were only slightly different. Notably, these banana fixed oils were all found to contain

*Mj. Int. J. Sci. Tech.*, **2007**, *01(02)*, 222-228

unusually high amounts of linoleic acid, although, similar to the previous finding [10], no oleic acid was detected in any of the oils studied.

The antioxidant activity of the banana oils before transesterification was evaluated using DPPH method and the results are shown in Table 2.

**Table 2**. Antioxidant activity of banana oils using DPPH method

| Bananas | KK | KN | KH |
|---|---|---|---|
| $IC_{50}$ (μg/ml)* | 90 | 73 | 81 |

* $IC_{50}$ of Vitamin E = 12.55 ppm

It was clear that the banana oils of KK, KN and KH showed moderate antioxidant activities compared to vitamin E when assayed by DPPH.

**Acknowledgements**

The authors are grateful to the Biology Department of Maejo University for GC/MS facilities. They would also like to thank the Chemistry Department of Maejo University for the undergraduate grant to R. M., a final year chemistry student.

**References**

1. K. Kayisu, L. F. Hood, and P. J. Vansoest, "Characterization of starch and fiber of banana fruit", *J. Food Sci.*, **1981**, *46*, 1885-90.
2. F. Lheureux, N. Laboureau, E. Muller, B. E. L. Lockhart, and M. L. Iskra-Caruana, "Molecular characterization of banana streak acuminata Vietnam virus isolated from Musa acuminata siamea (banana cultivar)", *Archives of Virology*, **2007**, *152*, 1409-1416.
3. M. Hagg, S. Ylikoski, and J. Kumpulainen, "Vitamin C content in fruits and berries consumed in Finland", *J. Food Comp. Anal.*, **1995**, *8*, 12-20.
4. E. T. Happi, R. H. Andrianaivo, B. Wathelet, J. T. Tchango, and M. Paquot, "Effects of the stage of maturation and varieties on the chemical composition of banana and plantain peels", *Food Chem.*, **2007**, *103*, 590-600.
5. S. Agrawal, R. K. Patel, S. D. Pandey, "Influence of higher levels of nitrogen and potassium on growth and yield potential of in-vitro Banana (cv. Robusta)", *Mysore J. Agri. Sci.*, **1998**, *32*, 275-

280.

6. H. Shiota, "New esteric components in the volatiles of banana fruit *(Musa sapientum* L.) ", *J. Agric. Food Chem.,* **1993**, *41,* 2056-2062.
7. J. M. F. Nogueira, P. J. P. Fernandes, and A. M. D. Nascimento, "Composition of volatiles of banana cultivars from Madeira Island", *Phytochem. Anal*., **2003**, *14*, 87-90.
8. J. Wabg, Y. Z. Li, R. R. Chen, J. Y. Bao, and G. M. Yang, "Comparison of volatiles of banana powder dehydrated by vacuum belt drying, freeze-drying and air-drying", *Food Chem*., **2007**, *104*, 1516-1521.
9. J. A. Pino, A. Ortega, R. Marbot, and J. Aguero, "Volatile components of banana fruit (*musa sapientum L*.) "Indio" for Cuba" *J. Essent. Oil. Res*., **2003,** *15*, 70-71
10. İ. Orhan, Ş. Küsmenoğlu, and B. Şener. "Fatty acid profile of fresh and dried banana (*Musa sapientum* L. var. *cavendishii* Lamb.) Peel Oils", *J. Fac. Pharm. Ankara*., **2002**, *31*, 13-19.
11. W. Phutdhawong, S. Kaewkong, and D. Buddhasukh, "GC-MS analysis of fatty acids in Thai durian aril." *Chiang Mai J. Sci.*, **2005**, *32*, 169-172.
12. W. Phutdhawong, R. Kawaree, S. Sanjaiya, W. Sengpracha, and D. Buddhasukh, "Microwave-assisted isolation of essential oil of *Cinnamomum iners* Reinw. ex Bl.: comparison with conventional hydrodistillation", *Molecules*, **2007**, *12*, 868-877.